SYNTHESIS OF Ti, Cr, Mn, Fe, Co, Ni, Cu, Zn SULFIDES BY SOLID-GAS REACTIONS, INVESTIGATION OF STRUCTURAL AND CONDUCTING PROPERTIES

A THESIS SUBMITTED TO
THE GRADUATE SCHOOL OF NATURAL AND APPLIED SCIENCES
OF
MIDDLE EAST TECHNICAL UNIVERSITY

BY

MUSTAFA FATİH GENİŞEL

IN PARTIAL FULFILLMENT OF THE REQUIREMENTS
FOR
THE DEGREE OF MASTER OF SCIENCE
IN
CHEMISTRY

NOVEMBER 2005

Approval of the Graduate School of Natural and Applied Sciences

_____

Prof. Dr. Canan Özgen
Director

I certify that this thesis satisfies all the requirements as a thesis for the degree of Master of Science.

_____

Prof. Dr. Hüseyin İşçi
Head of Department

This is to certify that we have read this thesis and that in our opinion it is fully adequate, in scope and quality, as a thesis for the degree of Master of Science.

_____

Assis. Prof. Dr. Ayşen Yılmaz
Supervisor

Examining Committee Members

Prof. Dr. Hüseyin İşçi	(METU,CHEM)	_____
Assis. Prof. Dr. Ayşen Yılmaz	(METU,CHEM)	_____
Prof. Dr. Ali Usanmaz	(METU,CHEM)	_____
Assoc. Prof. Dr. Gülsün Gökağaç	(METU,CHEM)	_____
Dr. Güller Gürbüz	(T.Ç.M.B.)	_____

I hereby declare that all information in this document has been obtained and presented in accordance with academic rules and ethical conduct. I also declare that, as required by these rules and conduct, I have fully cited and referenced all material and results that are not original to this work.

Name, Last name:

Signature:

ABSTRACT

SYNTHESIS OF Ti, Cr, Mn, Fe, Co, Ni, Cu, Zn SULFIDES BY SOLID-GAS REACTIONS, INVESTIGATION OF STRUCTURAL AND CONDUCTING PROPERTIES

Genişel, Mustafa Fatih

M.S., Department of Chemistry

Supervisor: Assis. Prof. Dr. Ayşen Yılmaz

November 2005, 130 pages

In this study some of the first row transition metal oxides were transformed to metal sulfides by new solid gas reaction system.

Transition metal sulfides have wide application area in industry and technology. Several techniques are known for the production of metal sulfides. Such as reactions between metal or metal oxide with H_2S, precipitation in several liquid medium, reaction between metal and sulfur in closed vessel, chemical vapor deposition (CVD) technique. These techniques will have some disadvantages; for example, reactants are rarely available or expensive materials, their production systems are complicated and hard to set up these systems, products contain oxygen or hydrogen or corresponding metal sulfate as impurities.

In our new sulfidizing system the reactants are metal oxides, carbon and SO_2. These materials can be found easily. Especially, SO_2 usage in this system is a big advantage of giving possibility of usage the hazardous waste product of SO_2 in industry.

The sulfidizing gas mixture was obtained by passing SO_2 over activated carbon at 750 ^{O}C in a vertical tubular furnace. The obtained gas contains, mainly, CS_2, CO and COS. The sulfidizing reactions took place in the horizontal tubular furnace at 450^{O}C-1250 ^{O}C. The duration of the reaction, (three hours), and flow rate (60ml/min) of the SO_2 gas were kept constant. The products were examined by X-ray powder diffraction and Raman scattering spectroscopy.

All examined metal oxides were transformed to metal sulfides by sulfidizing gas mixture successfully. Ti_3S_5 was obtained from TiO_2. Cr_2S_3 was obtained from Cr_2O_3. MnS (Alabandite) was obtained from MnO_2. FeS and $Fe_{1-x}S$ (Pyrrhotite) were obtained from Fe_2O_3. Co_9S_8 (Cobaltpentlandite) and CoS (Jaipurite) were obtained from Co_3O_4. NiS was obtained from NiO. $Cu_{7.2}S$, $Cu_{1.6}S$ (Calcocite-Q), $Cu_{1.81}S$, Cu_7S_4 (Anilite) Cu_9S_5 (Digenite), Cu_8S_5 (Geerite) were obtained from CuO, ZnS was obtained from ZnO.

The electrical conductivity character of each product obtained by sulfidizing reaction was analyzed in the temperature range of 77 K-300 K. Titanium sulfide, cobalt sulfide and nickel sulfide showed metallic conductivity, cupper sulfide and iron sulfide showed semiconductor behavior in this temperature range.

Keywords: Transition metal oxide, Transition metal sulfide, Conductivity Raman Scattering spectra, X-ray powder diffraction pattern, Sulfidizing reactions.

ÖZ

KATI-GAS TEPKİMELERİ İLE Ti, Cr, Mn, Fe, Co, Ni, Cu, Zn SÜLFÜR BİLEŞİKLERİNİN SENTEZİ, YAPISI VE İLETKENLİK ÖZELLİKLERİNİN İNCELENMESİ

Genişel, Mustafa Fatih
Yüksek Lisans, Kimya Bölümü
Tez Yöneticisi: Yard.Doç.Dr. Ayşen Yılmaz

Kasım 2005, 130 sayfa

Bu çalışmada bazı ilk sıra geçiş metal oksit bileşiklerinin metal sülfür bileşiklerine dönüşümleri laboratuarımızda kurulan katı-gaz tepkime sistemiyle gerçekleştirilmiştir.

Geçiş metallerinin sülfürlü bileşiklerinin endüstri ve teknolojide geniş kullanım alanlarına sahip olmalarından dolayı bu maddelerin üretim yöntemlerinin geliştirilmesi önemlidir. Günümüzde metallerin sülfürlü bileşiklerinin üretimi; metal veya metal oksidin H_2S ile tepkimesi, çeşitli sıvı fazlarda çökeltme, metal ile kükürdün kapalı sistemde tepkimesi ve kimyasal buhar biriktirme (CVD) gibi tekniklerle sağlanmaktadır. Bütün bu tekniklerin bazı dezavantajları vardır. Örneğin; tepkimeye giren maddelerin az bulunur ve pahalı olması, üretim sistemlerinin karmaşık ve oluşturulmalarının zor olması, üretilen maddelerin oksijen ve hidrojeni safsızlık olarak içermesi veya tepkime sonucunda metal sülfat oluşması, gibi.

Bu araştırmada kullandığımız sülfürleme sisteminde tepkimeye giren

maddeler metal oksitler, karbon ve SO_2 kolay bulunabilen bileşiklerdir. Özellikle endüstrinin ürettiği tehlikeli atık madde olan SO_2'nin yeniden kullanımının bu araştırmada önerilen yöntem ile sağlanabilme olasılığı büyük bir avantaj olacaktır.

Bu tezde kullanılan sülfürleyici gaz karışımı, SO_2'nin 750 ^{O}C'de aktive olmuş kömür ile dolu dikey tüp fırından geçirilmesi ile elde edildi. Elde edilen gaz karışımı büyük ölçüde CS_2,CO ve COS gazlarını içermektedir. Tepkime 450 ^{O}C–1250 ^{O}C'de yatay tüp fırında gerçekleştirildi. Tepkime süreleri, (üç saat), SO_2 gazının akış hızı (60 ml/dak) sabit tutuldu. Elde edilen ürünlerin X-ışınları toz kırınım desenleri ve Raman saçılımı spektrumları incelendi.

Çalışılan bütün metal oksitler sülfürleyici gaz karışımı ile başarılı bir şekilde metal sülfürlere dönüştürülmüşlerdir. TiO_2 den Ti_3S_5, Cr_2O_3 den Cr_2S_3, MnO_2 den MnS (Alabandite), Fe_2O_3 den FeS ve $Fe_{1-x}S$ (Pyrrhotite), Co_3O_4 den Co_9S_8 (Cobaltpentlandite) ve CoS (Jaipurite), NiO den NiS, CuO den $Cu_{7.2}S$, $Cu_{1.6}S$ (Calcocite-Q), $Cu_{1.81}S$, Cu_7S_4 (Anilite) Cu_9S_5 (Digenite) ve Cu_8S_5 (Geerite), ZnO den ZnS üretilmiştir.

Elde edilen metal sülfür bileşiklerinin elektrik iletkenliği davranışları 77 K–300 K sıcaklıkları arasında incelenmiştir. Titanyum sülfür, kobalt sülfür ve nikel sülfür bu sıcaklık aralığında metalik iletkenlik özelliği gösterirken; bakır sülfür ve demir sülfür yarı iletken özelliğe sahiptirler.

Anahtar Kelimeler: Geçiş metal oksitleri, Sülfürlü geçiş metalleri, iletkenlik, Raman saçılım spektrumu, X-ışınları toz kırınım desenleri. Sülfürleme Tepkimeleri.

To my family

ACKNOWLEDGEMENTS

I would like to express my sincere gratitude to Assis. Prof. Dr. Ayşen Yılmaz for her unceasing support, guides, and supervision throughout in this study.

I would like to express my sincere feelings of gratitude and appreciation to Prof. Dr. Meral Kızılyallı for directing me in this interesting study and for her skillful guidance, endless support, and encouragement in this tedious work. It has been a great honor for me to work with her.

I am indebted to Prof. Dr. O. Yavuz Ataman for giving moral support throughout in my university carrier. I owe much to him for his help to overcome difficulties I have encountered.

I also give my thanks to all the members of our research group; Semih Seyyidoğlu, Selcan Tuncel, Yasemin Özdil, Seher Karabıçak, Volkan Değirmenci and especially Ersin Yıldız.

Thanks are also extended to Kürşad Tosun, Nuh Sadi Yüksek, Mustafa Alp Ertem, Taner Atalar, Selçuk Gümüş and Emre Yazıcıoğlu for their unique friendships.

Finally, my special appreciation and gratitude is devoted to my family for their endless encouragement and moral support, which makes everything possible.

TABLE OF CONTENTS

LIST OF TABLES

Tables

LIST OF FIGURES

FIGURES

CHAPTER 1

INTRODUCTION

1. General Considerations

1.1 Sulfides

Almost, all known elements react with sulfur, forming sulfides and poly sulfides. It has been attempted to discuss at least the most important features of some binary sulfides.

Since 70's and 80's the synthesis and characterization of new binary, ternary and quaternary type of metal sulfides have received considerable attention. Important technological applications found for many of these materials as well as their remarkable relationships in structure and properties. These applications force the effort in synthesis and characterization of sulfide compounds, within the developing sophisticated synthesis and compound characterization techniques.

Almost all metal can be obtained as metal sulfide or metal oxide compounds. In addition to resemblance between metal sulfides and corresponding metal oxides, the structure and bonding of most binary metal sulfides differ significantly from those of corresponding metal oxides. The difference, primarily reside in the higher covalence of metal sulfur interactions relative to metal oxygen.

The lower electronegativity of the sulfur relative to the oxygen leaves the valence 3s and 3p sulfur bands much closer in energy to the transition metal d-orbital manifold (i.e., greater covalence). In many compounds, such as the copper

sulfides, formal oxidation states become ambiguous and oxidation-reduction chemistry may involve the sulfide bands more than the transition metal d-orbital bands.[1]

Transition metal binary sulfides have wide application area. In general cases they are used; in production of ammonia,[2] in hydrocarbon conversion process,[3] in production of nanocarbon material,[4,5] in recovery of metals,[6,7] in batteries, as cathode or anode materials.[8-15]Zinc sulfides are used as photocatalyst,[16] nanocables,[17] electroluminescent or phosphorescent materials,[18] fluorescent labeling materials,[19] in solar batteries, cathode ray luminescent, in laser diode in optical recording,[20] in blue LED's[21] and in the production of $ZnCl_2$.[22-28] Cupper sulfides are used in solar cells with CdS,[29, 30] in device for rectifying alternating current.[31] Nickel sulfides are used production of metallic nickel.[32] Cobalt sulfides are used as semiconductor photo electrode arrays in unassisted photolytic water splitting equipment[33]. Iron sulfides are used in adsorption of radioactive and heavy metals[34-36], as agents for air and water purification[38,39], building materials[40] hard magnetic alloys,[41] coating for steel in H_2S surroundings[42,43] in sulfur isotope production,[44] as coating for electrode material used in hydrogen production by electrolysis[45], in giant magnetic resistant with manganese sulfide.[46] Manganese sulfides are used; in steel to improve hot-work ability of steel[47] and in photo electrochemical production of hydrocarbons.[48]

1.2 Methods for Metal Sulfide Production

There are also lots of methods that are used for production of the metal sulfides.

Some of these methods are;

1) Precipitation in various solvent with various reactant:[49-53] In these techniques small solubility of the metal sulfides is used. Metals are dissolved as

soluble salts such as; metal chloride, metal bipyridine etc. and sulfide are dissolved as soluble salt such as; Li_2S, H_2S. Precipitation reactions occur in various solvent such as H_2O, OEt_2, hydrazine, THF. This technique is mainly used to obtain nano-crystalline product. If we consider that the main source of the metals as oxide minerals which have low solubility, finding soluble metal salt will be a problem.

2) Solid-gas reactions:[54-60] In this technique high temperature is mainly used. Metals or metal compounds such as metal sulfate, metal oxides heated under specific gas atmosphere such as; H_2, H_2/H_2S, H_2S, S, SO_2. H_2 is used with metal sulfate compounds but metal oxide is also obtained as by product. H_2/H_2S mixture or H_2S are used with metal or metal oxides. When SO_2 is used with metal beside metal sulfide, metal oxide production occurs.

3) Thin film production with Chemical Vapor Deposition (CVD): In this technique volatile starting materials are mixed at a suitable temperature and solid product synthesis out in the wall of the vessel and on substrate. Single crystals or thin films are obtained by CVD. Very complicated and sophisticated equipments are used in this technique. Typical starting materials are hydride halide and organometalic compounds. Obtaining suitable starting materials is also another problem.

4) Reaction between metal and elemental sulfur in closed vessel: In this technique elemental metal and sulfur put in a closed chemically inactive and strong vessel and heated.

In our sulfidizing method SO_2, carbon and metal oxide are used as reactant. All of these entire compounds can be found easily. Especially this method will be suitable for usage of SO_2 gas, which is a waste product of industry. The reducing power of our sulfidizing gas and controllable partial replacement make the method useful for obtaining electric conductivity the in material science. This method was used before in our laboratory to obtain NaS,

$YBa_2Cu_3S_7$ and FeCuS.[61-64]

1.3 Preparation of Sulfides Through Solid Gas Reactions

1.3.1 Thermodynamics of Carbon Disulfide Synthesis

Owen et al. [65] studied the details of the thermodynamics of carbon disulfide synthesis. Carbon disulfide can be synthesized by four different ways given below. The last one was used in our laboratory.

(a) CO_2 (g) + $2H_2S$ (g) ;
(b) CO_2 (g) + $2H_2S$ (g) + excess C (graphite);
(c) $2H_2S$ (g) + excess C (graphite);
(d) SO_2 (g) + excess C (graphite);

Owen et al.[65] calculated the equilibrium constants for the following equations and then the partial pressures of the gases were given according to the reaction temperature.

$SO_2 + 2C \longleftrightarrow COS + CO$
$2COS \longleftrightarrow CS_2 + CO_2$
$COS \longleftrightarrow 2CO + S_2$
$C + S_2 \longleftrightarrow CS_2$

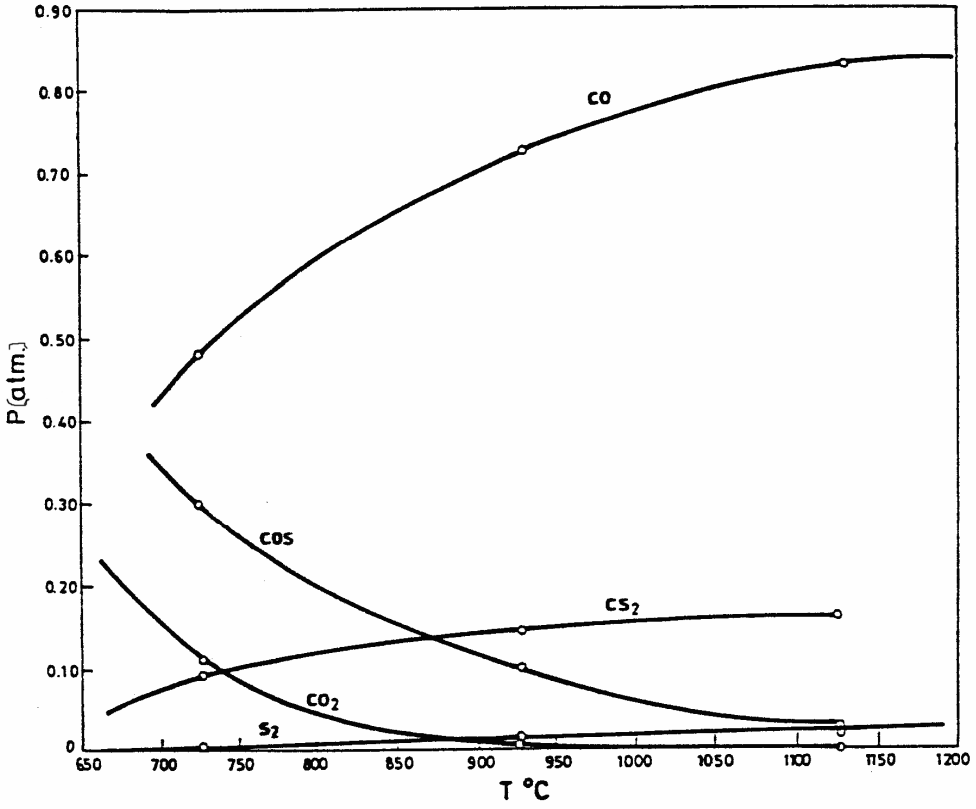

Figure 1.3.1: Plot of Partial Pressures vs. Reaction Temperature

The partial pressures of carbon disulfide, sulfur and carbon monoxide increase with increase of temperature where the partial pressures of the carbon dioxide and carbonyl sulfide decrease. In fact the reaction mechanism of carbon with sulfur dioxide is very complex but, it is known that sulfur dioxide is reduced at high temperatures. The partial pressure of carbon monoxide is 4.3×10^{-8} atm at 725 °C in the sulfidizing gas mixture, (Figure 1.3.1) [65]

All the reactions are assumed to occur at a constant total pressure of 1 atm at temperatures of 1000 K, 1200 K and 1400 K. The result of the last system is given in Table 1.3.1.1, contains the partial pressures of all the gases. [65]

Table 1.3.1.1: Equilibrium Partial Pressures (atm) of product obtained from SO_2 (g) + excess C (graphite) Reaction.

SO_2 (g) + excess C (graphite)			
	1000 K	1200 K	1400 K
CO	0.4830	0.7303	0.7800
CO_2	0.1132	0.0087	0.0009
COS	0.3019	0.0099	0.0326
CS_2	0.0940	0.1455	0.1646
S_2	0.0081	0.0163	0.0220
SO_2	$4.3*10^{-8}$	$8.6*10^{-9}$	$2.2*10^{-9}$

1.3.1 Production of Metal sulfide

Welch[66] proposed that metal sulfides from metal oxides or metals, could be obtained by using mentioned reducing and sulfidizing gas mixture discussed by Owen et al[65]. When a metal oxide, MO, is heated in the flow of carbondisulfide, CS_2, carbonyl sulfide, COS, or with the mixture of carbon monoxide, CO and sulfur, S_2, the following reactions would take place:

$$2MO + CS_2 \longrightarrow 2MS + CO_2,$$

$$MO + COS \longrightarrow MS + CO_2$$

$$2MO + S_2 + 2CO \longrightarrow 2MS + 2CO_2$$

1.4 Conductivity

Charge transfer is the fundamental idea of the electrical conductivity. Band model will help us to understand electrical conductivity. The orbitals in the separated atoms, become bands in solid compounds. These bands can be thought as road for charge to move.

The electrical conductivity related with the response of the charge to the applied electric field. We shall see that electrons in crystals are arranged in energy bands (Figure 1.4.1) separated by regions in energy for which no wavelike electron orbitals exist. Such forbidden regions are called energy gaps or band gaps, and result from the interaction of the conduction electron waves with the ion cores of the crystal.[67]

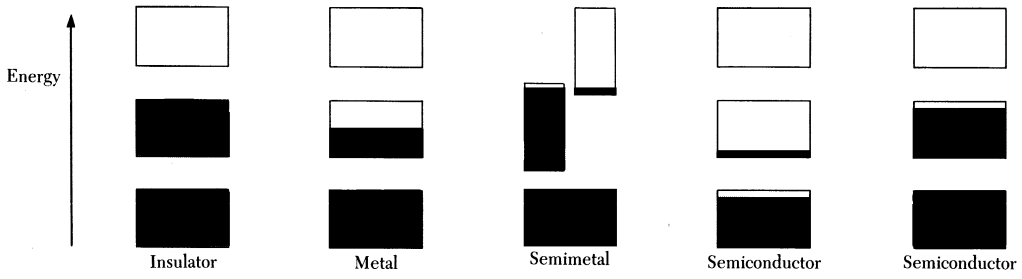

Figure 1.4.1.: Band Model and types of conductivity the shaded areas indicate the regions filled with electrons

Figure 1.4.1 shows schematic electron occupancy of allowed energy bands for an insulator, metal, semi-metal, and semiconductor. The vertical extent of the boxes indicates the allowed energy regions; the shaded areas indicate the

regions filled with electrons. In a semimetal (such as bismuth) one band is almost filled and another band is nearly empty at absolute zero, but a pure semiconductor (such as silicon) becomes an insulator at absolute zero. The left of the two semiconductors shown is at a finite temperature, with carriers excited thermally. The other semiconductor is electron-deficient because of impurities.[67]

The crystal behaves as an insulator if the allowed energy bands are either filled or empty, for then no electrons can move in an electric field. The crystal behaves as a metal if one or more bands are partly filled, say between 10 and 90 percent filled. The crystal is a semiconductor or a semimetal if one or two bands are slightly filled or slightly empty.[67]

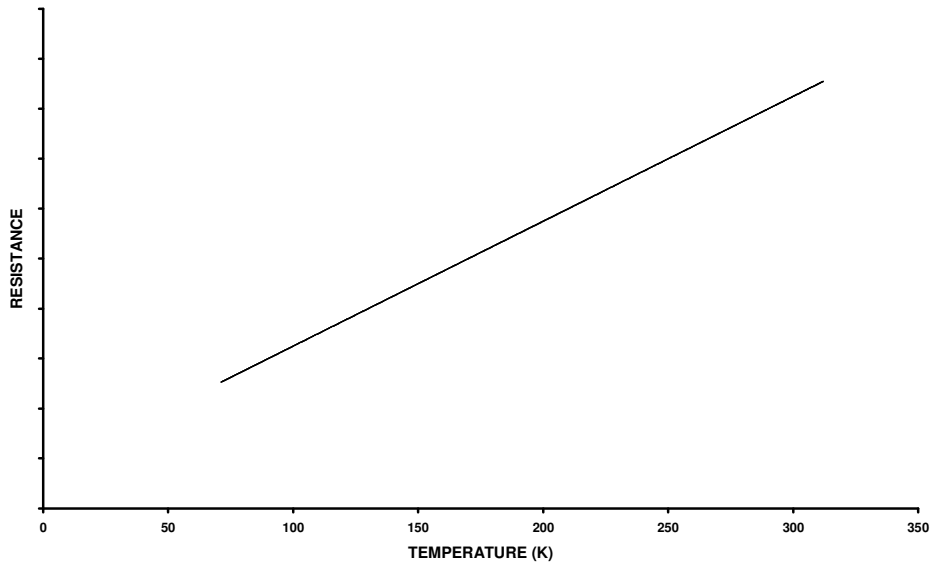

Figure 1.2.2: Typical Temperature vs Resistance Graph of Metallic Conductors

The temperature has an effective role on conductivity. In metallic conductivity, since the phonon-electron interaction increases with increasing temperature, the conductivity decreases at high temperatures, in semiconductors, conductivity increase with the increasing temperature. Because the number of freely movable charge carriers increase with increasing temperature. Figure 1.2.2 shows typical temperature vs resistance graph of metallic conductivity. In intrinsic semiconductors the typical temperatures vs resistance graph is seen in Figure 1.2.3.[68]

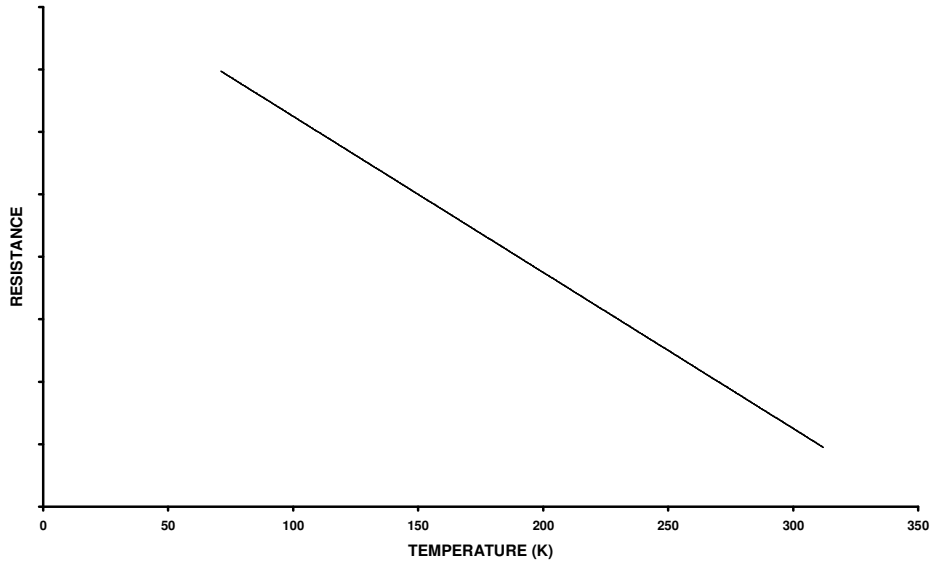

Figure 1.2.3: Typical Temperature vs Resistance Graph of Semiconductors

1.4.1 Conducting Properties of Transition Metal Sulfides

Just as in the case of sulfides of the main group metals, the 4s and 4p orbitals of the transition metals will combine with the 3p and 3s orbitals of

sulfur to form a valence band (mainly due to sulfur) and a conduction band (mainly due to metal). These are broad bands (of the order of 10 eV) the energy gap between them is one to a few eV in most transition-metal sulfides. The 3d orbitals of the transition metal will also overlap with the sulfur orbital, but much less than the 4s and 4p orbitals of the metal. Narrow bands will be formed, but in many cases we may treat the nd orbitals as essentially localized on the metal. If this energy lies within the energy gap between the top of the valence band and the bottom of the conduction band the compound will be a semiconductor. If, however, the energy of the oxidized state also lies below top of the valence band, the cation will be (partly) reduced, holes will be created in the valence band and the compound will be broad-band metallic conductor.

During the formation of metallic crystals from the isolated atoms, the valence electrons of the latter (in the case of the transition metals, the s + d electrons) are partially localized at the frameworks of the atoms and partially pass over to the non-localized state. The localized part of the electrons forms the stable d^0, d^5, and d^{10} configurations, the statistical weight of which varies within wide limits with a variation of the number of electrons in the d-shell of the isolated atom (nd); d^0 and d^5 stable configurations and d^5 and d^{10} configurations are formed in the case of the transition metals with $nd \leq 5$ and $nd > 5$, respectively. The S atom in the isolated state has a configuration of valence electrons s^2p^4, tending towards a finishing construction at the expense of the electrons of the partners (S itself or the transition metals) up to a stable configuration of the s^2p^6 type. The tendency towards a finishing construction to a stable s^2p^6 configuration is expressed, for S in particular, by the capacity of forming structural units in the crystals lattices of the sulfides.[69]

1.5 Purpose of the Work

Since the transition metal sulfides have wide application area in industry and technology, the production of the transition metal sulfides from easily

obtainable reactants are very important. The aim of this work is to propose a new method to transform metal oxide to metal sulfide by using solid gas reaction system. SO_2 gas is used in solid gas reaction system which makes it is possible to recycle the waste hazardous side product of SO_2 in industry. In literature there was not any synthetic method similar to our method, which is the reaction of the metal oxides with the sulfidizing gas mixture.

Beside SO_2 the first raw of the transition metal oxides are other reactants. The oxygen can be replaced with the solid gas reaction using the sulfidizing gas mixture (CS_2, COS, and S_2) which was obtained with the reaction of SO_2 gas with carbon.

Previous works,[61-64] which were performed in our laboratory shows that metal sulfides can be prepared with this known solid gas reaction. In this work the sulfide materials which were obtained at 450 ^{O}C-1250 ^{O}C with sulfidizing gas reactions had the same X-ray powder diffraction (XRD) pattern with known metal sulfide compounds.

In this thesis we will try to clarify following questions by heating at different temperatures with constant heating duration and with constant flow rate of SO_2. Is it possible to transform transition metal oxides into transition metal sulfides? If it is possible what would be the product that obtained at studied temperature and what is the minimum temperature to obtain metal sulfides? If the transition metal sulfides were obtained what would be their structural properties?

CHAPTER 2

EXPERIMENTAL TECHNIQUES

2.1. Chemical Substances

All chemicals, obtained from Merck, Fluka, Aldrich and Sigma, was analytical grade. Nitrogen, N_2, and sulfur dioxide, SO_2, gases and activated charcoal were obtained from local distributors. The gases were passed through $CaCl_2$ for the removal of water.

All chemicals were dried at 100 ° C before using in solid-state reactions.

2.2. Instrumentation

Rigaku Miniflex diffractometer was used for taking X-ray diffraction of the powders with Cu K_α (λ =1.54050 Å). All measurements were made with 0.05 degree steps and 1 degree / minute rate.

Jobin Yvon Horiba was used for Raman scattering Spectra. This instrument has He-Ne laser wavelength of 632.83 nm and Peltier cooled CCD detector. Laser power was 10 mWatt, detector worked at -75 ^{O}C the slit width was 200 μm, and grating, with 600 blazes/cm, was used. Data accumulation duration was 60 second, and each accumulation was done for 6 times

A horizontal type of LABSCO (Laboratory Supply Company Ollmann & Co KG) furnace was used. In this furnace heating elements were silicon carbide rods.

Resistance measurements were carried out with the four probe technique, pellet. Low resistance electrical contacts were made with a silver paint. Temperature was controlled by a cryostat, JANIS Research VPF-475.

2.2.1. Conductivity Measuring System

The system composed of the following equipments.

I) Lakeshore 331 Temperature controller

II) Model 580 Micro-ohmmeter

III) Capital Equipment Corp. IEEE-488 Interface Card and its special software program.

IV) Janis VPF-475 Cryostat.

A PC was added to the system

To measure and control the temperature calibrated Lakeshore Model 331 Tempetature Controller was used. The resistivity change was measured with Model 580 Micro-Ohmmeter using four probe techniques.

These two instruments were connected to the PC with IEEE-488 interface card. There are several alternatives to choose the program from the software, we have chosen program that written in LabWiev 6.0i. The program was written in C language in our laboratory. It controls the instruments automatically and reads the resistance and temperature, controls temperature values of the set samples. The data were used to draw graphics (R (ohm) vs. Temp. (K)). The program also controls the Lakeshore model 331 Temperature Controller, Model 580 Micro-ohmmeter automatically at the same time.

2.2.2 Device for Solid-Gas Reactions

A horizontal tubular furnace with a silica tube of 4 cm diameter and 60 cm length, which was designed in our laboratory was used as a reaction chamber.

A vertical tube filled with activated charcoal and inserted vertically in the furnace was used as a reduction chamber.

The temperature control was made with Cr-Ni thermocouple using thermometer type of heat control system.

Polyethylene tubes with glass connections and glass valves were used in the system. In order to prevent gas leakage, silicone type of adhesive material was employed at the connections of the system. The residual gases were discarded outside through the tube from the window.

A gas mask was used for safety purposes, because sulfur dioxide and reduced gases are dangerous for human health.

The flow sheet of the system is given in Figure 2.2.2.1.

2.3. Procedures

2.3.1. Preparation of Sulfide Compounds

Each reactant was sulfidized in order to observe the type of sulfides formed in our experiments. The following compounds were sulfidized using the device described in section 2.2.2.

TiO_2, Cr_2O_3, MnO_2, Fe_2O_3, Co_3O_4, NiO, CuO, ZnO.

The reactant raw materials were weighed in porcelain boats, and put into the reaction chamber. Before starting the flow of sulfidizing gas mixture, nitrogen gas was passed through the system to remove the oxygen present. The furnace was heated under the nitrogen atmosphere until the desired temperature was reached. Sulfidizing gas mixture was allowed to pass from system, with a flow rate of 60ml/min and introduced into the reaction chamber, heated at different temperatures between 450-1350 °C. The furnace was allowed to cool in nitrogen atmosphere. The amount of the reactant kept constant. The samples were weighed for stoichiometric calculations for the end products. The products were examined by X-Ray Powder Diffraction (XRD) and Raman Scattering Spectra.

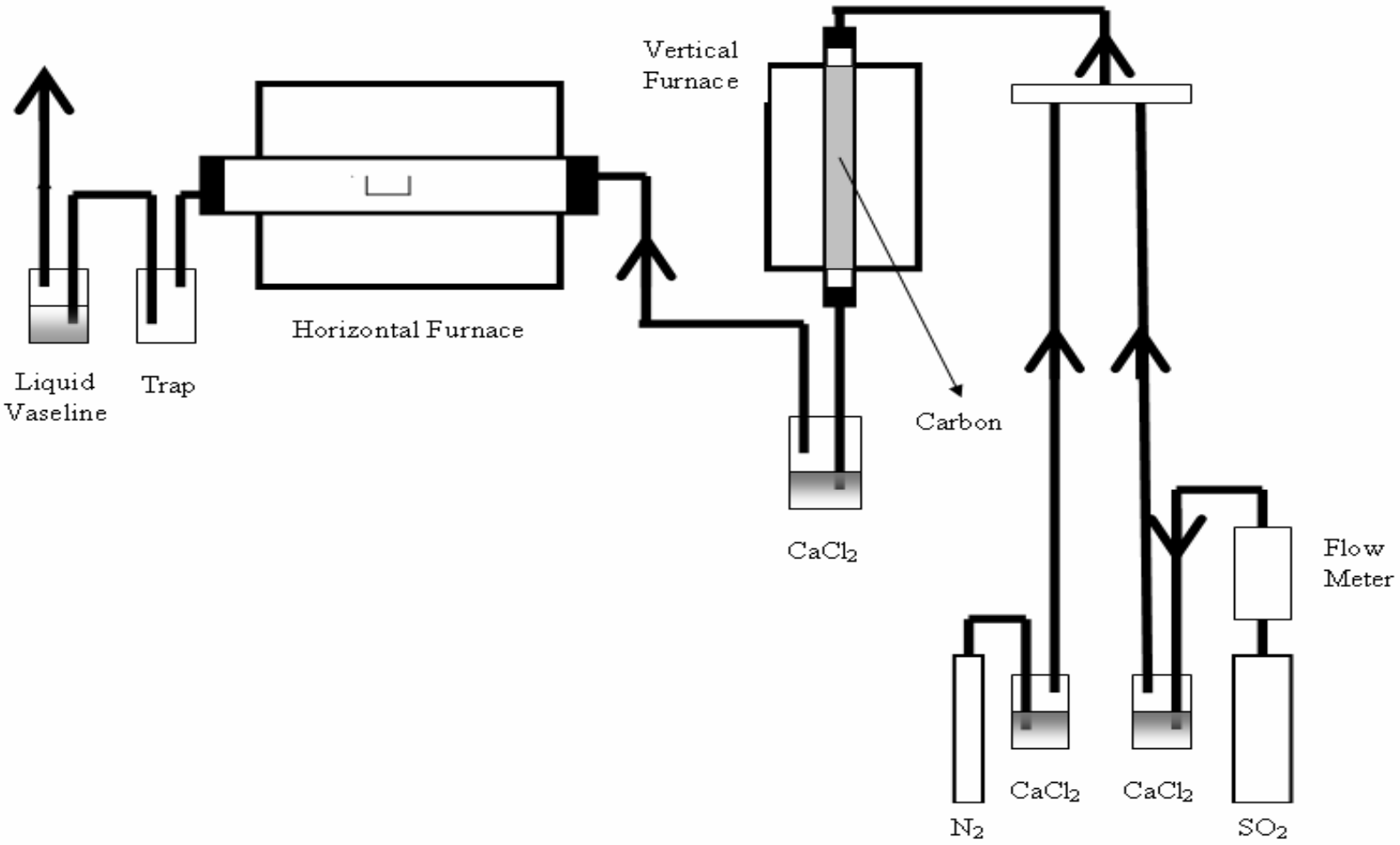

Figure 2.2.2.1: Flow Sheet of the Solid-Gas System

CHAPTER 3

RESULTS AND DISCUSSION

3.1. Preparation of Sulfide Compounds

Each reactant was heated in a sulfidizing gas mixture according to the process described in section 2.3.1. The following experiments were performed by heating metal oxides at various temperatures in the presence of SO_2 for three hours. After each experiment the products were checked by X-ray powder diffraction in order to control the sulfide formation. X-ray powder diffraction data of the product was recorded and compared with the JCPDS data. The JCPDS card numbers were given in round brackets.

In this work some transition metal sulfides were synthesized by using our new method which was not reported before in the literature. The calculated and observed weight gains are in good agreement.

3.1.1. Sulfidizing of TiO_2

The reactant in this synthesis was Anatase, TiO_2 (JCPDS Card No: 21-1272). The reactant is in tetragonal system with cell parameters a = b = 3.785 Å and c = 9.514 Å.) Reactions were done at 450 ^{O}C, 850 ^{O}C and 1250 ^{O}C. The X-ray powder diffraction patterns, Raman scattering spectra of the products and reactants and the data which was obtained from these analysis techniques were given in APPENDIX A. The changes in the XRD pattern with temperature can be seen in Figure 3.1.1.1.

The data which were obtained from XRD pattern of the products indicate that our new sulfidizing system converted successfully the TiO_2 to Ti_3S_5 by using

SO_2 and carbon, at 850 ^{O}C and 1250 ^{O}C temperatures. Table 3.1.1.1 shows the studied temperature and obtained corresponding products. The star, which was in the boxes, used to label the compound that has maximum intensity in XRD pattern.

Table 3.1.1.1: Summary of the result from the sulfidizing reaction of Titanium.

Temperature	Reactant	Products
450 ^{O}C	TiO_2 Anatase	★ TiO_2 Anatase + TiO_2 Rutile
850 ^{O}C	TiO_2 Anatase	TiO_2 (Anatase) + ★TiO_2 (Rutile) + Ti_3S_5
1250 ^{O}C	TiO_2 Anatase	★TiO_2 Rutile + Ti_3S_5

Rutile TiO_2 (JCPDS Card No: 76-1938) which was obtained from sulfidizing reaction at all studied temperature as by product, is in tetragonal system with cell parameters a = b = 4.593 Å and c = 2.959 Å.

The obtained Ti_3S_5 (JCPDS Card no: 27-908) is in hexagonal system with the cell parameters a = b = 3.422 Å and c = 11.457 Å.

Titanium sulfide has layered structure which consists of sulfur and titanium layers. The sequence is like this: S-S-Ti-S-S-Ti-S-S-Ti-… Additional titanium atoms equally distributed in between S layers. This phenomenon is called intercalation.[70].

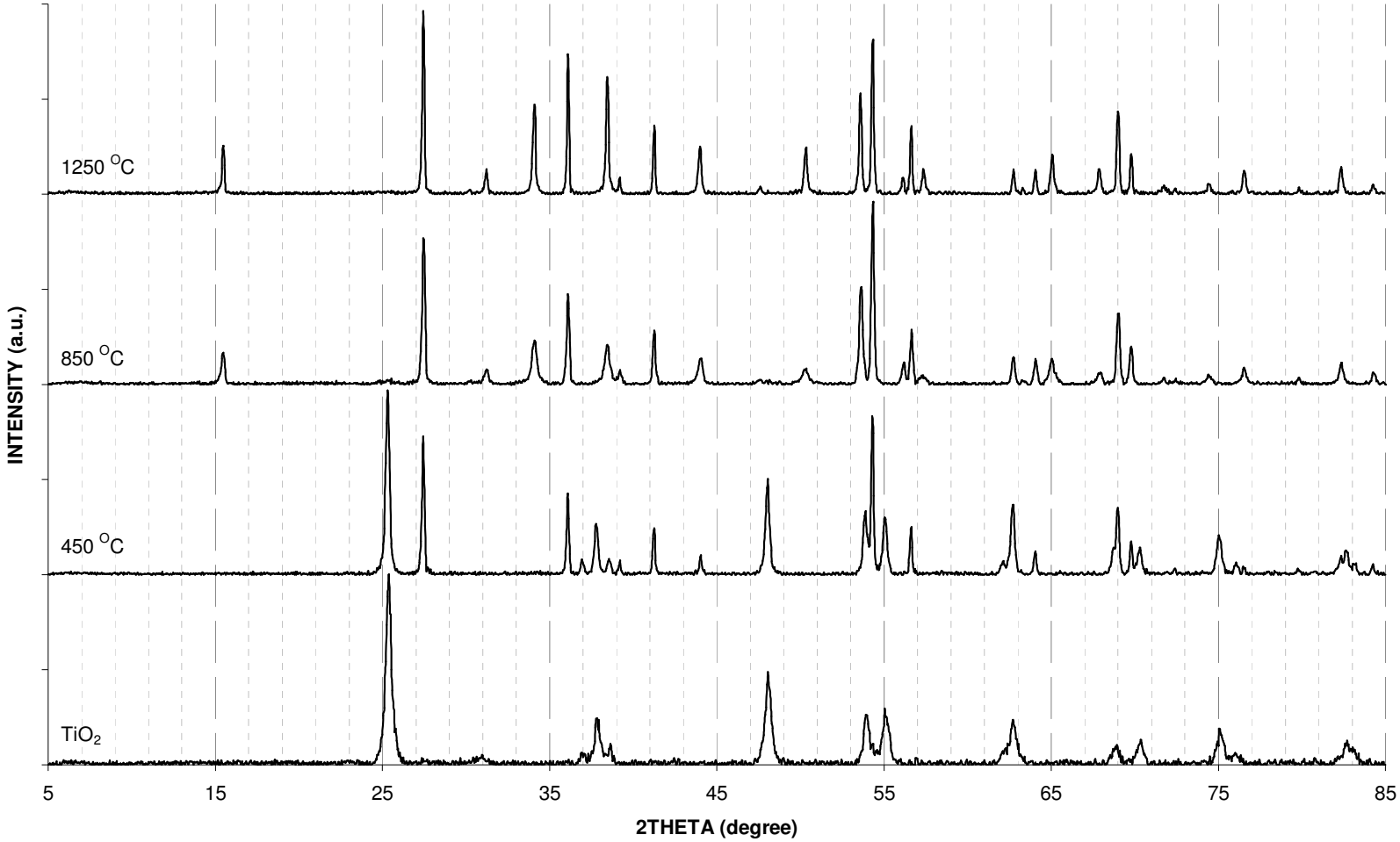

Figure 3.1.1.1: X-Ray Powder Diffraction Patterns of Reactant and Products that used in the Sulfidizing Reaction of TiO_2

In conclusion, our new sulfidizing system achieves to convert TiO_2 to Ti_3S_5 by using SO_2 gas and carbon at 850 ^{O}C and 1250 ^{O}C. To convert all of the reactants to Ti_3S_5 the sulfidizing reaction need more time at 850 ^{O}C and 1250 ^{O}C. The remained reactant changed its structure and was converted into another polymorph of TiO_2, rutile TiO_2.

In the literature there is only one reported method about the production of Ti_3S_5 which was called vapor transfer method.[71]

In Raman scattering spectra, there are four peaks at 610 cm^{-1},440 cm^{-1}, 261 cm^{-1} and 150 cm^{-1} this peaks are belongs to Rutile, TiO_2.

3.1.2. Sulfidizing of Cr_2O_3

The reactant in this synthesis was Eskolaite, Cr_2O_3 (JCPDS Card no: 84-1616). The reactant is in hexagonal system with the cell parameters a = b = 4.952 Å and c = 13.599 Å. The X-ray powder diffraction patterns, Raman scattering spectra of the products and reactants and the data which was obtained from these analysis techniques were given in APPENDIX B. The changes in the XRD pattern with temperature can be seen in Figure 3.1.2.1.

The data which were obtained from XRD pattern of the products indicate that our new sulfidizing system convert successfully the Cr_2O_3 into Cr_2S_3 by using SO_2 and carbon at studied temperatures. Table 3.1.2.1 shows the studied temperature and obtained corresponding products. The star, which was in the boxes, used to label the compound that has maximum intensity in XRD pattern.

Table 3.1.2.1: Summary of the result from the sulfidizing reaction of Chromium

Temperature	Reactant	Products
650 ^{O}C	Cr_2O_3	Cr_2O_3 + ★ Cr_2S_3 (10-340)
850 ^{O}C	Cr_2O_3	Cr_2O_3 + ★ Cr_2S_3 (10-340)
1250 ^{O}C	Cr_2O_3	Cr_2O_3 + Cr_2S_3 (10-340) + Cr_2S_3 (11-007)

XRD pattern examination proved that the obtained Cr_2S_3 has two polymorphic structures: Both of them are in hexagonal and Ni-As type with very close a and b cell parameters with different c cell parameters. These are Cr_2S_3 (JCPDS Card no: 10-340, a = b = 5.939 Å and c = 16.650 Å) and Cr_2S_3 (JCPDS Card no: 11-007 a = b = 5.942 Å and c = 11.188 Å). The obtained chromium sulfides were same in the crystal system with different c values on the other hand close a and b parameters.

In conclusion, our new sulfidizing system achieves to convert Cr_2O_3 to Cr_2S_3 by using SO_2 gas and carbon at studied temperatures. The small number of very weak peaks in the XRD pattern belonging to the reactant indicate that the duration of the sulfidizing reaction was not sufficient to convert all of the reactant to sulfide compound at studied temperature.

Raman scattering spectra of the chromium oxide and sulfides have highly intense background. This gives a hint to us that the samples have photoluminescence character.[72]

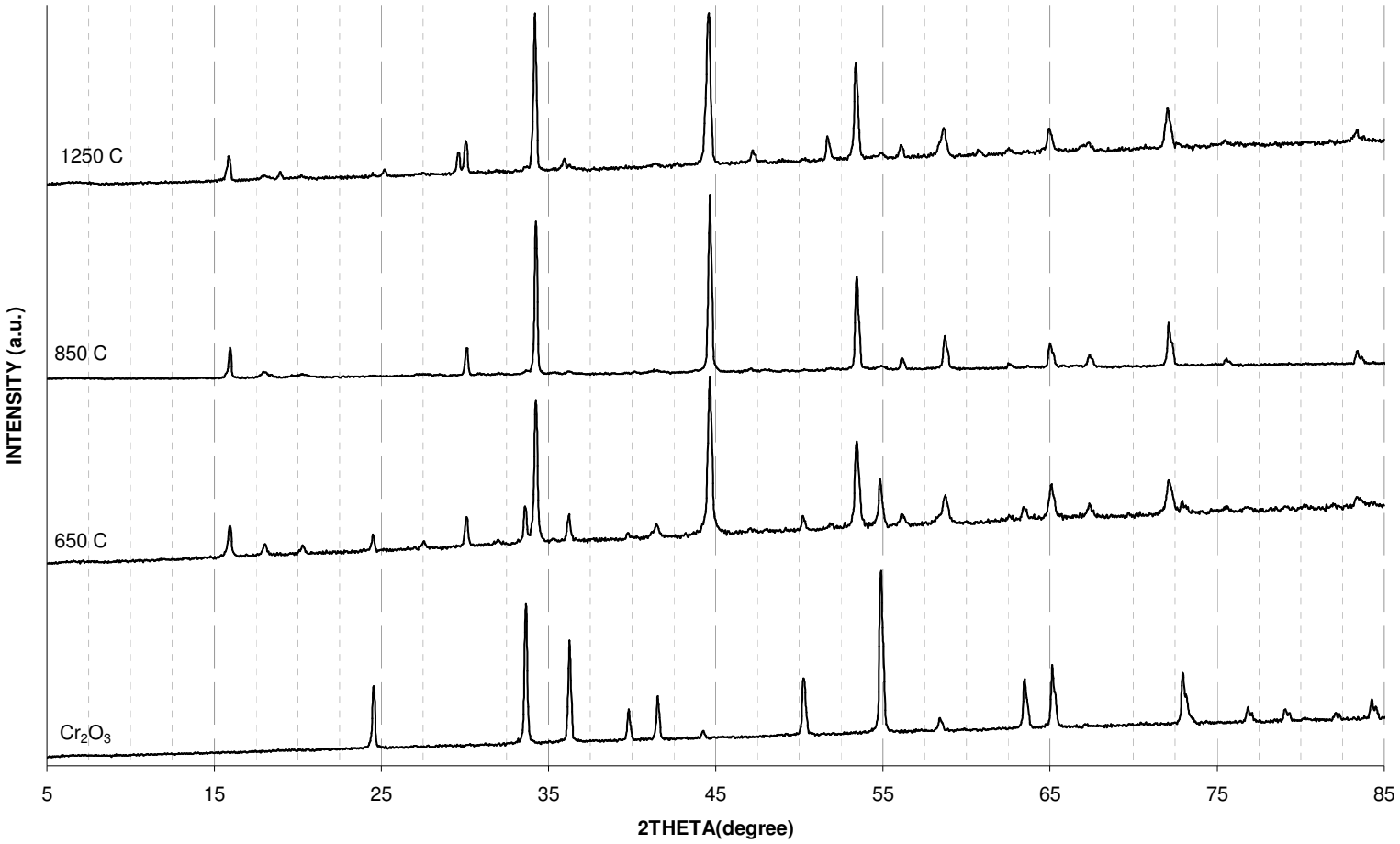

Figure 3.1.2.1: X-Ray Powder Diffraction Patterns of Reactant and Products that used in the Sulfidizing Reaction of Cr_2O_3

3.1.3. Sulfidizing of MnO_2

The reactant in this synthesis was Pyrolusite, MnO_2 (JCPDS Card no: 72-1982) in tetragonal system with cell parameters a = b = 4.388 Å, c = 2,865 Å.[73] Reactions were done at 550 ^{O}C, 650 ^{O}C, 850 ^{O}C, 950 ^{O}C and 1150 ^{O}C. The X-ray powder diffraction patterns, Raman scattering spectra of the products and reactants and the data which was obtained from these analysis techniques were given in APPENDIX C. The changes in the XRD pattern with temperature can be seen in Figure 3.1.3.1.

The data which were obtained from XRD pattern of the products indicate that our new sulfidizing system converted successfully the MnO_2 to alabandite MnS by using SO_2 and carbon, at studied temperatures. Table 3.1.3.1 shows the studied temperature and obtained corresponding products. The star, which was in the boxes, used to label the compound that has maximum intensity in XRD pattern. Unfortunately, none of the product has monophase sulfide compound, MnO as by product and unknown product peaks were also observed at all studied temperatures.

Table 3.1.3.1: Summary of the result from the sulfidizing reaction of Manganese.

Temperature	Reactant	Products
550 ^{O}C	MnO_2	★ Alabandite MnS + Mangonosite MnO
650 ^{O}C	MnO_2	★ Alabandite MnS + Mangonosite MnO
850 ^{O}C	MnO_2	★ Alabandite MnS + Mangonosite MnO
950 ^{O}C	MnO_2	★ Alabandite MnS + Mangonosite MnO
1150 ^{O}C	MnO_2	★ Alabandite MnS + Unknown

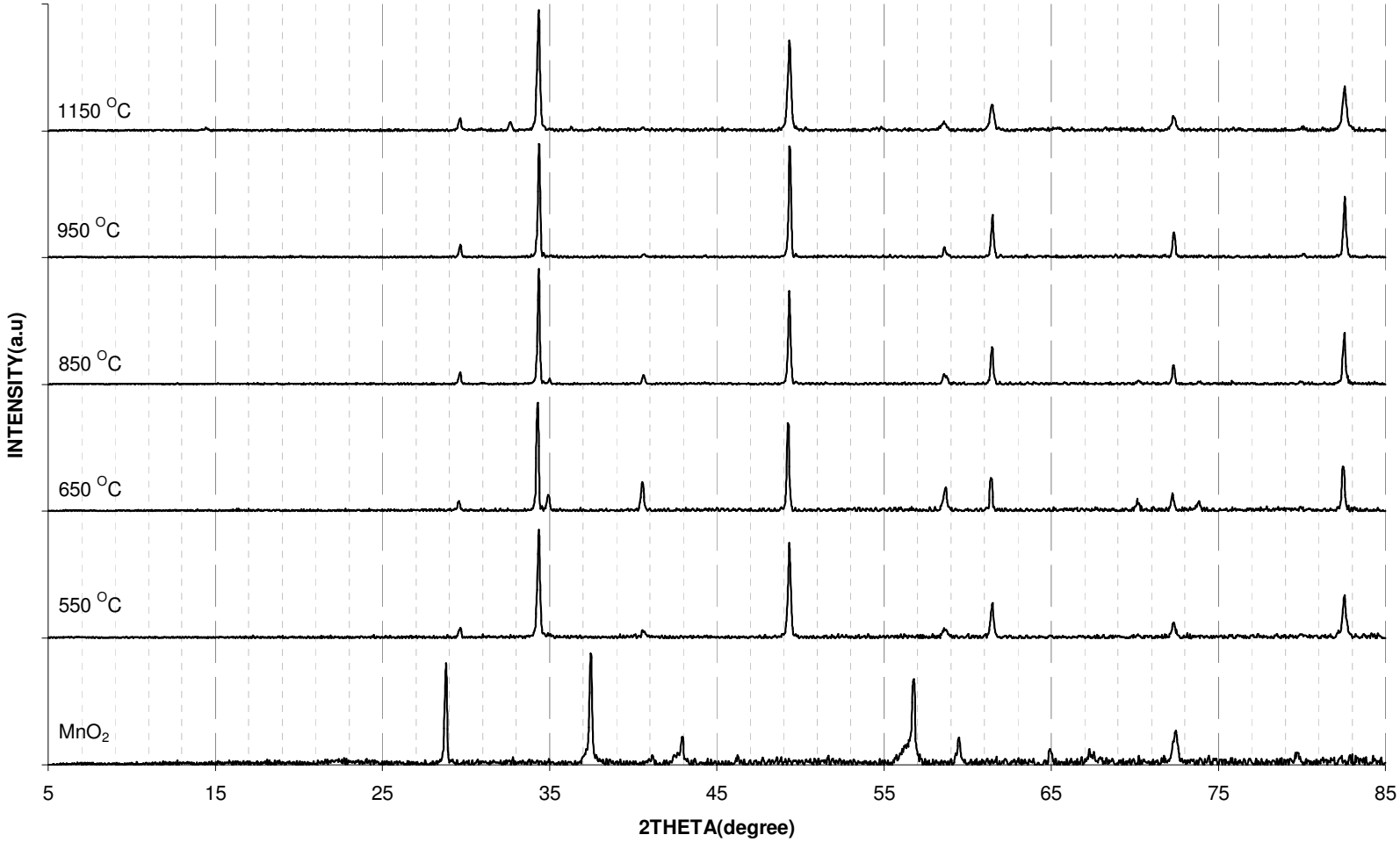

Figure 3.1.3.1: X-Ray Powder Diffraction Patterns of Reactant and Products that used in the Sulfidizing Reaction of MnO_2

Mangonosite MnO (JCPDS Card no: 7-230) is in cubic system with the cell parameters a = b = c = 4.445 Å. At 535 ^{O}C the MnO_2 started to decompose, reduced from 4+ oxidation state to 2+ oxidation state so the unreacted MnO_2 turned into MnO. [74]

Alabandite, MnS (JCPDS Card no: 06-518) is in NaCl structure and in cubic system with cell parameters a = b = c = 5.224 Å.

In conclusion, our new sulfidizing system achieves to convert MnO_2 to MnS by using SO_2 gas and carbon at studied temperatures. The duration of the sulfidizing reaction was not sufficient to convert all of the reactant at studied temperature except 1150 ^{O}C. The remained reactant decomposes and converted into MnO. There were not any MnO peak in XRD pattern of the product which was obtained at 1150 ^{O}C but there were four peaks which were belong to unidentified compound.

In Raman scattering spectra of Mn derivatives there were four main peaks at 650 cm^{-1}, 355 cm^{-1}, 305 cm^{-1}, 280 cm^{-1}.

3.1.4. Sulfidizing of Fe_2O_3

The reactant in this synthesis was Hematite, Fe_2O_3 (JCPDS Card no: 33-664). The reactant is in hexagonal system with the cell parameters a = b = 5.036 Å and c = 13.749 Å. Reactions were done at 450 ^{O}C, 650 ^{O}C, and 850 ^{O}C. The X-ray powder diffraction patterns, Raman scattering spectra of the products and reactants and the data which was obtained from these analysis techniques were given in APPENDIX D. The changes in the XRD pattern with temperature can be seen in Figure 3.1.4.1.

The obtained XRD data indicate that our sufidizing system converted Fe_2O_3 into iron sulfide successfully by using SO_2 and carbon at studied

temperatures. Table 3.1.4.1 shows the studied temperatures and obtained corresponding products. The star, which was in the boxes, used to label the compound that has maximum intensity in XRD pattern.

Table 3.1.4.1: Summary of the results from the sulfidizing reaction of Iron.

Temperature	Reactant	Products
450 ^{O}C	Fe_2O_3	★ Fe_2O_3 + FeS
650 ^{O}C	Fe_2O_3	$Fe_{1-X}S$ (Pyrrhotite-4H)
850 ^{O}C	Fe_2O_3	Fe_7S_8 (Pyrrhotite-3T)

450 ^{O}C temperature was not enough convert all of the reactant to FeS, the peaks of remaining Fe_2O_3 were observed in powder XRD pattern. The obtained FeS (JCPDS Card no: 42-1340) was in cubic system with cell parameters a = b = c = 5.418 Å.

650 ^{O}C temperature and three hours heating was enough to transform all Fe_2O_3 to pyrrhotite-4H $Fe_{1-X}S$ (JCPDS Card no: 22-1120) in hexagonal system with the cell parameters a = b = 6.880 Å and c = 22.900 Å.

Increasing temperature to 850 ^{O}C for heating three hours caused to phase transition in crystal structure to new form of iron sulfide: Pyrrhotite-3T Fe_7S_8 (JCPDS Card no:76-2308) in hexagonal system with the cell parameters a = b = 6.866 Å and c = 17.088 Å.

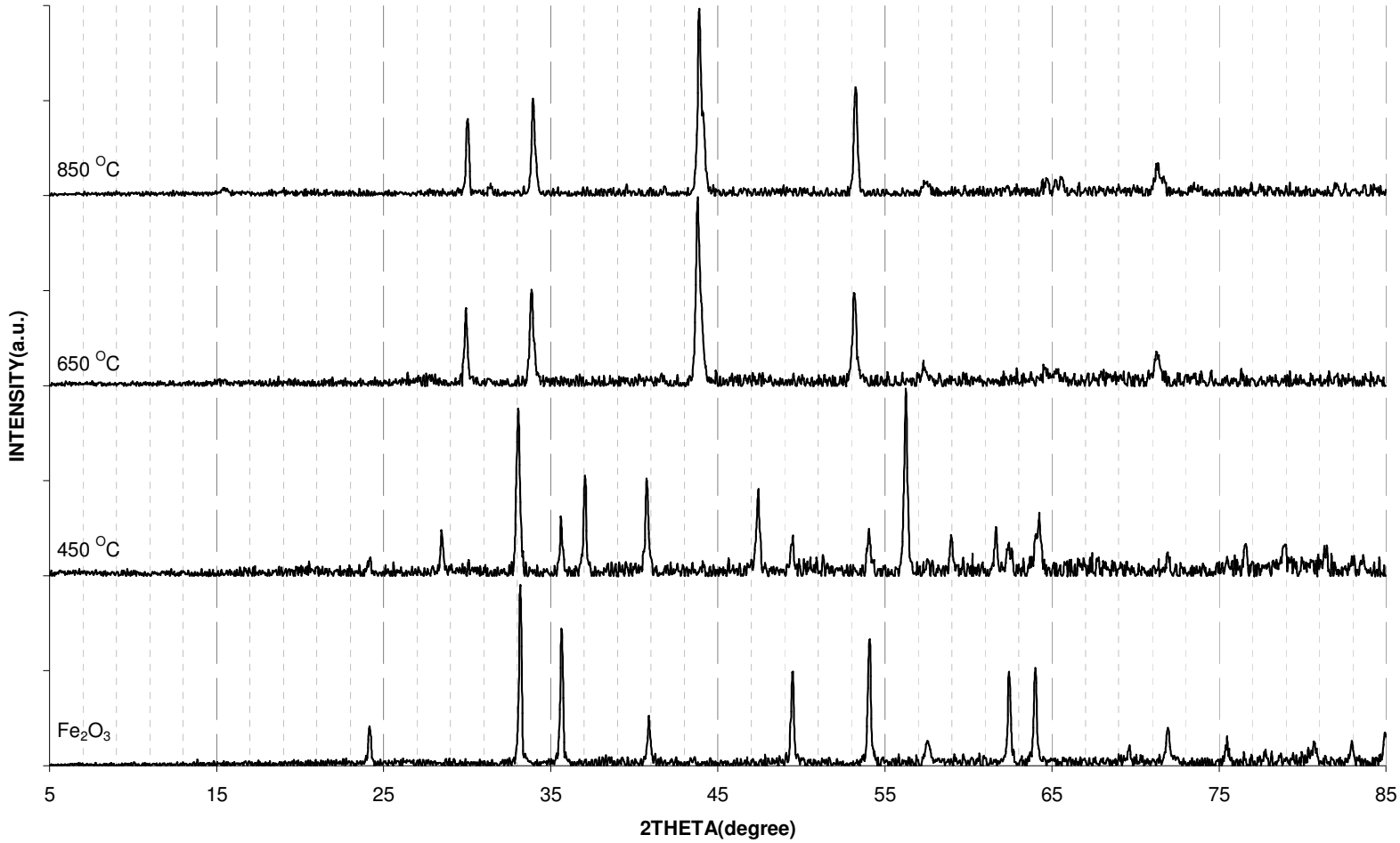

Figure 3.1.4.1: X-Ray Powder Diffraction Patterns of Reactant and Products in the Sulfidizing Reaction of Fe_2O_3

In conclusion, our new sulfidizing system achieves to convert iron oxide to iron sulfide by using SO_2 gas and carbon at studied temperatures. The reactant peaks which appear in XRD pattern of the product that was obtained at 450 ^{O}C, shows that the duration of the sulfidizing reaction was not sufficient to convert all of the reactant at 450 ^{O}C. At 650 ^{O}C and 850 ^{O}C the products were pyrrhotite.

There are several peaks in Raman scattering spectra; 650 cm^{-1}, 610 cm^{-1}, 390 cm^{-1}, 350 cm^{-1}, 280 cm^{-1}, 210 cm^{-1}. These peaks slightly changed their positions in each sample.

3.1.5. Sulfidizing of Co_3O_4

The reactant in this synthesis was Co_3O_4 (JCPDS Card No: 76-1802). The reactant is in cubic system with the cell parameters a = b = c = 8.072 Å. Reactions were done at 550 ^{O}C, 650 ^{O}C, 850 ^{O}C, 950 ^{O}C and 1150 ^{O}C. The X-ray powder diffraction patterns, Raman scattering spectra of the products and reactants and the data which was obtained from these analysis techniques were given in APPENDIX E. The changes in the XRD pattern with temperature can be seen in Figure 3.1.5.1.

The XRD pattern of the products indicates that our new sulfidizing system converted Co_3O_4 to cobalt sulfide successfully at studied temperatures by using SO_2 and carbon. Table 3.1.5.1 shows the studied temperature and obtained corresponding products. The star, which was in the boxes, used to label the compound that has maximum intensity in XRD pattern.

Table 3.1.5.1: Summary of the result from the sulfidizing reaction of Cobalt.

Temperatures	Reactant	Products
550 ^{O}C	Co_3O_4	Jaipurite, CoS
650 ^{O}C	Co_3O_4	Jaipurite, CoS
850 ^{O}C	Co_3O_4	Jaipurite, CoS
950 ^{O}C	Co_3O_4	★ (Cobaltpentlandite) Co_9S_8 + Jaipurite, CoS
1150 ^{O}C	Co_3O_4	★ (Cobaltpentlandite) Co_9S_8 + Unknown

The product at 550 ^{O}C, 650 ^{O}C and 850 ^{O}C was CoS which was a mineral and called as Jaipurite, CoS (JCPDS Card no: 75-605) in hexagonal system with the cell parameters a = b = 3.377 Å, c = 11.457 Å.

Experiments at 950 ^{O}C produced another mineral as Cobaltpentlandite, Co_9S_8 (JCPDS Card no: 86-2273) in cubic system with the cell parameters a = b = c = 9,923 Å.

In conclusion, our new sulfidizing system achieves to convert Co_3O_4 to Cobalt sulfide by using SO_2 gas and carbon at studied temperatures. The product which was obtained at 950 ^{O}C was mixture of to cobalt sulfide jaipurite and cobaltpentlandite. There were three unidentified peaks together with the peaks belonging to cobaltpentlandite in the XRD pattern of the product that obtained at 1150 ^{O}C.

In Raman scattering spectra of the product five peaks were observed at 670 cm^{-1}, 610 cm^{-1}, 505 cm^{-1}, 490 cm^{-1}, 190 cm^{-1}.

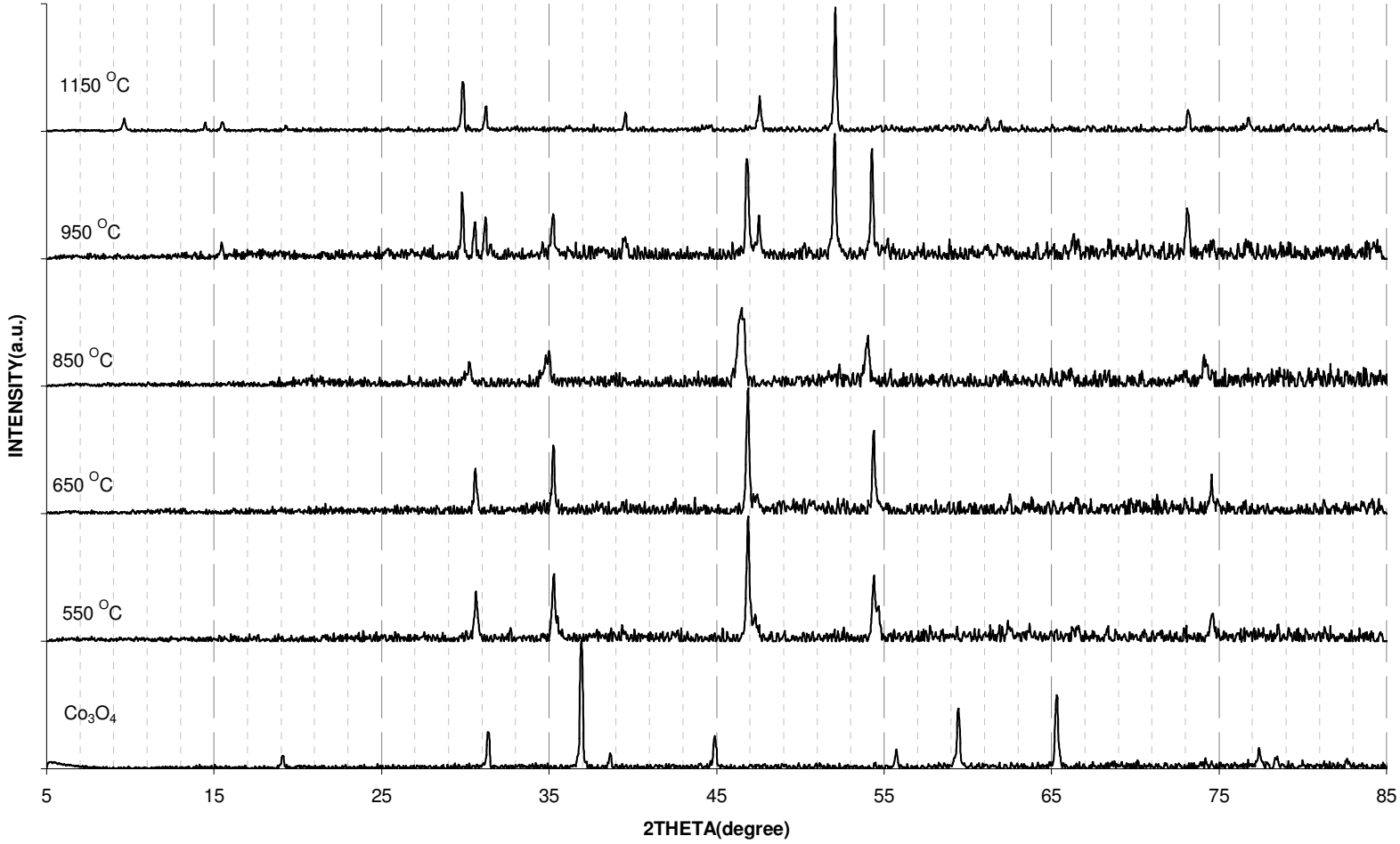

Figure 3.1.5.1: X-Ray Powder Diffraction Patterns of Reactant and Products in the Sulfidizing Reaction of Co_3O_4

3.1.6. Sulfidizing of NiO

The reactant in this synthesis was NiO (JCPDS Card No: 73-1523) in cubic system with the cell parameters a = b = c = 4,180 Å. Reactions were done at 450 ^{O}C and 650 ^{O}C. The X-ray powder diffraction patterns, Raman scattering spectra of the products and reactants and the data which was obtained from these analysis techniques were given in APPENDIX F. The changes in the XRD pattern with temperature can be seen in Figure 3.1.6.1.

The obtained data from the XRD of the sulfidizing reaction products indicate that our new sulfidizing system converted NiO into NiS successfully by using SO_2 and carbon at studied temperature. Table 3.1.1.1 shows the studied temperature and obtained corresponding products. The star, which was in the boxes, used to label the compound that has maximum intensity in XRD pattern.

Table 3.1.6.1: Summary of the result from the sulfidizing reaction of Nickel

Temperatures	Reactant	Products
450 ^{O}C	NiO	NiS
650 ^{O}C	NiO	★ NiS + Unknown

The product was NiS (JCPDS Card No: 77-1624) in hexagonal system with cell parameters a = b = 3.439 Å and c = 5,324 Å.

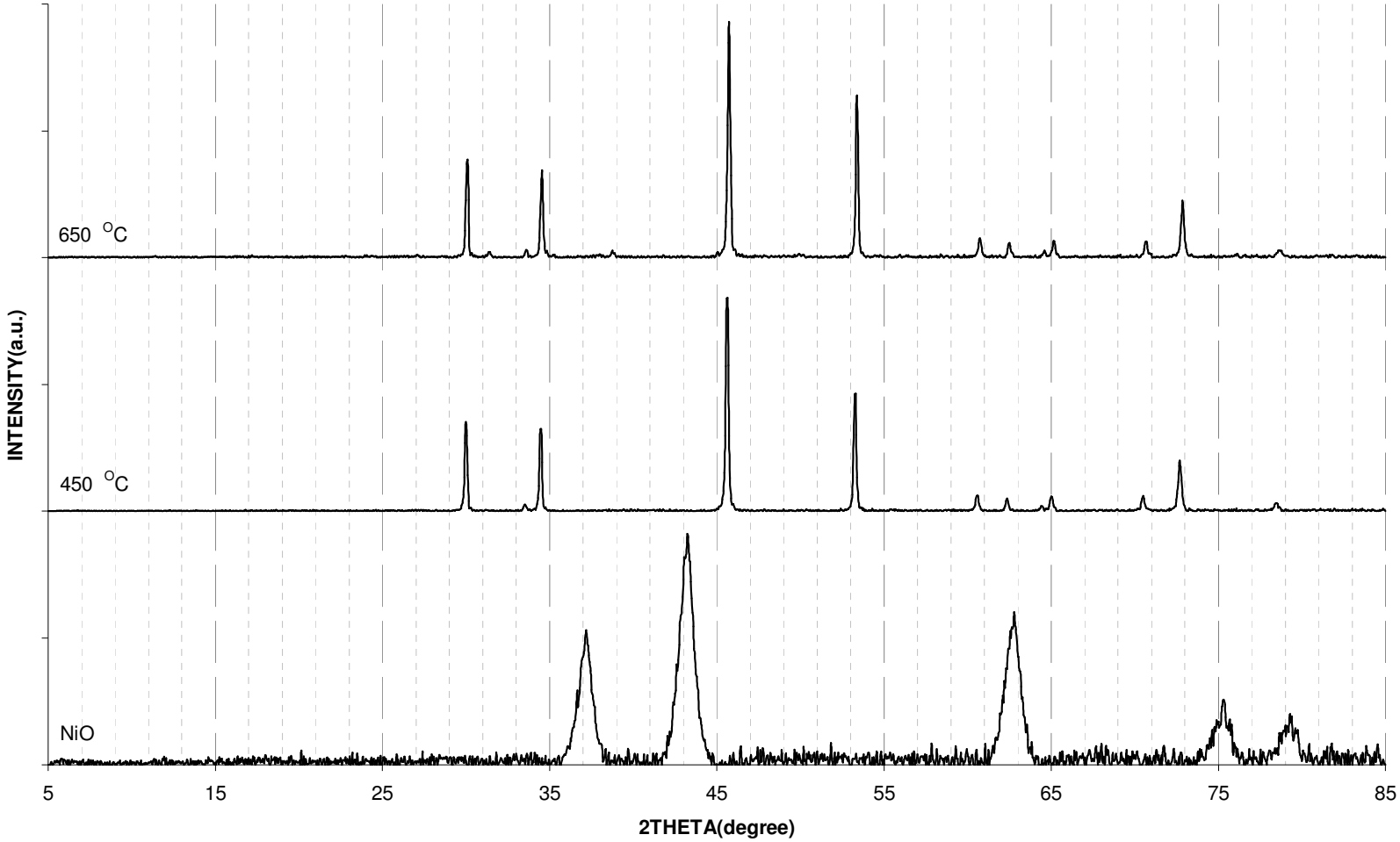

Figure 3.1.6.1: X-Ray Powder Diffraction Patterns of Reactant and Products in the Sulfidizing Reaction of NiO

In conclusion, our new sulfidizing system achieves to convert NiO to NiS by using SO_2 gas and carbon at studied temperatures. NiS melts at above 735 ^{O}C, so the experiments were done at 450 ^{O}C and 650 ^{O}C. There were four unknown peaks in the XRD pattern of the product that obtained 650 ^{O}C.

Raman scattering spectra of the nickel oxide and sulfides were not helpful for characterization due to highly intense background. This problem is common for the samples having photoluminescence character.[72]

3.1.7. Sulfidizing of CuO

The reactant in this synthesis was Tenorite, CuO (JCPDS Card No: 72-629). The reactant is in monoclinic system with cell parameters a = 4.684 Å, b = 3.423 Å, c = 5.129 Å and $\alpha = \gamma = 90^{O}$, $\beta = 99.540^{O}$. Reactions were done at 650 ^{O}C, 850 ^{O}C and 1150 ^{O}C. The X-ray powder diffraction patterns, Raman scattering spectra of the products and reactants and the data which was obtained from these analysis techniques were given in APPENDIX G. The changes in the XRD pattern with temperature can be seen in Figure 3.1.7.1.

The data which were obtained from XRD pattern of the products indicate that our new sulfidizing system converted successfully the CuO into cupper sulfide by using SO_2 and carbon, at 650 ^{O}C 850 ^{O}C and 1150 ^{O}C temperatures. Table 3.1.7.1 shows the studied temperatures and obtained corresponding products. The star, which was in the boxes, used to label the compound that has maximum intensity in XRD pattern.

Table 3.1.7.1: Summary of the results from the sulfidizing reaction of Cupper.

Temperatures	Reactant	Products
650 ^{O}C	CuO	$Cu_{1.6}S + Cu_{1.81}S + Cu_{7.2}S_4$
850 ^{O}C	CuO	$Cu_{1.6}S + Cu_7S_4 + Cu_9S_5$
1150 ^{O}C	CuO	$Cu_{1.6}S + Cu_{1.81}S + Cu_{7.2}S_4 + Cu_8S_5$

The products were mixture of Chalcocite-Q, $Cu_{1.6}S$ (JCPDS Card No: 29-578) in tetragonal system with the cell parameters a = b = 3.996 Å and c = 11.278 Å, $Cu_{7.2}S_4$ (JCPDS Card No: 24-61) in cubic system with the cell parameters a = b = c = 5.570 Å, $Cu_{1.81}S$ (JCPDS Card no: 41-959) in tetragonal system with the cell parameters a = b = 7.558 Å and c = 18.340 Å, Anilite, Cu_7S_4 (JCPDS Card no: 33-489) in orthorhombic system with the cell parameters a = 7.906 Å, b = 7.822 Å, c = 11.078 Å, Digenite, Cu_9S_5 (JCPDS Card no: 47-1748) in hexagonal system with the cell parameters a = b = 3.930 Å, c = 48.140 Å and Geerite, Cu_8S_5 (JCPDS Card no: 33-491) in hexagonal system with the cell parameters a = b = 3.863 Å and c = 46.100 Å

The various mixtures of many cupper sulfide compounds were observed in the literature. The crystal structure of the compounds determined by the arrangements of the sulfide ion. The crystal structure is hexagonal closed packing or cubic closed packing of sulfide ions. The cupper ions are in the interstitial space of the crystal structure [75]

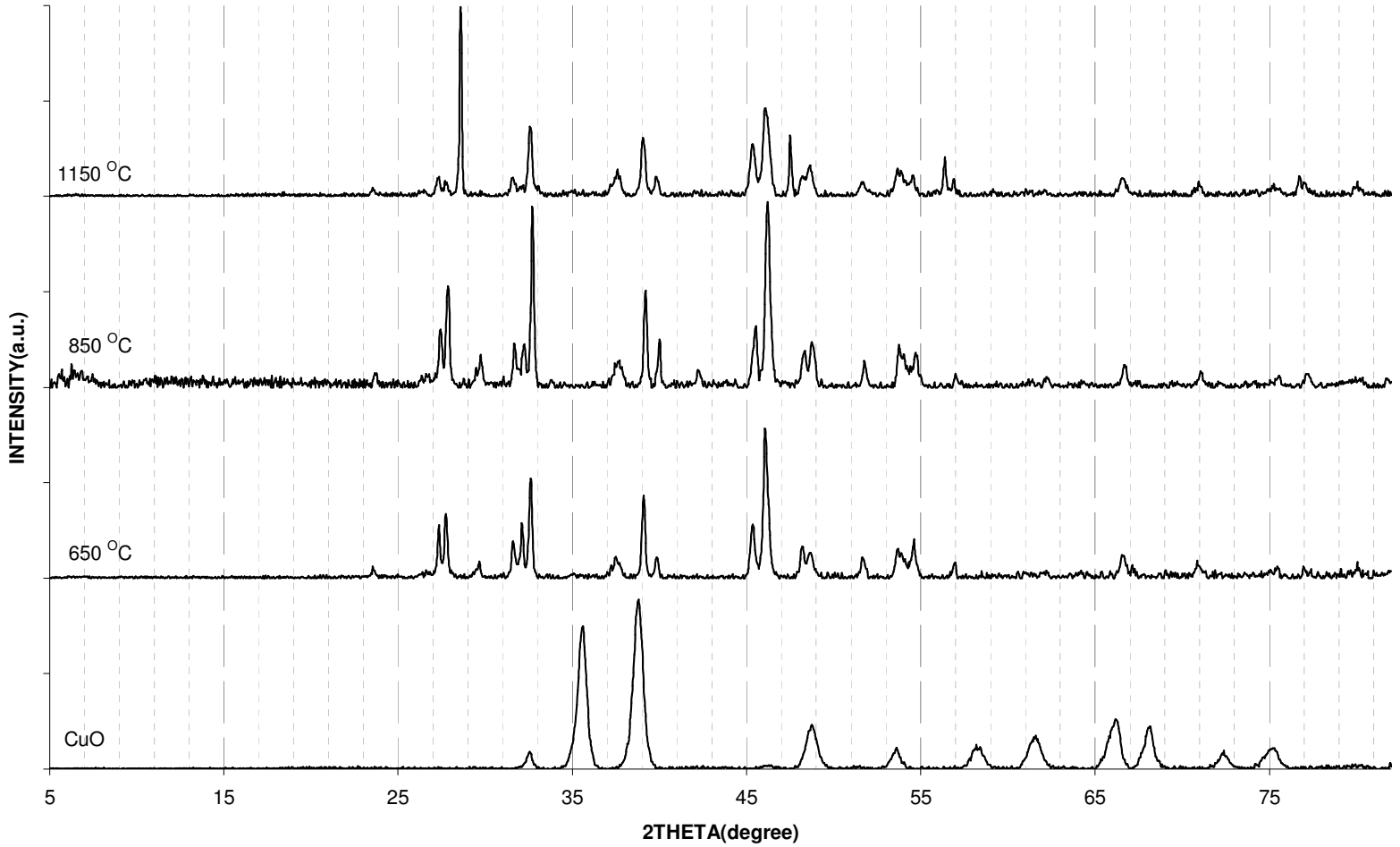

Figure 3.1.7.1: X-Ray Powder Diffraction Patterns of Reactant and Products in the Sulfidizing Reaction of CuO

In conclusion, our new sulfidizing system achieves to convert CuO into cupper sulfide by using SO_2 gas and carbon at 650 ^{O}C, 850 ^{O}C and 1250 ^{O}C. On the other hand the products were not pure single phase; they were mixture of different polymorph of cupper sulfide. All these compounds were in $Cu_{2-x}S$ formula, where $0.19<x<0.4$. This was common in cupper sulfide synthesis.

Raman scattering spectra of the cupper oxide and sulfides were not helpful for characterization due to highly intense background. This problem is common for the samples having photoluminescence character.[72]

3.1.8. Sulfidizing of ZnO

The reactant in this synthesis was ZnO (JCPDS Card No: 75-576).[76] The reactant is in hexagonal system with the cell parameters a = b = 3.243 Å and c = 5.195 Å. Reactions were done at 450 ^{O}C, 550 ^{O}C, 650 ^{O}C, 850 ^{O}C, 950 ^{O}C and 1150 ^{O}C. The X-ray powder diffraction patterns, Raman scattering spectra of the products and reactants and the data which was obtained from these analysis techniques were given in APPENDIX H. The changes in the XRD pattern with temperature can be seen in Figure 3.1.8.1.

The data which were obtained from XRD pattern of the products indicate that our new sulfidizing system convert successfully the ZnO to ZnS by using SO_2 and carbon, at studied temperatures. Table 3.1.8.1 shows the studied temperatures and obtained corresponding products. The star, which was in the boxes, used to label the compound that has maximum intensity in XRD pattern.

Table 3.1.8.1: Summary of the result from the sulfidizing reaction of Zinc.

Temperatures	Reactant	Products
450 ^{O}C	ZnO	★ ZnO + ZnS Wurtzite-2H + ZnS Sphalerite
550 ^{O}C	ZnO	ZnO + ZnS Wurtzite-2H + ZnS Sphalerite
650 ^{O}C	ZnO	ZnS Wurtzite-2H + ZnS Sphalerite
850 ^{O}C	ZnO	ZnS Wurtzite-2H + ZnS Sphalerite
950 ^{O}C	ZnO	ZnS Wurtzite-2H + ZnS Sphalerite
1150 ^{O}C	ZnO	ZnS Wurtzite-2H + ZnS Sphalerite

One of the product was Sphalerite, ZnS (JCPDS Card no: 05-566) in cubic system with the cell parameters a = b = c = 5.406 Å.[77]

Wurtzite-2H, ZnS (JCPDS Card No: 36-1450) in hexagonal system was observed as another polymorph of the product with the cell parameters a = b = 3.821 Å and c = 6.257 Å.

In conclusion, our new sulfidizing system achieves to convert ZnO to ZnS by using SO_2 gas and carbon at studied temperatures. The ZnO peaks in the XRD pattern of the products that were obtained at 450 ^{O}C and 550 ^{O}C indicate that the duration of the sulfidizing reaction was not sufficient to convert all of the reactant at 450 ^{O}C and 550 ^{O}C.

In Raman scattering spectra of the Zn derivatives peaks were observed at 668 cm^{-1}, 637 cm^{-1}, 613 cm^{-1}, 450 cm^{-1}, 419 cm^{-1}, 396 cm^{-1}, 348 cm^{-1}, 331 cm^{-1}, 298 cm^{-1}, 272 cm^{-1}, 216 cm^{-1} and 177 cm^{-1}. These values are in agreement with the data in the literature.[78]

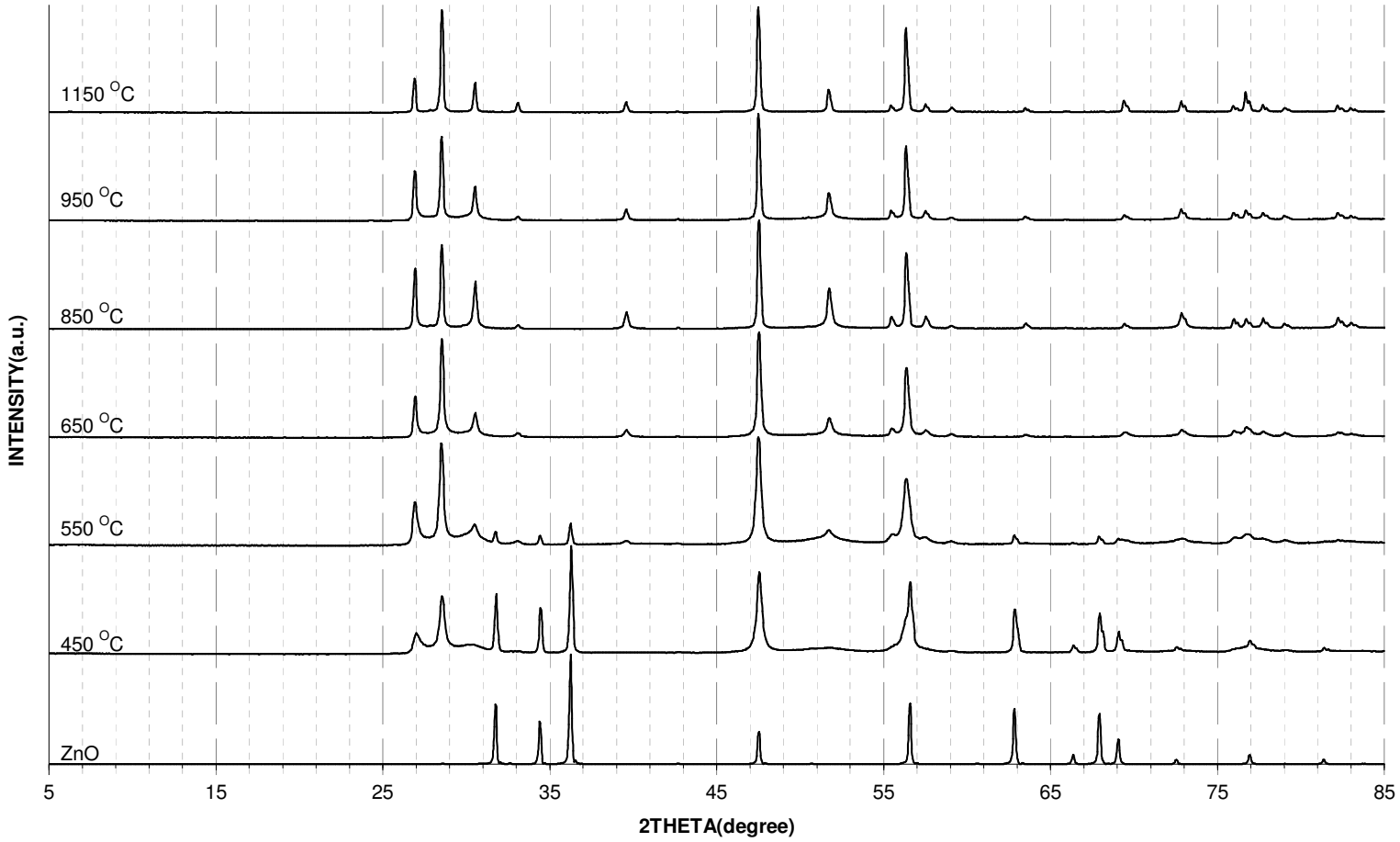

Figure 3.1.8.1: X-Ray Powder Diffraction Patterns of Reactant and Products in the Sulfidizing Reaction of ZnO

3.2. Conductivity Measurements

The conductivity of some products was examined by our conductivity measuring system which was described in detail in section 2.2.1. In figures, normalized resistance values, R/R_0, where R_0 is the resistance measured at 300 K, are given. Absolute resistivity depends on the sample size (length and cross section) which was difficult to adjust and to measure, but the conductivity characteristic of the sample was founded.

The product, obtained from the sulfidizing reaction of TiO_2 at 1250 ^{O}C, was pressed and annealed at 800 ^{O}C for two hours in N_2 atmosfer. The obtained Temperature vs Relative Resistance graph is shown in Figure 3.2.1. The sample has in metallic conductivity property, this agrees with the literature.[79] TiS_2 is semiconductor but with the increasing Ti concentration titanium sulfide becomes metallic conductor.

The product, obtained from the sulfidizing reaction of Cr_2O_3 at 1250 ^{O}C, was pressed and annealed at different temperatures and different annealing durations. Unfortunately an appropriate pellet can not be obtained. They were in fine powdery form so the contact with the silver paint could not achieved. In the literature the conductivity of the single crystal of Cr_2S_3 was measured and it was found in semi-conducting character.[80]

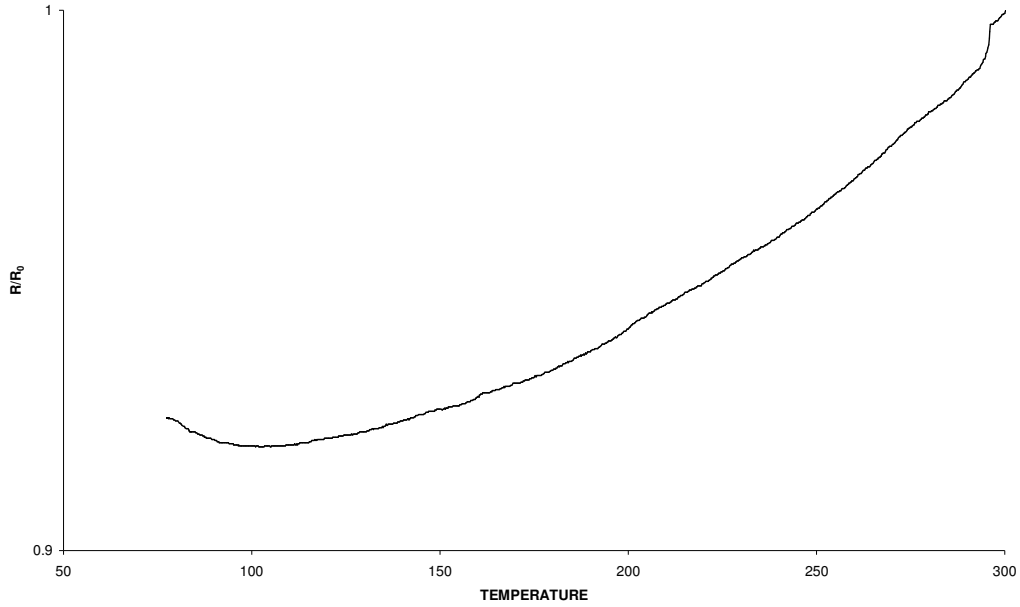

Figure 3.2.1: Temperature vs Relative Resistance Graph of the Product obtained from Sulfidizing Reaction of TiO_2 at 1250 ^{O}C.

The product obtained from the sulfidizing reaction of MnO_2 at 950 ^{O}C, was pressed and annealed at 800 ^{O}C for one hour in N_2. The obtained Temperature vs Relative Resistance graph is shown in Figure 3.2.2. Although the resistance character of the sample seems very complicated, it is in agreement with the literature.[81] Aplesnin et al. studied electrical conductivity of single crystal alabandite MnS, and they reported complicated electrical conductivity character. Our results agree with the data in the literatures: Conductivity of MnS results from the motion of holes in the e_g and t_{2g} bands. The holes in e_g band are responsible for the temperature-independent behavior of conductivity at low temperatures. The sharp decrease in the resistivity at T< 200 K was caused by the thermal activation of the holes in the degenerate t_{2g} band. The nonlinear behavior at T = 250 K and temperature hysteresis of the conductivity at around 250 K arised from partial lifting of degeneration of the holes in t_{2g} subbands observed at 250 K. One of the three t_{2g} subbands at T = 250 K and one of the two e_g subbands

at T = 160 K induces the charge instability due to the competition between the on-site Coulomb interaction of the holes in different orbitals and small hybridization of the subbands. Above 250 K, MnS become metallic conductor.

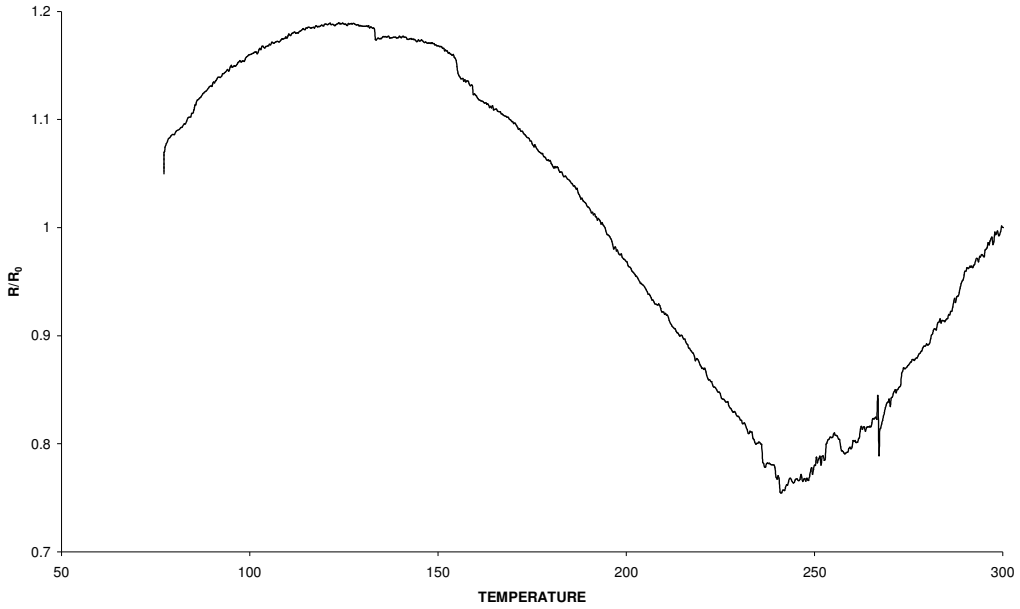

Figure 3.2.2: Temperature vs Relative Resistance Graph of the Product obtained from Sulfidizing Reaction of MnO_2 at 950 ^{O}C.

The product obtained from the sulfidizing reaction of Fe_2O_3 at 650 ^{O}C, was pressed and annealed at 800 ^{O}C for one hour in N_2. Temperature vs Relative Resistance graph, obtained by the electrical conductivity measurements, is shown in Figure 3.2.3. The result of the measurement shows that the sample was in semiconductor character. This behavior is constant with the literature.[82]

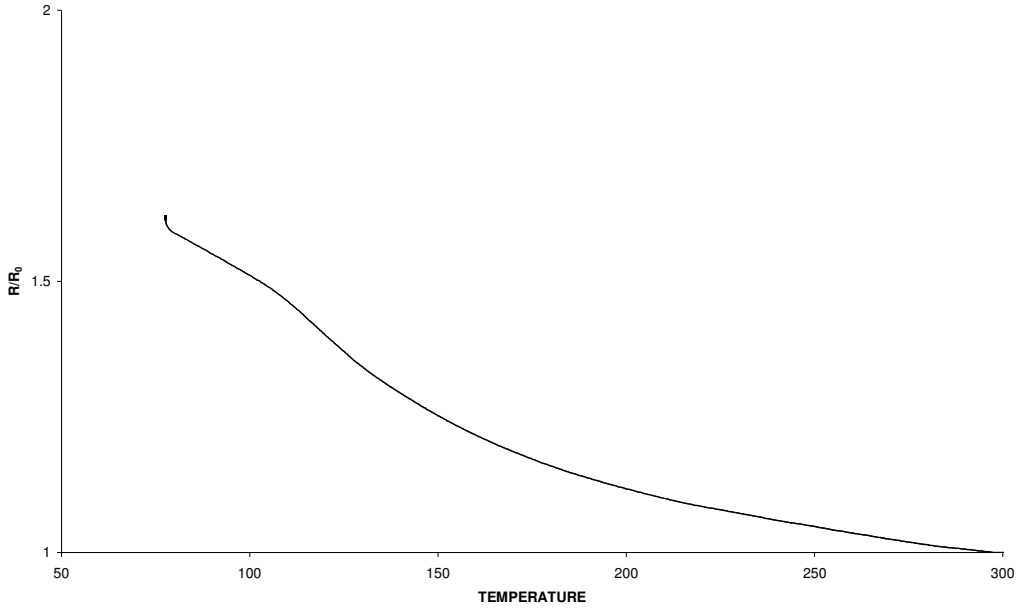

Figure 3.2.3: Temperature vs Relative Resistance Graph of the Product obtained from Sulfidizing Reaction of Fe_2O_3 at 650 ^{O}C

The product obtained from the sulfidizing reaction of Co_3O_4 at 950 ^{O}C, was pressed and annealed at 800 ^{O}C for one hour in N_2. The Temperature vs Relative Resistance graph, obtained by the electrical conductivity measurement, is shown in Figure 3.2.4. The result of the measurement shows that the sample was in metallic conductivity character and this behavior agrees with literature.[83]

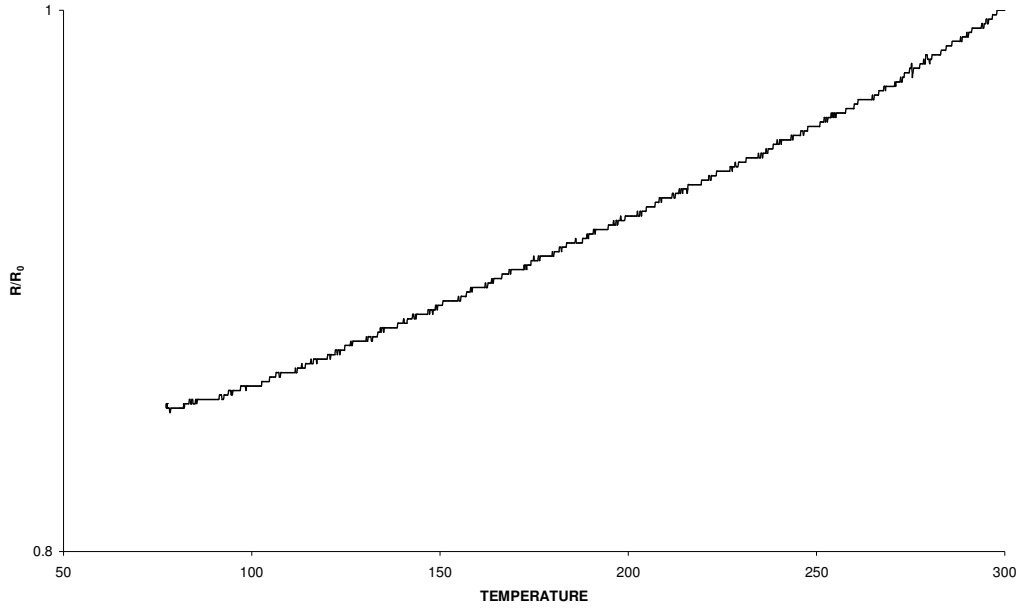

Figure 3.2.4: Temperature vs Relative Resistance Graph of the Product obtained from Sulfidizing Reaction of Co_3O_4 at 950 ^{O}C

The product obtained from the sulfidizing reaction of NiO at 450 ^{O}C, was pressed and annealed at 750 ^{O}C for one hour in N_2. The Temperature vs Relative Resistance graph, obtained by the electrical conductivity measurement, is shown in Figure 3.2.5. The result of the measurement shows that the sample was in metallic conductivity character and this behavior agrees with literature.[84]

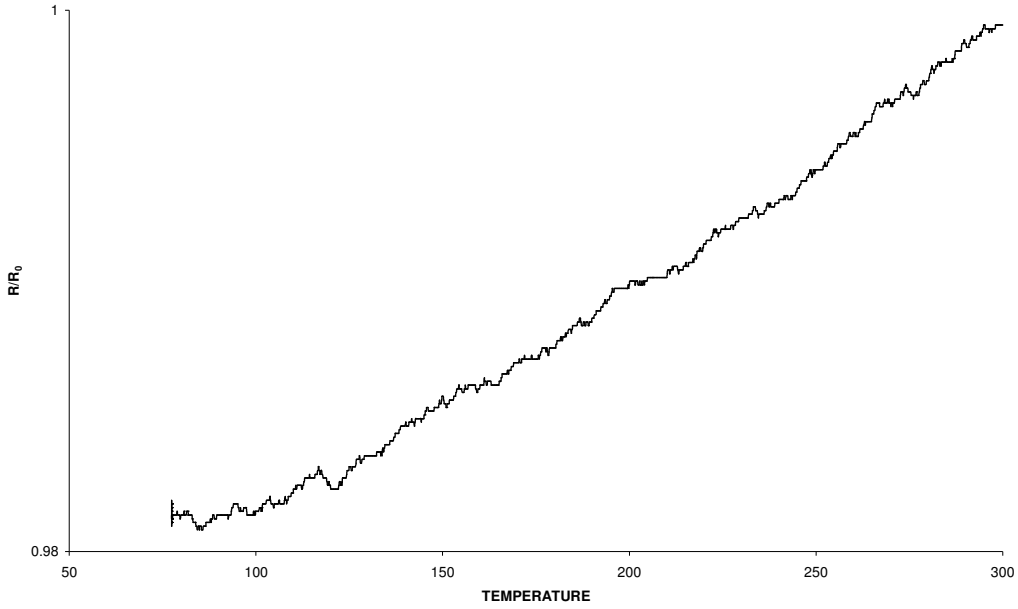

Figure 3.2.5: Temperature vs Relative Resistance Graph of the Product obtained from Sulfidizing Reaction of NiO at 450 ^{O}C

The product obtained from the sulfidizing reaction of CuO at 850 ^{O}C, was pressed and annealed at 750 ^{O}C for one hour in N_2. The Temperature vs Relative Resistance graph, obtained by the electrical conductivity measurement, is shown in Figure 3.2.6. Sample shows semi-conducting behavior, this behavior agrees with literature.[85] Ermolenko et al. reported that these kind of cupper sulfides, Cu_{2-x} S, where $0.19 < x < 0.4$, are p type semiconductors.

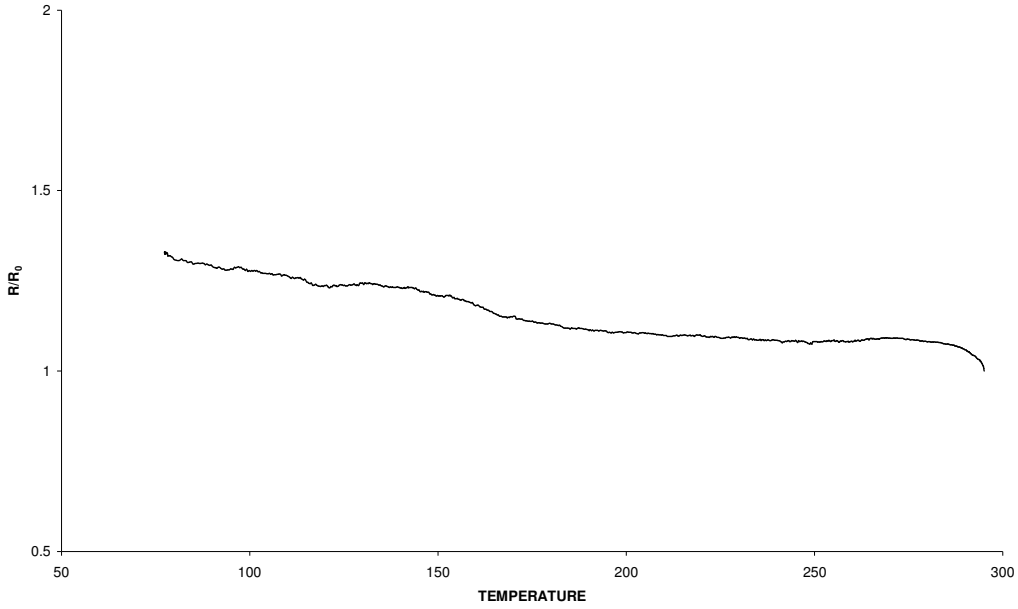

Figure 3.2.6: Temperature vs Relative Resistance Graph of the Product obtained from Sulfidizing Reaction of CuO at 850 ^{O}C

The product obtained from the sulfidizing reaction of ZnO at 850 ^{O}C, was pressed and annealed at 1150 ^{O}C for two hours in N_2. The Temperature vs Relative Resistance graph obtained by electrical conductivity measurement, is shown in Figure 3.2.7. Although ZnS is a well known semiconductor, the sample showed complex behavior. The reason is that surface of the pellet is dusty.

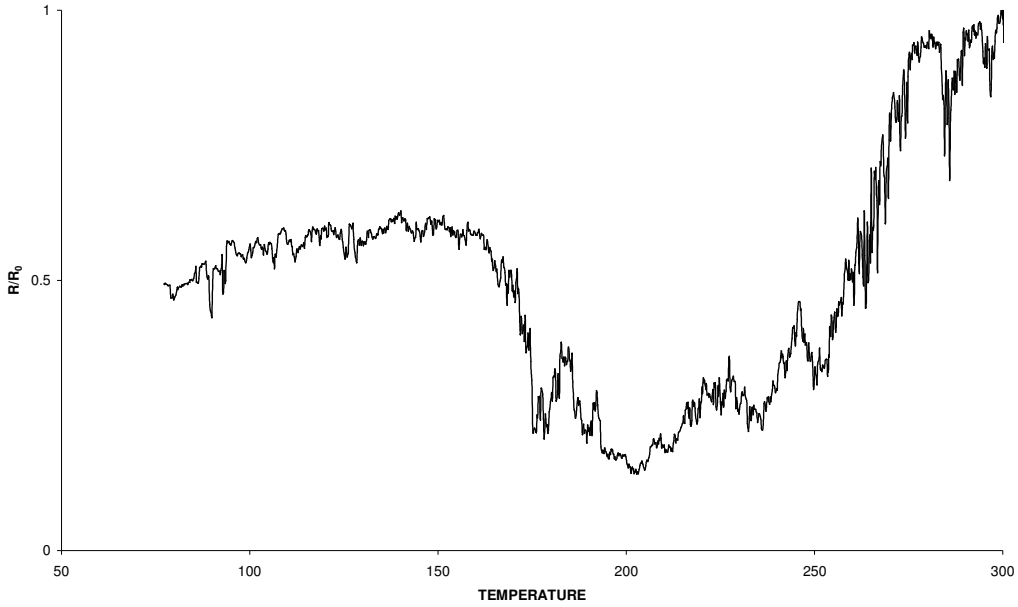

Figure 3.2.7: Temperature vs Relative Resistance Graph of the Product obtained from Sulfidizing Reaction of ZnO at 850 ^{O}C

CHAPTER 4

GENERAL CONCLUSION

In this work, some of the first row transition metal sulfides were synthesized from their oxides by a new sulfidizing and reducing method which was not reported in the literature. This method was used in our laboratory before for the synthesis of $CuFeS_2$, CdS, Na_2S and sulfide derivatives of Perovskite type superconductors. The obtained products were analyzed by x-ray powder diffraction and Raman scattering spectroscopy. Their electrical conductivity behavior was also searched.

In TiO_2 case, 450 ^oC is not enough to give reaction between TiO_2 and sulfidizing gas mixture, but Anatase reactant starts to turn into Rutile. 850 ^oC and 1250 ^oC are enough for activation energy of reaction but the reaction duration; three hours, is not enough to convert all TiO_2 to titanium sulfide. Conductivity data agree with the literature.

In Cr_2O_3 case, 650 ^oC is enough to activate the reaction but again the duration is not enough to convert all oxide to sulfide. At 1250 ^oC, all reactant turns into Cr_2S_3, but there is an unidentified peak in x-ray powder diffraction pattern. The conductivity measurement couldn't be performed for this product due to difficulty in annealing. So the contacts couldn't be attached to product.

In MnO_2 case, all products has MnS peaks in x-ray powder diffraction pattern, but the reaction duration is not enough, except at 1250 ^oC, to convert all MnO_2 to MnS. MnO_2 decomposes to MnO at 535 ^oC. Under normal condition with the help of the CO content, as reducing agent, all unreacted MnO_2 decomposed to MnO. The product of 1250 ^oC has unknown peaks at the x-ray powder diffraction pattern. Conductivity measurement data agree with previous researchers' data.

In Fe_2O_3 case, sulfidizing reaction was achieved at 450 ^oC. X-Ray powder diffraction pattern has iron sulfide peaks. But duration of the reaction is insufficient to convert the entire oxide compound to sulfide compound. At 650 and 850 ^oC, there was no oxide peaks in X-ray powder diffraction pattern. All products has same crystal structure, pyrrhotite. Conductivity measurement data agree with literature.

In Co_3O_4 case, 450 ^OC and was enough to convert all oxide to sulfide in three hours. Reaction conditions produce Co_9S_8, cobaltpentlandite, at 550 ^OC, 650 ^OC and 850 ^OC. At higher temperatures, 950 ^OC and 1150 ^OC, the product was CoS, jaipurite. Conductivity measurement data agree with the literature, the product is metallic conductor.

NiO turns into NiS at 450 ^OC and 650 ^OC in three hours. At 795 ^OC the NiS start to melt[86] so the sulfidizing reaction at higher temperatures were not studied. The conductivity measurement data agree with literature. The product has metallic conductivity.

In CuO case, at all temperatures, the reactant CuO turns into cupper sulfide, the sulfidizing reaction time was enough. Although the products were mixture, the conductivity measurements data agree with previous researchers' data. Non stochiometric cupper sulfide compounds are semiconductors.

In ZnO case, at 450 ^OC, the reaction has been started but the sulfidizing reaction duration was not enough to complete the reaction. At 650 ^OC and over this temperature the reaction completes in three hours. Products were mixture of ZnS polymorph; wurtzite and sphalerite.

All studied first row transition metal oxides were converted to their sulfide derivatives successfully. The sulfidizing gas mixture can be used for production of studied metals' sulfide from their oxides.

In future, the affect of the flow rate of the gas nd the sulfidizing reaction duration on varieties of products may be examined. The detailed structural research on obtained products may be done to clarify phase diagrams of metal sulfides

REFERENCES

[1] Güler Halil, Ph.D Thesis 'Synthesis and Characterization of Some Conducting Oxides and Sulfides' March 1996 Chemistry Department METU pages:1-11.

[2] Weigand, Wolfgang; Kreisel, Guenter; Kaessbohrer, Johannes; Sammler, Marina; Grunert, Renate. Ger. Offen. (2000), 4

[3] Bedard, Robert L.; Vail, Lawrence D.; Wilson, Stephen T.; Flanigen, Edith M. (UOP Inc., USA). U.S. (1990), 20 pp.

[4] Kawakami, Soichiro; Yamamoto, Tomoya; Sano, Hitomi; Tani, Atsushi. Eur. Pat. Appl. (2003) 34 pp.

[5] Saito, Yahachi; Nakahira, Takako; Uemura, Sashiro; Nagamawari, Takeshi. Jpn. Kokai Tokkyo Koho (2003), 8

[6] Simons, C. S. Metallurgical Society Conferences [Proceedings] (1963), 24 592-615, discussion 615-16

[7] Vaschetti, A. Metallurgia Italiana (1968), 60(5), 387-94

[8] Henriksen, G. L.; Vissers, D. R. Journal of Power Sources (1994), 51(1-2), 115-28.

[9] Shembel, Elena Moiceevna; Nagirniy, Viktor Mihaylovich; Apostolova, Raisa Danilovna; Novak, Petr Yakovlevich PCT Int. Appl. (2005), 17

[10] Hwang, Duck-chul; Park, Zin; Lee, Jae-woan. U.S. Pat. Appl. Publ. (2004), 11

[11] Tomczuk, Zygmunt. U.S. (1979), 4.

[12] Ritchie, Andrew Grahame; Bowles, Peter George. PCT Int. Appl. (2000), 9

[13] Kwon, Ho Jin. Repub. Korean Kongkae Taeho Kongbo (2001).

[14] Sanyo Electric Co., Ltd., Japan. Jpn. Kokai Tokkyo Koho (1985), 2

[15] Hitachi Maxell, Ltd., Japan. Jpn. Kokai Tokkyo Koho (1984), 3 .

[16] Hu, Jin-Song; Ren, Ling-Ling; Guo, Yu-Guo; Liang, Han-Pu; Cao, An-Min; Wan, Li-Jun; Bai, Chun-Li. Angewandte Chemie, International Edition (2005), 44(8), 1269-1273.

[17] Bando, Yoshio; Zhu, Yingchun. Jpn. Kokai Tokkyo Koho (2005), 6 pp

[18] Shirata, Masashi. U.S. Pat. Appl. Publ. (2005), 13 pp

[19] Hirai, Hiroyuki; Sugihara, Keiko; Nishigaki, Junji. U.S. Pat. Appl. Publ. (2005), 12 pp.

[20] Bando, Yoshio; Zhu, Yingchun. Jpn. Kokai Tokkyo Koho (2005), 5 pp

[21] Oda, Shunri; Kukimoto, Hiroshi. IEEE Transactions on Electron Devices (1977), ED-24(7), 956-8

[22] Broser, Immanuel; Reichardt, Werner. Zeitschrift fuer Physik (1952), 134 222-44.

[23] Eliseev, E. I. USSR. (1972), No. 204 41-5

[24] Sedlacek, Jiri. Sbornik Vysoke Skoly Chem. Technol. v Praze, Oddil Tak. Anorg. a Org. Technol. (1958), 573-94

[25] Tombak, M. I.; Popova, A. V.; Komar, O. F.; Bundel, A. A. Izvestiya Akademii Nauk SSSR, Seriya Fizicheskaya (1959), 23 1363-9

[26] Levshin, V. L.; Borodin, N. S.; Neronova, G. P. Optika i Spektroskopiya (1957), 3 258-66

[27] Ellefson, Bennett S. (1949), U.S.

[28] Stalony-Darbovski, J. Roczniki Chemii (1925), 5 193-214

[29] Schurich, Bernd. Zentralabt. Forsch. Entwickl., Technol. Forsch. Entwickl. (1984), 56 pp

[30] Brody, T. P.; Shirland, F. A. Proc. Symp. Mater. Sci. Aspects Thin Film Syst. Sol. Energy Convers. (1974), (PB-239 270), 170-92

[31] Hambuechen, Carl. (1938), US

[32] Kohlmeyer, E. J.; Gerlach, J.; Hondelmann, D.; Kleist, H. G.; Pawlek, F. Metall (Isernhagen, Germany) (1968), 22(5), 400-4.

[33] Smotkin, E. S.; Cervera-March, S.; Bard, A. J.; Campion, A.; Fox, M. A.; Mallouk, T.; Webber, S. E.; White, Journal of Physical Chemistry (1987), 91(1), 6-8.

[34] Bazylinski, Dennis A.; Frankel, Richard B.; Heywood, Brigid R.; Mann, Stephen; King, John W.; Donaghay, Percy L.; Hanson, Alfred K. Applied and Environmental Microbiology (1995), 61(9), 3232-9.

[35] Watson, J. H. P.; Croudace, I. W.; Warwick, P. E.; James, P. A. B.; Charnock, J. M.; Ellwood, D. C. Department of Physics and Astronomy, Separation Science and Technology (2001)

[36] Watson, J. H. P.; Ellwood, D. C.; Deng, Qixi; Mikhalovsky, S.; Hayter, C. E.; Evans, J. Minerals Engineering (1995), 8(10), 108

[37] Takemura, Yozo; Noda, Tamio. Jpn. Kokai Tokkyo Koho (1992), 5 pp

[38] Ito, Daisuke; Miura, Kuniaki; Ichimura, Tetsunari; Ihara, Ikkou; Watanabe, Tsuneo. IEEE Transactions on Applied Superconductivity (2004), 14(2), 1551-1553

[39] Feigenbaum, Simon. Foote Prints on Chemicals, Metals, Alloys and Ores (1956), 26(No. 1), 10-15.

[40] Akutsu, Kenji; Marushima, Norio. Jpn. Kokai Tokyo Koho (1975), 4 pp

[41] Taranov, O. G.; Rakitina, Z. A.; Shatov, Yu. S.; Nuzhdina, T. A. U.S.S.R. (1975),

[42] Dautovich, D. P.; Hay, M. G. Materials Performance (1978), 17(8), 15-19

[43] Peculea, Marius; Beca, Titus; Dogaru, Constantin; Dogaru, Elvira; Mihai, Mircea; Smaranda, Dumitru. Rom. (1986), 4 pp.

[44] Kalashnikov, A. L.; Ushakov, O. S.; Istomin, V. Ja; Afanas'ev, V. G.; Malyi, E. N. Russ. (1999)

[45] Gonzalez, E. R.; Assuncao, N. A.; de Giz, M. J.; Tremiliosi-Filho, G. Hydrogen Energy Progress XI, Proceedings of the World Hydrogen Energy Conference, (1996), 1 723-728.

[46] Ryabinkina, L. I.; Abramova, G. M.; Romanova, O. B.; Petrakovskii, G. A. Russ. (2005),

[47] Feigenbaum, Simon. Foote Prints on Chemicals, Metals, Alloys and Ores (1954), 26(No. 1), 3-6

[48] Zhang Xiang V; Martin Scot T; Friend Cynthia M; Schoonen Martin A A; Holland Heinrich D Journal of the American Chemical Society (2004 Sep 15), 126(36)

[49] German, Wm. L.; Brandon, Thomas W. Journal of the Chemical Society, (1940),

[50] Suryanarayana, Chittari V.; Kurian, Alice. Indian (1972), 12 pp

[51] Takeda, Mitsuo. Jpn. Kokai Tokkyo Koho (2004), 32 pp

[52] Ando, Koji; Kudo, Takashi. Jpn. Kokai Tokkyo Koho (2003), 3 pp

[53] Hoar, T. P.; Tucker, A. J. P. Journal of the Institute of Metals (1953), 81 665-79; (Paper No. 1485)

[54] Henderson, James R.; Johnson, Donald M.; Muramoto, Michiya. U.S. (1973), 10 pp

[55] Barret, Pierre; Delafosse, Denise. Bulletin de la Societe Chimique de France (1970), 1 82-5

[56] Xiao, Y.; Soons, J.; Lans, S. C.; van Sandwijk, A.; Reuter, M. A.; van der Plas, D. W. Light Metals 2003, Proceedings of the International Symposium on Light Metals, (2003), 101-117

[57] Clearfield, Abraham. Acta Cryst. (1963), 16 135-42

[58] Tran, T. T. M.; Fiaud, C.; Sutter, E. M. M.; Villanova, A. Corrosion Science (2003), 45(12), 2787-2802

[59] Xiao, Y.; Van Der Plas, D. W.; Soons, J.; Lans, S. C.; Van Sandwijk, A.; Reuter, M. A. Canadian Metallurgical Quarterly (2004), 43(2), 283-292

[60] Malur, J. Kristall und Technik (1966), 1 261-5.

[61] Kizilyalli, M.; Bilgin, M.; Kizilyalli, H. M.. Journal of Solid State Chemistry (1990), 85(2), 283-92.

[62] Guler, H.; Kesanli, B.; Kizilyalli, M.; Pamuk, O.; Morkan, A. Key Engineering Materials (2004), 264-268

[63] Guler, Halil; Kizilyalli, Meral; Firat, Tezer; Ozenbas, Macit. High Temperature and Materials Science (1999), Volume Date 1997, 38(1), 23-39.

[64] Kizilyalli, M.; Kizilyalli, H. M.. NATO ASI Series, Series B: Physics (1985), 129(Transp. Nonstoichiom. Compd.), 441-9.

[65] Owen A.J, Sykes , K.W., and Thomas D.J.D. Trans. Faraday Soc. 47, 419,1951.

[66] Welch J.E., Interim Report, Imperial Collage,1970

[67] Kittel, C. "Introduction to Solid State Physics"7th edition John Wiley & Sons. New york 1996.

[68] Smart,L; Moore, E. " Solid State Chemistry, an Introduction" 2nd edition, Chapman & Hall Press.1995.

[69] Oganesyan, V. Kh. Fizika (1967), 2(1), 55-64

[70] Shriver D.F., Atkins P.W. Langford C.H. Inorganic Chemistry 2nd Edition Oxford Press. pp 774 775

[71] Inoue, M.; Negishi, H.; Fujii, T.; Takase, K.; Hara, Y.; Sasaki, M. Journal of Physics and Chemistry of Solids (1996), 57

[72] Prawer S. Nemanich R. J. Philosophical Transactions: Mathematical, Physical and Engineering Sciences 362/1824 (2004) pp2537-2565.

[73] Kondrashev, Yu. D.; Zaslavskii, A. I. Seriya Fizicheskaya (1951), 15 179-86

[74] Weast R. "Handbook of Chemistry and Physics" 57th Edition CRC Press 1977. p B-131

[75] Goble, Ronald J. Canadian Mineralogist (1985), 23(1), 61-76

[76] Sabine, Terence M.; Hogg, Suzanne. Acta Crystallographica, Section B: Structural Crystallography and Crystal Chemistry (1969), 25(Pt. 11), 2254-6

[77] Swanson, Howard E.; Fuyat, Ruth K. National Bureau of Standards Circular (U. S.) (1953), 539(Vol. II), 65 pp.

[78] Hope G.A.,Woods r. Munce C.G;Mineral Engineering, 14/12, 1565-1577, 2001

[79] Molenda, J. Journal of Thermal Analysis (1992), 38(9), 2163-9.

[80] Iwahashi, Katsutoshi; Sugiura, Takeshi; Masuda, Yoshika. Journal of the Physical Society of Japan (1975), 39(3), 647-55.

[81] Aplesnin, S. S.; Ryabinkina, L. I.; Abramova, G. M.; Romanova, O. B.; Vorotynov, A. M.; Velikanov, D. A.; Kiselev, N. I.; Balaev, A. D. Physical Review B: Condensed Matter and Materials Physics (2005), 71(12).

[82] Oganesyan, V. Kh. Khal'kogenidy (Svoistva, Metody Poluch. Primen.), Mater. Seminara, 1st, Kiev (1967), Volume Date 1965, 160-6

[83] Le Brusq, Henri; Delmaire, Jean P.; Marion, Fernand. Comptes Rendus des Seances de l'Academie des Sciences, Serie C: Sciences Chimiques (1971), 273(2), 139-42

[84] Townsend,M.G.;Trembley, R.;Horwood, L.J. Journal of Physic C: Solid State Physics (1971), 4(5), 598-606.

[85] Ermolenko, Yu. E. USSR. Avail. SPSTL.Deposited Doc.(1980), (SPSTL 870 khp-D80), 3-8

[86] Weast R. "Handbook of Chemistry and Physics" 57th Edition CRC Press 1977 page: B-136

APPENDIXES

APPENDIX A

Table Appendix A.1: X-ray powder diffraction data of Reactant Anatase, TiO_2 (JCPDS Card No: 21-1272) that used in Sulfidizing Reactions of TiO_2

OBSERVED DATA		CARD DATA				
		Anatase TiO_2 (JCPDS Card No: 21-1272)				
d-values	I/I_0	d-values	I/I_0	h	k	l
3.517	100	3.52	100	1	0	1
2.431	10	2.431	10	1	0	3
2.378	35	2.378	20	0	0	4
2.330	11	2.332	10	1	1	2
1.892	57	1.892	35	2	0	0
1.700	42	1.700	20	1	0	5
1.667	44	1.666	20	2	1	1
1.492	8	1.493	4	2	1	3
1.480	37	1.481	14	2	0	4
1.364	17	1.364	6	1	1	6
1.338	20	1.338	6	2	2	0
1.279	31	1.280	2	1	0	7
1.265	31	1.265	10	2	1	5
1.250	9	1.251	4	3	0	1
1.189	2	1.189	2	0	0	8
1.172	3	1.173	2	3	0	3
1.166	18	1.166	6	2	2	4
1.161	8	1.161	4	3	1	2
1.060	3	1.060	2	2	1	7
1.051	9	1.052	4	3	0	5

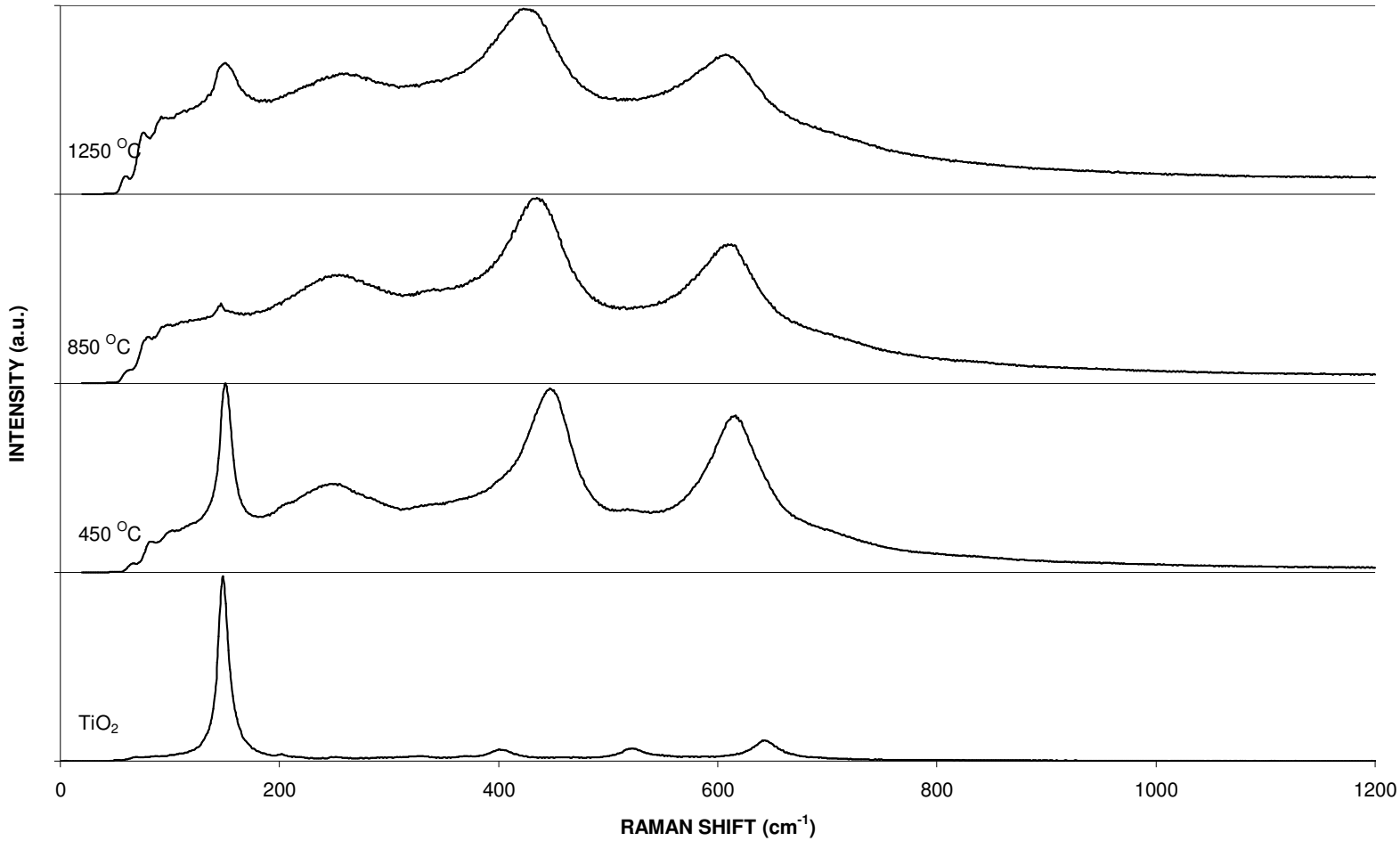

Figure Appendix A1: Raman Scattering Spectra of Reactant and Products of Sulfidizing Reactions of TiO_2

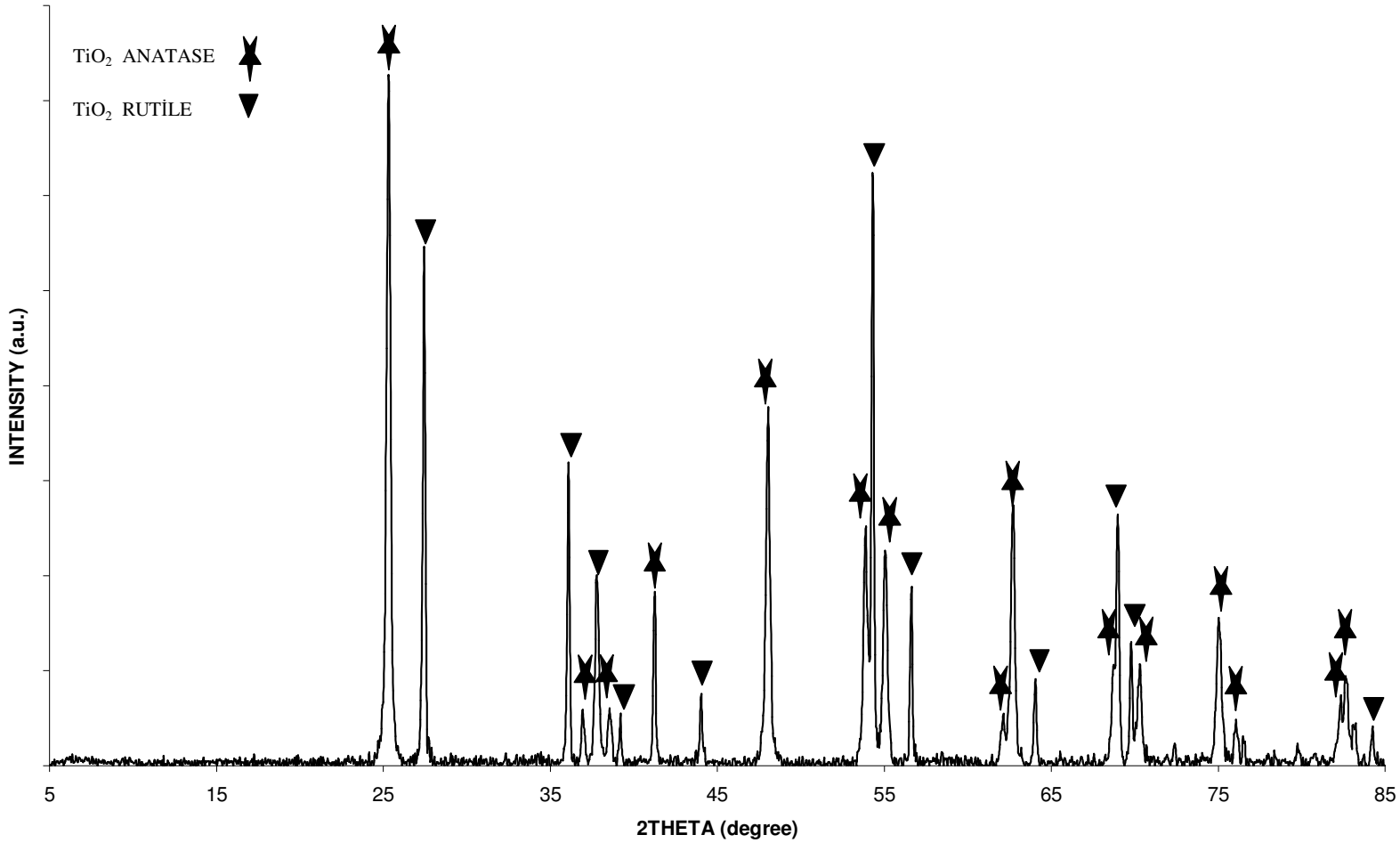

Figure Appendix A.2: X-Ray Powder Diffraction Pattern of Product obtained from the Sulfidizing Reactions of TiO_2 at 450 ^oC

Table Appendix A 2: X-Ray Powder Diffraction Data of the Product obtained From the Sulfidizing Reaction of TiO_2 at 450 ^{O}C

OBSERVED DATA		CARD DATA									
		Rutile, TiO_2 (JCPDS Card No: 76-1938)					Anatase TiO_2 (JCPDS Card No: 21-1272)				
d-values	I/I_0	d-values	I/I_0	h	k	l	d-values	I/I_0	h	k	l
3.510	100						3.520	100	1	0	1
3.246	76	3.247	100	1	1	0					
2.486	44	2.486	44	1	0	1					
2.431	9						2.431	10	1	0	3
2.378	28						2.378	20	0	0	4
2.333	9						2.332	10	1	1	2
2.187	26	2.187	17	1	1	1					
2.054	11	2.054	6	2	1	0					
1.892	52						1.892	35	2	0	0
1.700	35						1.700	20	1	0	5
1.688	86	1.687	49	2	1	1					
1.665	32						1.666	20	2	1	1
1.623	26	1.624	14	2	2	0					
1.492	8						1.493	4	2	1	3
1.479	38	1.479	7	0	0	2					
1.453	13	1.452	7	3	1	0					
1.364	37						1.364	6	1	1	6
1.360	15	1.359	16	3	0	1					
1.346	18	1.346	8	1	1	2					
1.338	15						1.338	6	2	2	0
1.263	22						1.265	10	2	1	5
1.250	7						1.251	4	3	0	1
1.170	11	1.170	3	3	2	1	1.173	2	3	0	3
1.167	14						1.166	6	2	2	4
1.148	6	1.148	2	4	0	0					

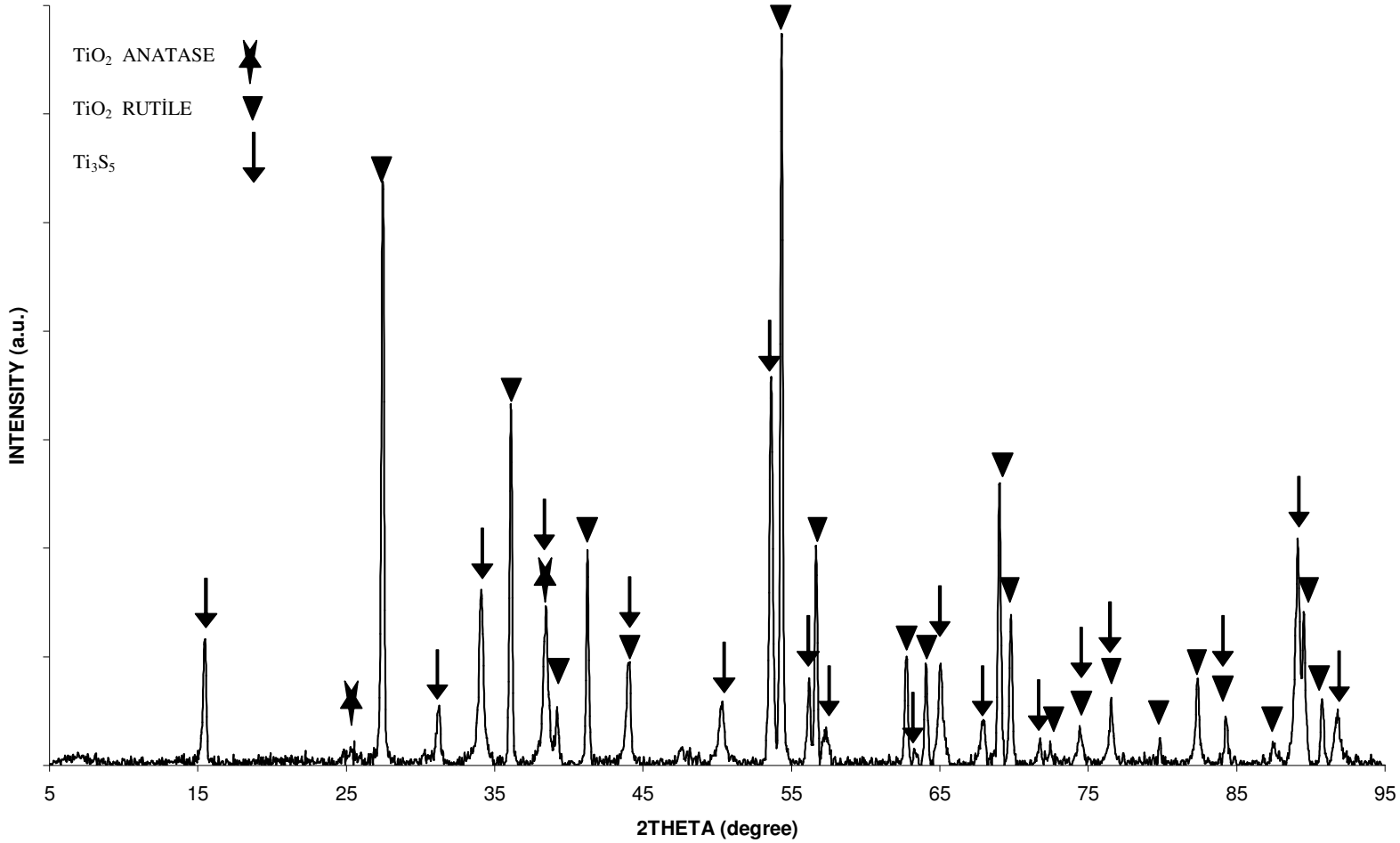

Figure Appendix A.3: X-Ray Powder Diffraction Pattern of Product obtained from the Sulfidizing Reaction of TiO_2 at 850 ^oC.

Table Appendix A.3: X-Ray Powder Diffraction Data of the Product obtained From the Sulfidizing Reaction of TiO_2 at 850 ^{O}C.

OBSERVED DATA		CARD DATA													
		Ti_3S_5 (JCPDS Card no: 27-908)					Rutile, TiO_2 (JCPDS Card No: 76-1938)					Anatase, TiO_2 (JCPDS Card No: 21-1272)				
d-values	I/I_0	d-values	I/I_0	h	k	l	d-values	I/I_0	h	k	l	d-values	I/I_0	h	k	l
5.712	33	5.730	80	0	0	2										
3.517	2											3.52	100	1	0	1
3.241	80						3.247	100	1	1	0					
2.855	9	2.870	70	1	0	1										
2.627	25	2.632	80	1	0	2										
2.486	50						2.486	44	1	0	1					
2.336	22	2.343	70	1	0	3						2.332	10	1	1	2
2.296	8						2.296	7	2	0	0					
2.184	33						2.187	17	1	1	1					
2.052	15	2.060	60	1	0	4	2.054	6	2	1	0					
1.811	9	1.813	10	1	0	5										
1.707	54	1.711	100	1	1	0										
1.687	100						1.687	49	2	1	1					
1.635	12	1.640	60	1	1	2										
1.623	31						1.624	14	2	2	0					
1.605	6	1.605	40	1	0	6										
1.478	15						1.479	7	0	0	2					
1.464	3	1.469	40	1	1	4										
1.453	14						1.452	7	3	1	0					
1.433	14	1.431	60	0	0	8										
1.377	7	1.381	70	2	0	3										
1.359	39						1.359	16	3	0	1					
1.346	21						1.346	8	1	1	2					
1.314	4	1.317	10	2	0	4										
1.303	4						1.304	1	3	1	1					
1.273	6	1.274	10	1	1	6	1.274	1	3	2	0					
1.244	10	1.244	70	2	0	5										
1.200	4						1.201	1	2	1	2					
1.169	12	1.170	40	1	0	9	1.170	4	3	2	1					
1.148	7						1.148	2	4	0	0					

Table Appendix A.3 (continued)

OBSERVED DATA		CARD DATA														
		Ti_3S_5 (JCPDS Card no: 27-908)					Rutile,TiO_2 (JCPDS Card No: 76-1938)					Anatase,TiO_2(JCPDS Card No: 21-1272)				
d-values	I/I_0	d-values	I/I_0	h	k	l	d-values	I/I_0	h	k	l	d-values	I/I_0	h	k	l
1.113	4						1.114	1	4	1	0					
1.098	32	1.098		2	0	7										
1.094	22						1.093	5	2	2	2					
1.082	10						1.083		3	3	0					
1.073	8	1.075		3	1	3										

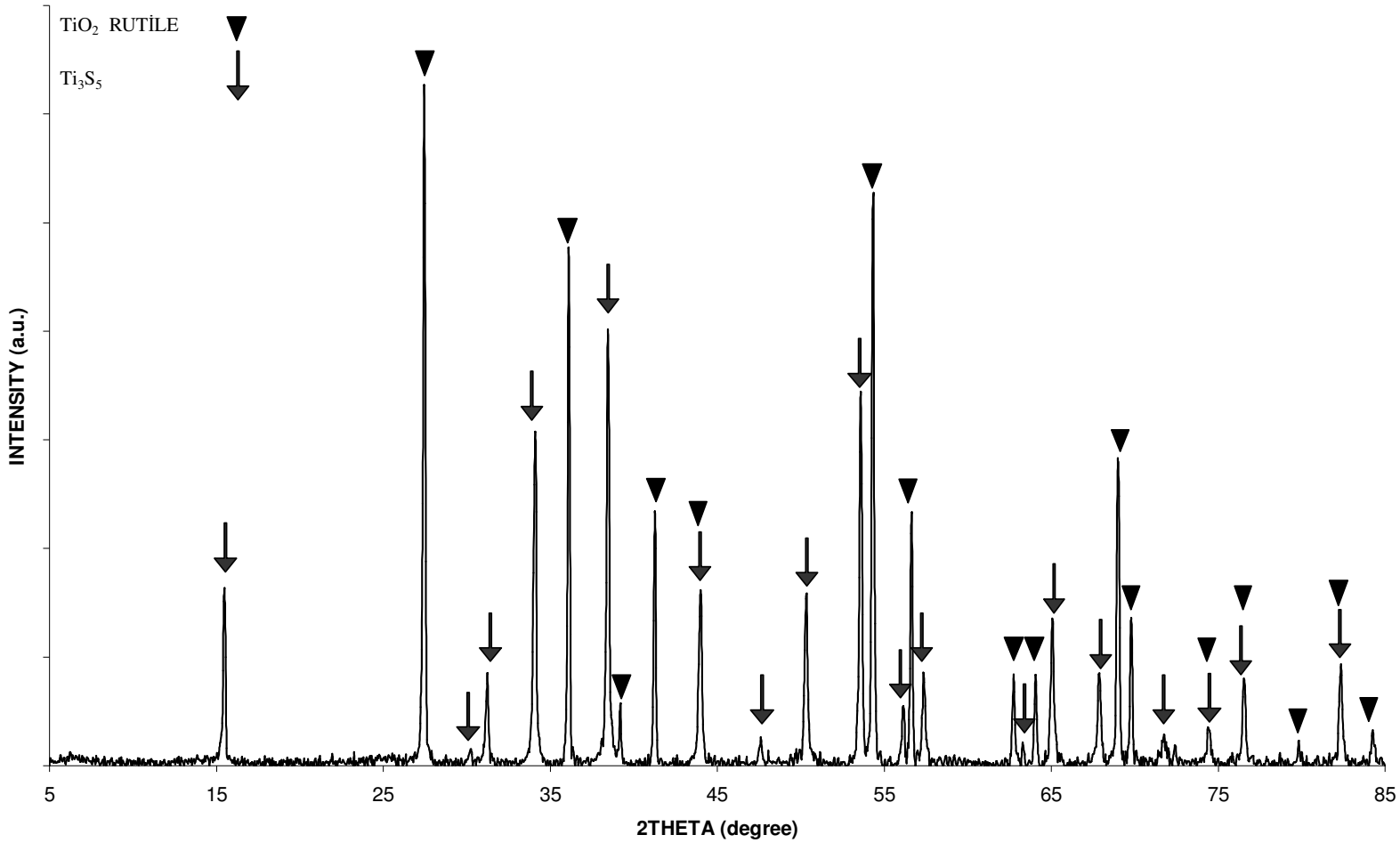

Figure Appendix A.4: X-Ray Powder Diffraction Pattern of Product that obtain from the Sulfidizing Reaction of TiO_2 at 1250 ^oC.

Table Appendix A.4: X-Ray Powder Diffraction Data of the Product obtained From the Sulfidizing Reaction of TiO_2 at 1250 ^{O}C.

OBSERVED DATA		CARD DATA									
		Ti_3S_5 (JCPDS Card no: 27-908)					Rutile, TiO_2 (JCPDS Card No: 76-1938)				
d-values	I/I_0	d-values	I/I_0	h	k	l	d-values	I/I_0	h	k	l
5.712	27	5.730	80	0	0	2					
3.246	100						3.247	100	1	1	0
2.952	3	2.964	10	1	0	0					
2.860	14	2.870	70	1	0	1					
2.627	50	2.632	80	1	0	2					
2.486	77						2.486	44	1	0	1
2.339	64	2.343	70	1	0	3					
2.296	10						2.296	7	2	0	0
2.187	38						2.187	17	1	1	1
2.056	26	2.060	60	1	0	4	2.054	6	2	1	0
1.909	5	1.908	5	0	0	6					
1.811	26	1.813	10	1	0	5					
1.708	55	1.711	100	1	1	0					
1.687	84						1.687	49	2	1	1
1.637	9	1.64	60	1	1	2					
1.623	38						1.624	14	2	2	0
1.604	14	1.605	40	1	0	6					
1.479	14						1.479	7	0	0	2
1.468	4	1.469	40	1	1	4					
1.453	14						1.452	7	3	1	0
1.432	22	1.431	60	0	0	8					
1.380	14	1.381	70	2	0	3					
1.360	46						1.359	16	3	0	1
1.346	22						1.346	8	1	1	2
1.314	5	1.317	10	2	0	4					
1.274	6	1.274	10	1	1	6	1.274	1	3	2	0
1.244	13	1.244	70	2	0	5	1.243	2	2	0	2
1.200	4						1.200	1	2	1	2
1.170	15	1.170	40	1	0	9	1.170	3	3	1	1
1.148	6						1.148	2	4	0	0

APPENDIX B

Table Appendix B.1: X-ray powder diffraction data of Reactant Eskolaite, Cr_2O_3 (JCPDS Card no: 84-1616) that used in Sulfidizing Reactions of Cr_2O_3.

OBSERVED DATA		CARD DATA				
		Eskolaite, Cr_2O_3 (JCPDS Card no: 84-1616)				
d-values	I/I_0	d-values	I/I_0	h	k	l
3.623	32	3.620	60	0	1	2
2.661	77	2.664	100	1	0	4
2.476	59	2.476	83	1	1	0
2.263	19	2.266	5	0	0	6
2.172	26	2.173	25	1	1	3
2.045	5	2.045	4	2	0	2
1.814	37	1.814	33	0	2	4
1.671	100	1.672	61	1	1	6
1.579	9	1.577	5	1	2	2
1.464	33	1.463	23	2	1	4
1.430	42	1.429	27	3	0	0
1.394	3	1.392	1	1	2	5
1.296	36	1.296	10	1	0	10
1.239	11	1.238	6	2	2	0
1.210	9	1.209	4	3	0	6
1.173	6	1.173	1	1	2	8
1.148	14	1.148	5	2	0	10
1.133	10	1.133	1	0	0	12
1.124	10	1.123	5	1	3	4
1.087	24	1.090	1	1	3	5

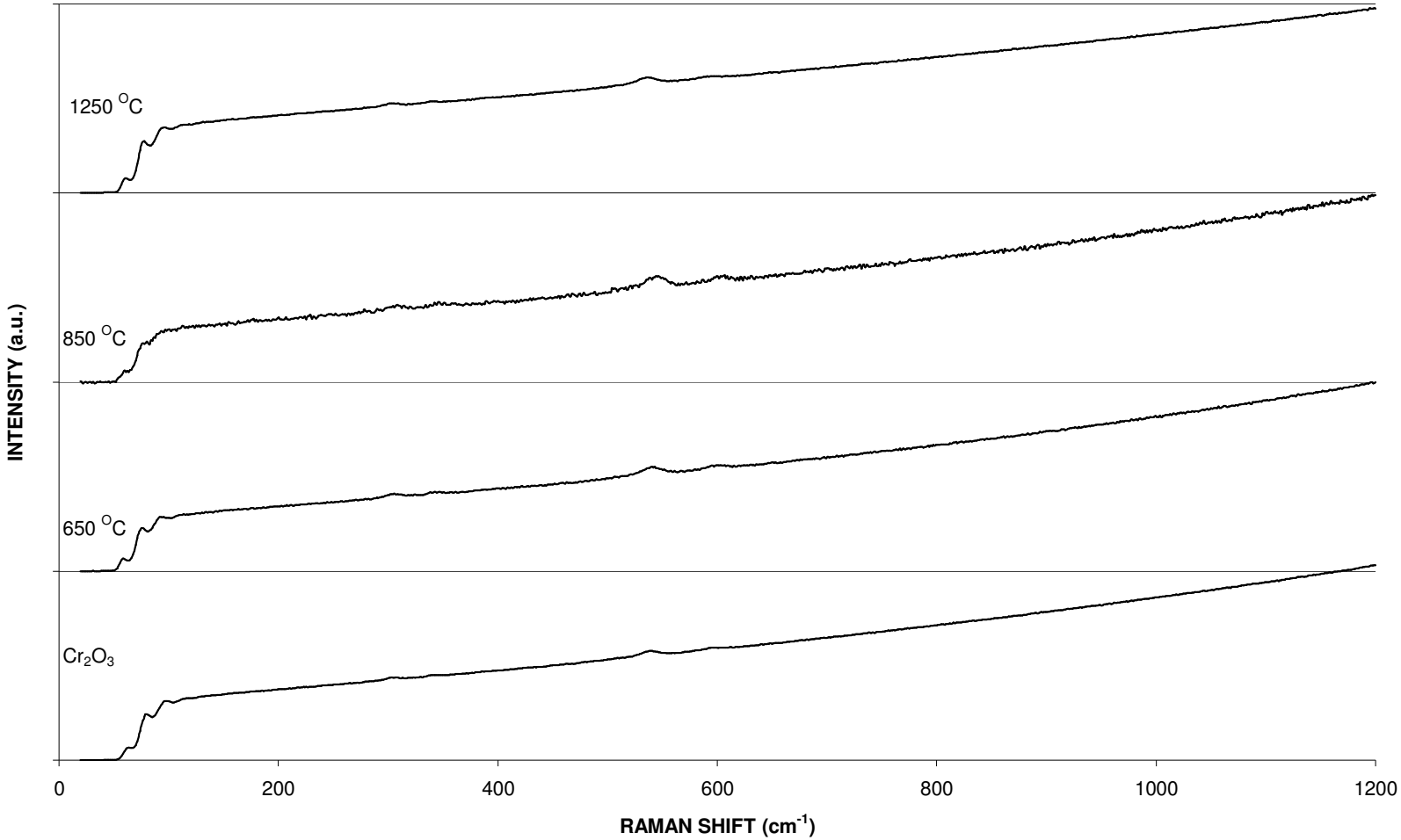

Figure Appendix B.1: Raman Scattering Spectra of Reactant and Product of Sulfidizing Reaction of Cr_2O_3

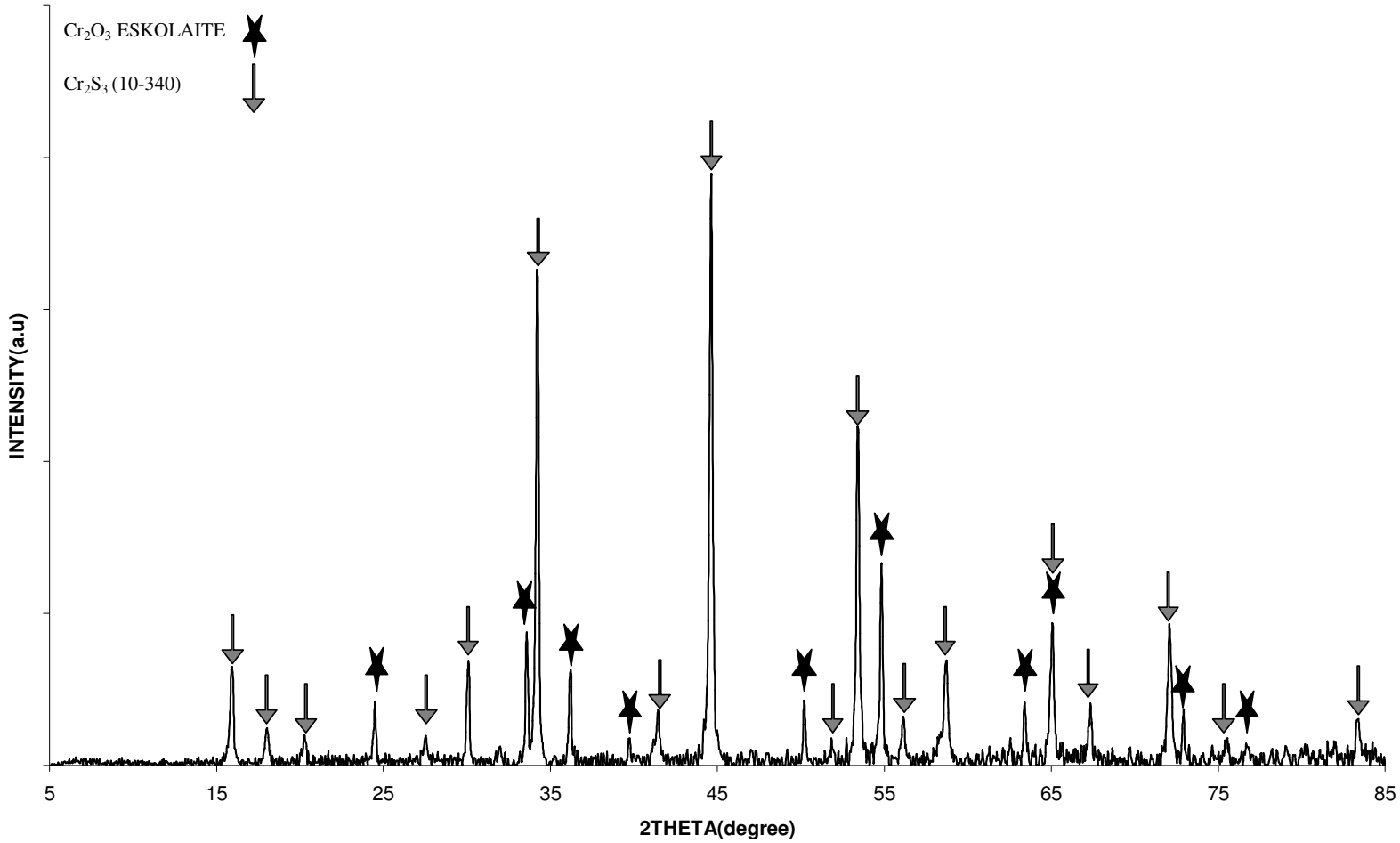

Figure Appendix B.2: X-Ray Powder Diffraction Pattern of Product obtained from the Sulfidizing Reaction of Cr_2O_3 at 650 ^oC

Table Appendix B.2: X-Ray Powder Diffraction Data of the Product obtained From the Sulfidizing Reaction of Cr_2O_3 at 650 ^{O}C

OBSERVED DATA		CARD DATA									
		Cr_2S_3 (JCPDS Card no: 10-340)					Eskolaite, Cr_2O_3(JCPDS Card no: 84-1616)				
d-values	I/I_0	d-values	I/I_0	h	k	l	d-values	I/I_0	h	k	l
5.552	17	5.550	16	0	0	3					
4.910	7	4.910	10	1	0	1					
4.371	6	4.370	8	0	1	2					
3.630	11						3.627	60	0	1	2
3.235	5	3.230	6	1	0	4					
2.966	18	2.960	16	1	1	0					
2.795	4	2.783	6	0	0	6					
2.665	23						2.664	100	1	0	4
2.616	84	2.613	80	1	1	3					
2.476	17						2.476	83	1	1	0
2.266	5						2.266	5	0	0	6
2.177	10	2.180	4	0	2	4	2.173	25	1	1	3
2.028	100	2.024	100	1	1	6					
1.816	11						1.814	33	0	2	4
1.762	5	1.759	4	2	1	4					
1.713	58	1.713	50	3	0	0					
1.672	35						1.672	61	1	1	6
1.637	9	1.636	8	3	0	3					
1.570	18	1.569	25	1	1	9					
1.484	5	1.484	4	2	2	0					
1.466	11						1.463	23	2	1	4
1.432	25	1.433	10	2	2	3	1.429	27	3	0	0
1.389	11	1.388	12	0	0	12					
1.309	24	1.308	20	2	2	6					
1.296	10						1.2960	10	1	0	10
1.257	5	1.258	8	3	0	9					
1.239	4						1.1238	5	1	3	4
1.158	8	1.158	8	2	2	9					

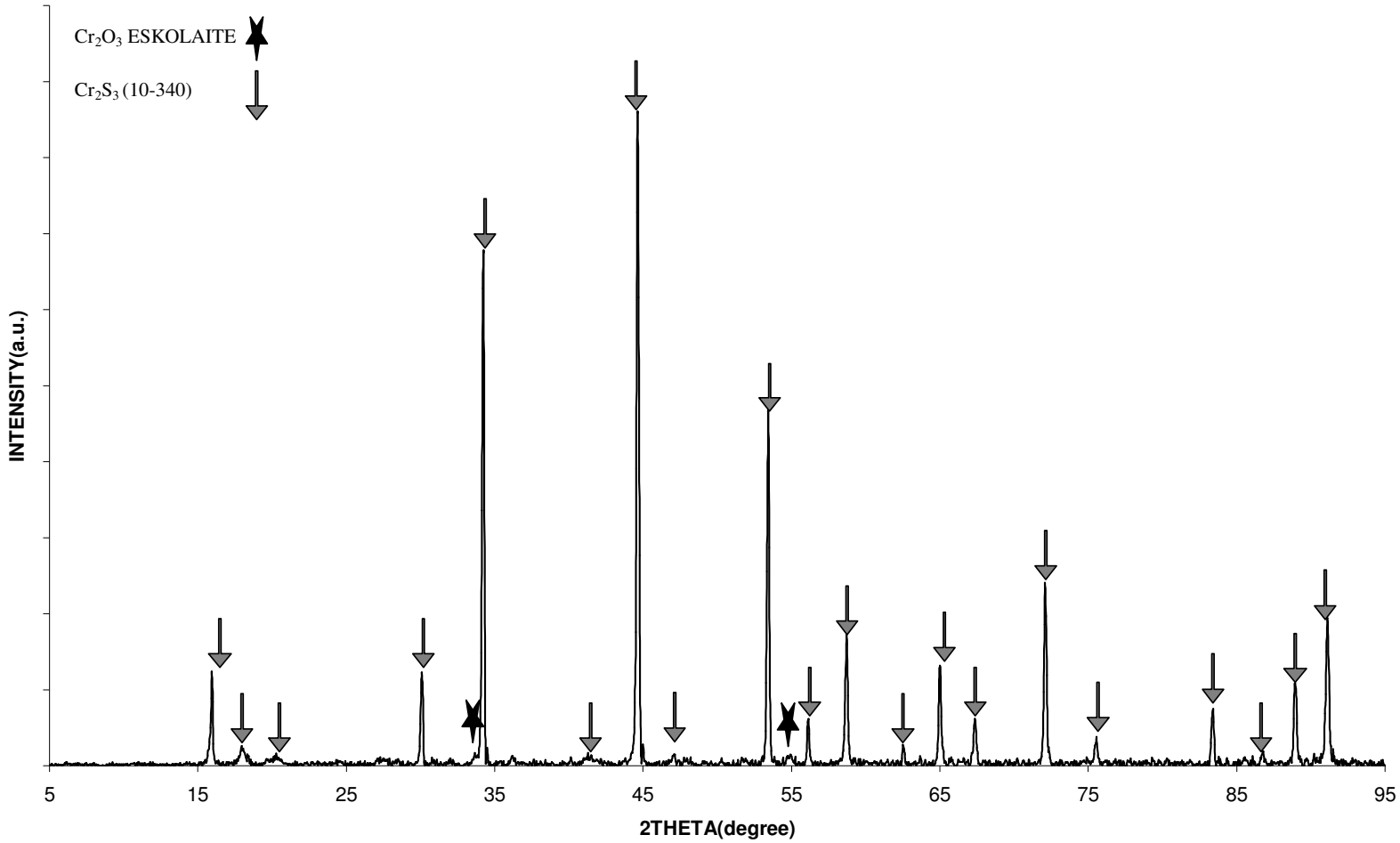

Figure Appendix B.3: X-Ray Powder Diffraction Pattern of Product obtained from the Sulfidizing Reaction of Cr_2O_3 at 850 ^oC

Table Appendix B.3: X-Ray Powder Diffraction Data of the Product obtained From the Sulfidizing Reaction of Cr_2O_3 at 850 ^{O}C

OBSERVED DATA		CARD DATA									
		Cr_2S_3 (JCPDS Card no: 10-340)					Eskolaite, Cr2O3 (JCPDS Card no: 84-1616)				
d-values	I/I_0	d-values	I/I_0	h	k	l	d-values	I/I_0	h	k	l
5.552	15	5.550	16	0	0	3					
4.937	4	4.910	10	1	0	1					
4.371	2	4.370	8	0	1	2					
2.966	15	2.960	16	1	1	0					
2.661	2						2.664	100	1	0	4
2.616	79	2.613	80	1	1	3					
2.184	2	2.180	4	0	2	4					
2.028	100	2.024	100	1	1	6					
1.928	2	1.926	4	0	1	8					
1.713	55	1.713	50	3	0	0					
1.671	2						1.672	61	1	1	6
1.637	8	1.636	8	3	0	3					
1.572	21	1.569	25	1	1	9					
1.485	4	1.484	4	2	2	0					
1.434	16	1.433	10	2	2	0					
1.389	8	1.388	12	0	0	12					
1.309	28	1.308	20	2	2	6					
1.257	5	1.258	8	3	0	9					
1.158	9	1.158	8	2	2	9					
1.121	3	1.122	4	4	1	0					
1.099	13	1.099	12	4	1	3					
1.079	23	1.079	20	2	0	14					

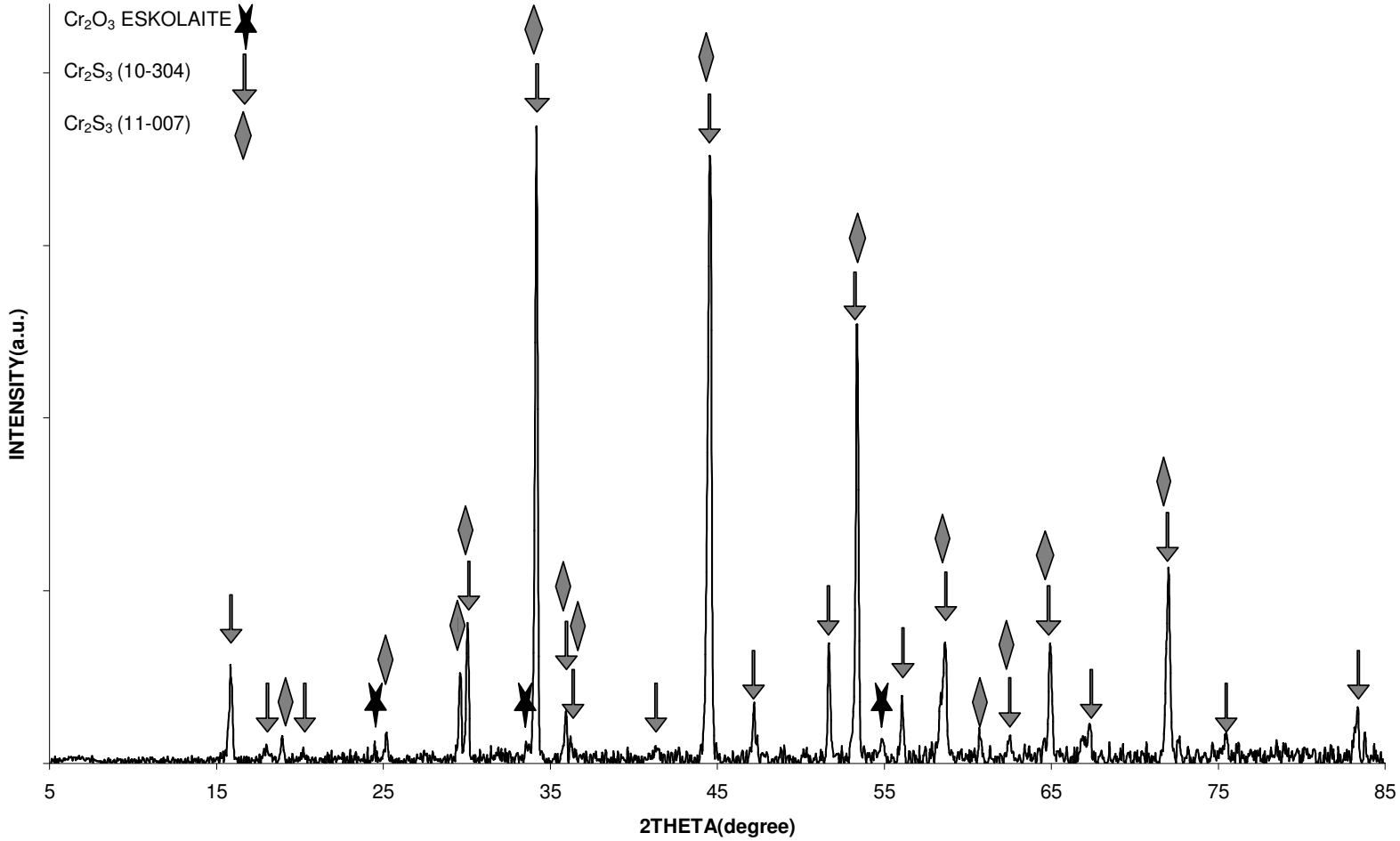

Figure Appendix B.4: X-Ray Powder Diffraction Pattern of Product obtained from the Sulfidizing Reaction of Cr_2O_3 at 1250 ^oC

Table Appendix B.4: X-Ray Powder Diffraction Data of the Product obtained From the Sulfidizing Reaction of Cr_2O_3 at 1250 ^{O}C

OBSERVED DATA		CARD DATA														
		Cr_2S_3 (JCPDS Card no: 10-340)					Cr_2S_3 (JCPDS Card no: 11-007)					Eskolaite, Cr_2O_3 (JCPDS Card no: 84-1616)				
d-values	I/I_0	d-values	I/I_0	h	k	l	d-values	I/I_0	h	k	l	d-values	I/I_0	h	k	l
5.569	16	5.550	16	0	0	3	5.560	15	0	0	2					
4.910	4	4.910	10	1	0	1										
4.679	5						4.670	15	1	0	1					
4.392	3	4.370	8	0	1	2										
3.630	4											3.627	60	0	1	2
3.531	5						3.538	15	1	0	2					
3.010	15						3.010	9	1	0	3					
2.971	23	2.960	16	1	1	0	2.970	15	1	1	0					
2.661	4											2.664	100	1	0	4
2.620	100	2.613	80	1	1	3	2.620	85	1	1	2					
2.496	9						2.505	5	2	0	1					
2.473	5											2.476	83	1	1	0
2.179	3	2.180	4	0	2	4										
2.030	99	2.024	100	1	1	6	2.036	100	1	1	4					
1.924	10	1.926	4	0	1	8										
1.767	20	1.759	4	2	1	4										
1.714	50	1.713	50	3	0	0	1.714	50	3	0	0					
1.672	4	1.678	4	1	2	5										
1.639	11	1.636	8	3	0	3										
1.579	12						1.579	25	1	1	6					
1.573	20	1.569	25	1	1	9										
1.524	6						1.527	3	1	0	7					
1.484	5	1.484	4	2	2	0	1.487	3	2	2	0					
1.435	20	1.433	10	2	2	3	1.435	15	2	2	2					
1.389	7	1.388	12	0	0	12										
1.310	32	1.308	20	2	2	6	1.311	30	2	2	4					
1.258	6	1.258	8	3	0	9										
1.158	10	1.158	8	2	2	9										

APPENDIX C

Table Appendix C.1: X-ray powder diffraction data of Reactant Pyrolusite, MnO_2 (JCPDS Card no: 24-735) that used in Sulfidizing Reactions of MnO_2

OBSERVED DATA		CARD DATA				
		Pyrolusite, MnO_2 (JCPDS Card no: 24-735)				
d-values	I/I_0	d-values	I/I_0	h	k	l
3.097	92	3.110	100	1	1	0
2.399	100	2.407	55	1	0	1
2.192	9	2.199	8	2	0	0
2.128	9	2.110	16	1	1	1
1.961	9	1.968	5	2	1	0
1.627	18	1.623	55	2	1	1
1.552	25	1.555	14	2	2	0
1.435	15	1.437	8	0	0	2
1.390	15	1.391	8	3	1	0
1.303	31	1.306 1.304	20 20	3 1	0 1	1 2
1.202	12	1.203	3	2	0	2
1.122	10	1.123	3	2	0	2
1.055	17	1.056	6	2	2	2

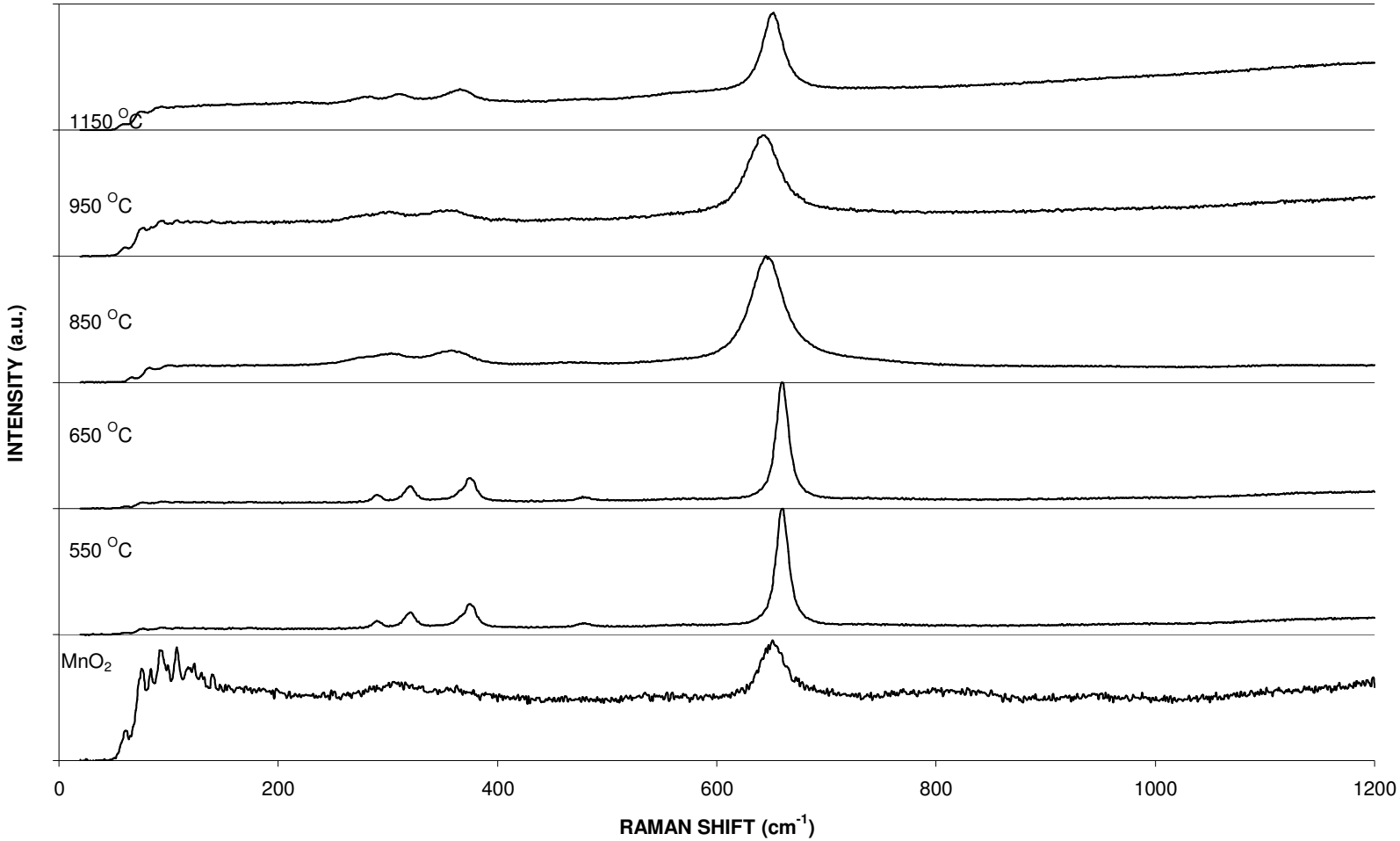

Figure Appendix C.1: Raman Scattering Spectra of Reactant and Products of Sulfidizing Reaction of MnO_2

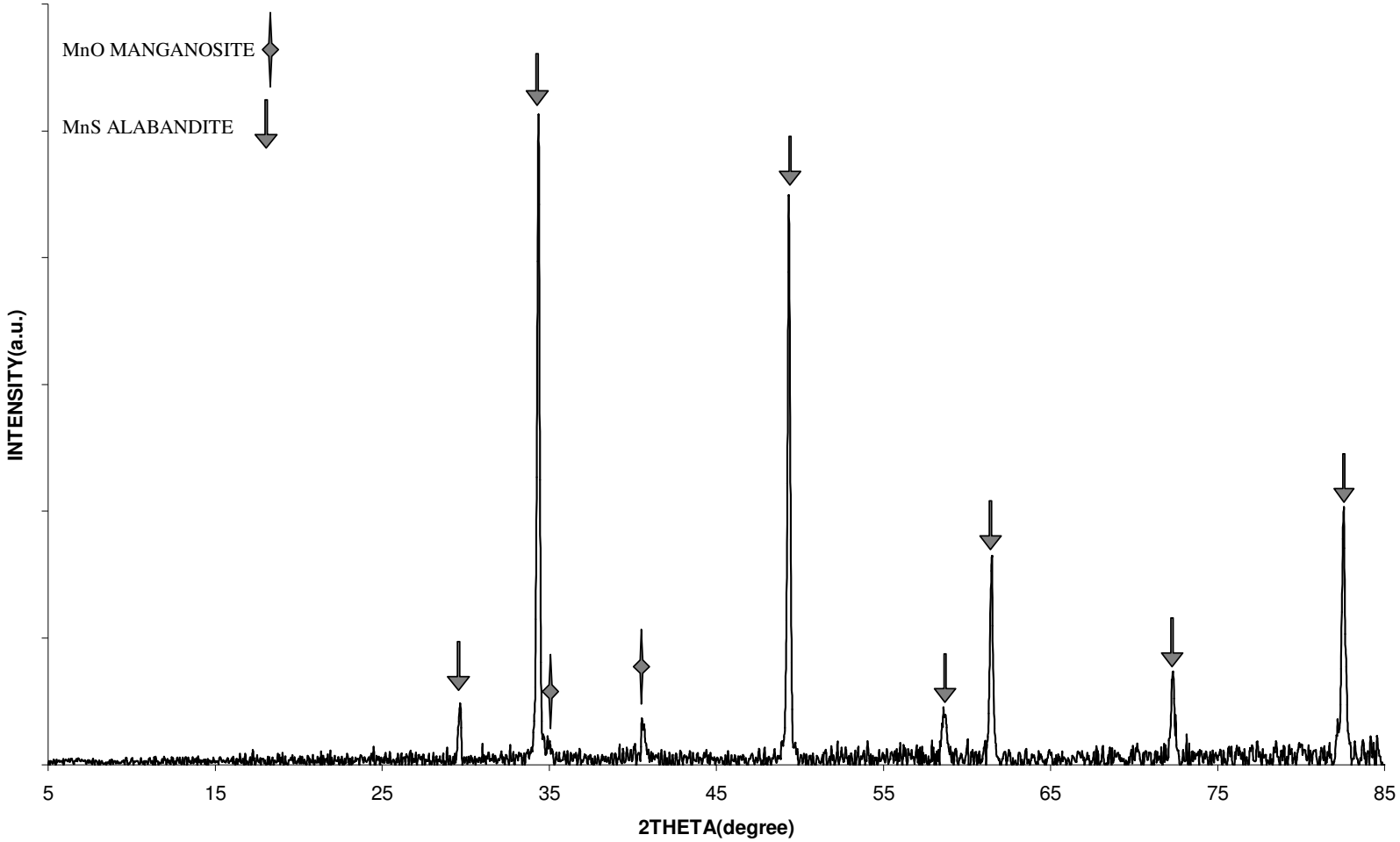

Figure Appendix C.2: X-Ray Powder Diffraction Pattern of Product obtained from the Sulfidizing Reaction of MnO_2 at 550 ^{o}C

Table Appendix C.2: X-Ray Powder Diffraction Data of the Product obtained From the Sulfidizing Reaction of MnO_2 at 550 ^{O}C

.

OBSERVED DATA		CARD DATA									
		Alabandite, MnS (JCPDS Card no:06-518)					Mangonosite, MnO (JCPDS Card no: 7-230)				
d-values	I/I_0	d-values	I/I_0	h	k	l	d-values	I/I_0	h	k	l
3.005	10	3.015	14	1	1	1					
2.605	100	2.612	100	2	0	0					
2.569	5						2.567	64	1	1	1
2.215	8						2.223	100	2	0	0
1.845	88	1.847	50	2	2	0					
1.570	9	1.575	6	3	1	1					
1.507	32	1.509	20	2	2	2					
1.305	15	1.306	8	4	0	0					
1.168	40	1.168	20	4	2	0					

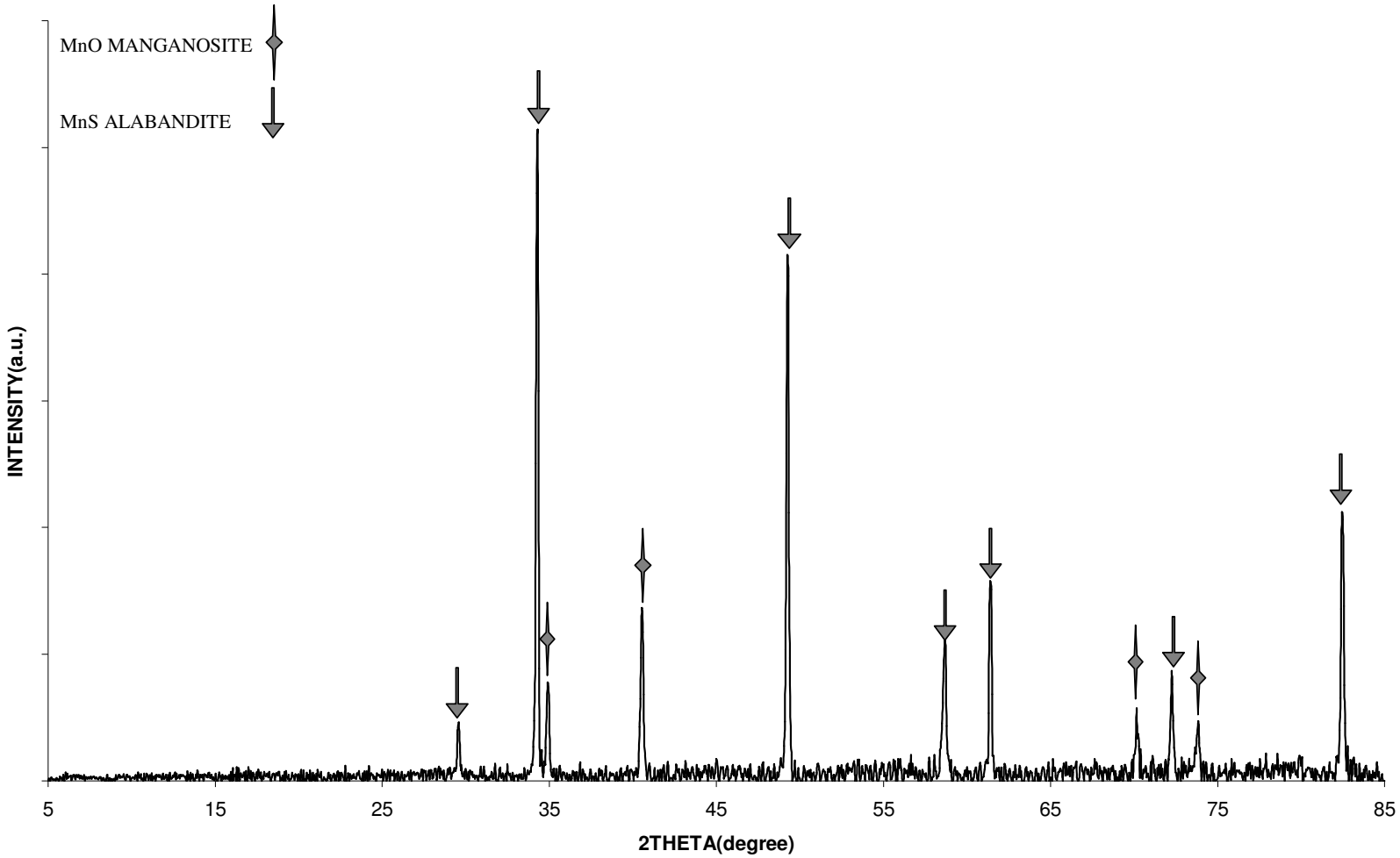

Figure Appendix C.3: X-Ray Powder Diffraction Pattern of Product obtained from the Sulfidizing Reaction of MnO_2 at 650 ^{o}C

Table Appendix C.3: X-Ray Powder Diffraction Data of the Product obtained From the Sulfidizing Reaction of MnO_2 at 650 ^{O}C

OBSERVED DATA		CARD DATA									
		Alabandite, MnS (JCPDS Card no:06-518)					Mangonosite, MnO (JCPDS Card no: 7-230)				
d-values	I/I_0	d-values	I/I_0	h	k	l	d-values	I/I_0	h	k	l
3.015	10	3.015	14	1	1	1					
2.612	100	2.612	100	2	0	0					
2.565	16						2.567	64	1	1	1
2.223	27						2.223	100	2	0	0
1.847	82	1.847	50	2	2	0					
1.572	22	1.575	6	3	1	1					
1.509	31	1.509	20	2	2	2					
1.340	12						1.341	20	3	1	1
1.307	17	1.306	8	4	0	0					
1.282	10						1.283	14	2	2	2
1.167	42	1.168	20	4	2	0					

Table Appendix C.4: X-Ray Powder Diffraction Data of the Product obtained From the Sulfidizing Reaction of MnO_2 at 850 ^{O}C

OBSERVED DATA		CARD DATA									
		Alabandite, MnS (JCPDS Card no:06-518)					Mangonosite, MnO (JCPDS Card no: 7-230)				
d-values	I/I_0	d-values	I/I_0	h	k	l	d-values	I/I_0	h	k	l
3.010	11	3.015	14	1	1	1					
2.609	100	2.612	100	2	0	0					
2.562	5						2.567	64	1	1	1
2.220	8						2.223	100	2	0	0
1.845	81	1.847	50	2	2	0					
1.574	9	1.575	6	3	1	1					
1.571	6						1.572	49	2	2	0
1.508	33	1.509	20	2	2	2					
1.340	4						1.341	20	3	1	1
1.305	17	1.306	8	4	0	0					
1.168	45	1.168	20	4	2	0					

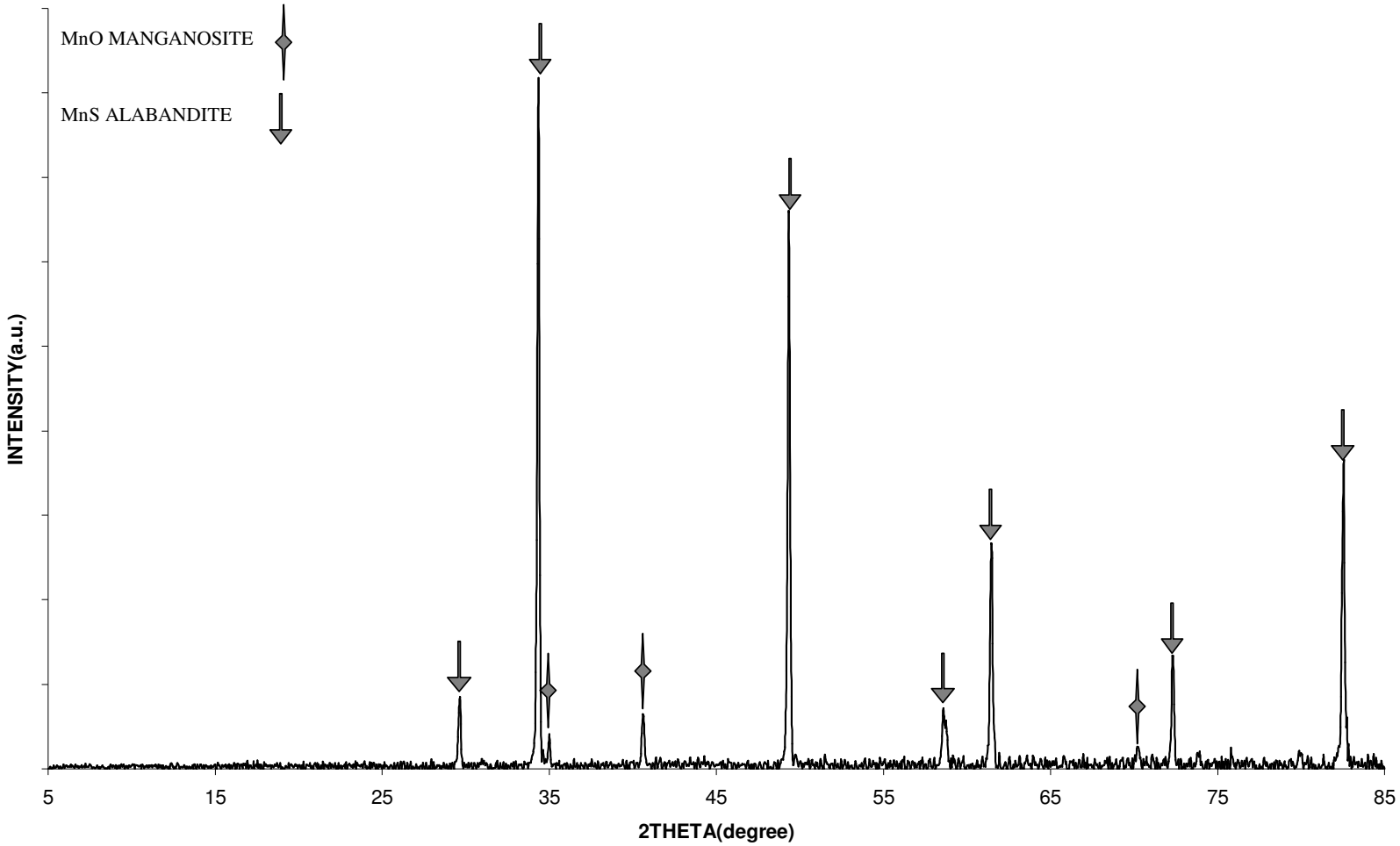

Figure Appendix C.4: X-Ray Powder Diffraction Pattern of Product obtained from the Sulfidizing Reaction of MnO_2 at 850 ^{o}C

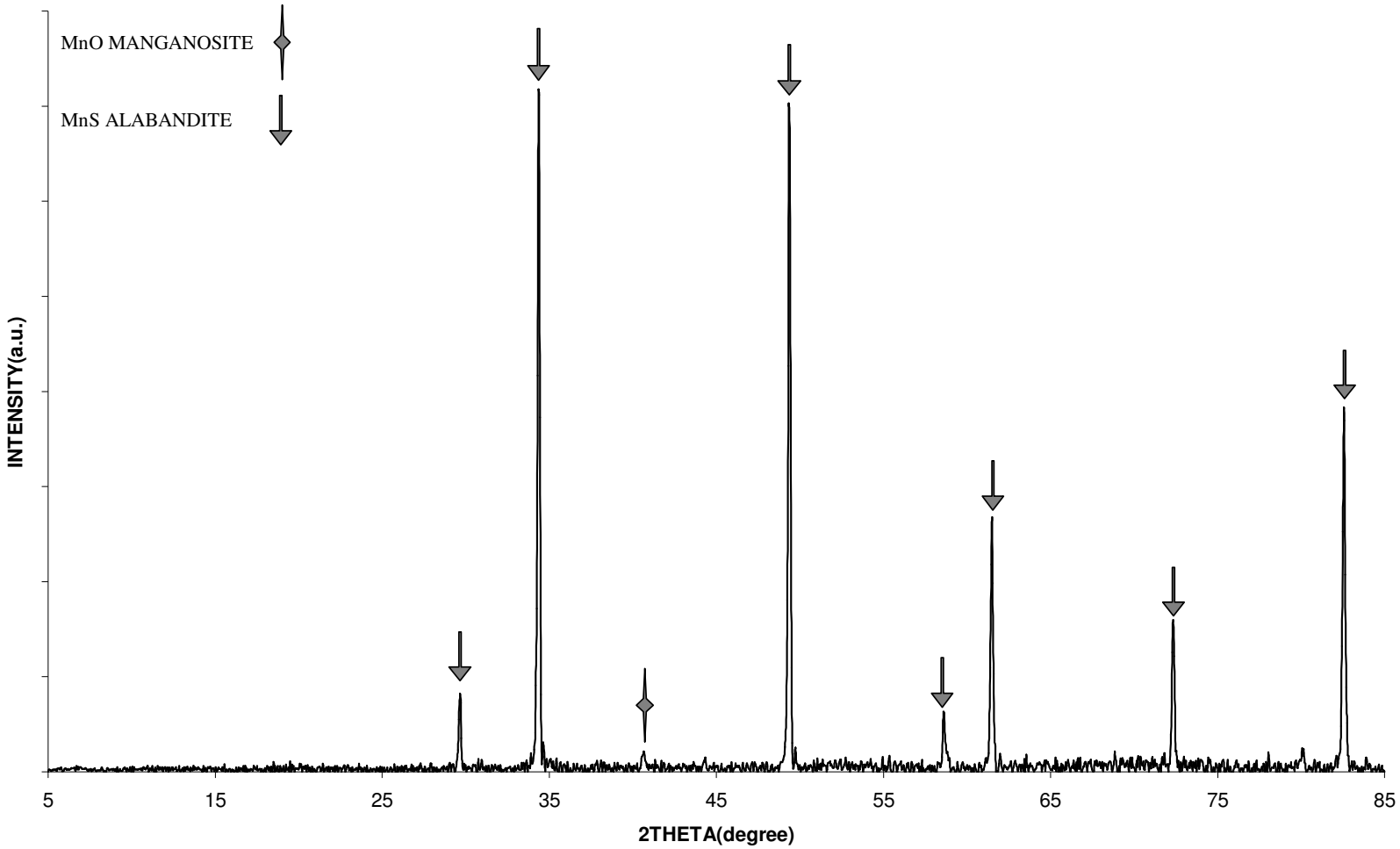

Figure Appendix C.5: X-Ray Powder Diffraction Pattern of Product obtained from the Sulfidizing Reaction of MnO_2 at 950 ^{o}C

Table Appendix C.5: X-Ray Powder Diffraction Data of the Product obtained From the Sulfidizing Reaction of MnO_2 at 950 ^{O}C

OBSERVED DATA		CARD DATA									
		Alabandite, MnS (JCPDS Card no:06-518)					Mangonosite, MnO (JCPDS Card no: 7-230)				
d-values	I/I_0	d-values	I/I_0	h	k	l	d-values	I/I_0	h	k	l
3.015	12	3.015	14	1	1	1					
2.612	100	2.612	100	2	0	0					
2.220	17						2.223	100	2	0	0
1.847	99	1.847	50	2	2	0					
1.575	9	1.575	6	3	1	1					
1.509	38	1.509	20	2	2	2					
1.307	23	1.306	8	4	0	0					
1.168	54	1.168	20	4	2	0					

Table Appendix C.6: X-Ray Powder Diffraction Data of the Product obtained From the Sulfidizing Reaction of MnO_2 at 1150 ^{O}C

OBSERVED DATA		CARD DATA				
		Alabandite, MnS (JCPDS Card no:06-518)				
d-values	I/I_0	d-values	I/I_0	h	k	L
6.125	3					
3.010	11	3.015	14	1	1	1
2.740	8					
2.609	100	2.612	100	2	0	0
2.473	4					
2.366	4					
2.220	4					
1.845	75	1.847	50	2	2	0
1.574	8	1.575	6	3	1	1
1.508	22	1.509	20	2	2	2
1.306	13	1.306	8	4	0	0
1.168	37	1.168	20	4	2	0

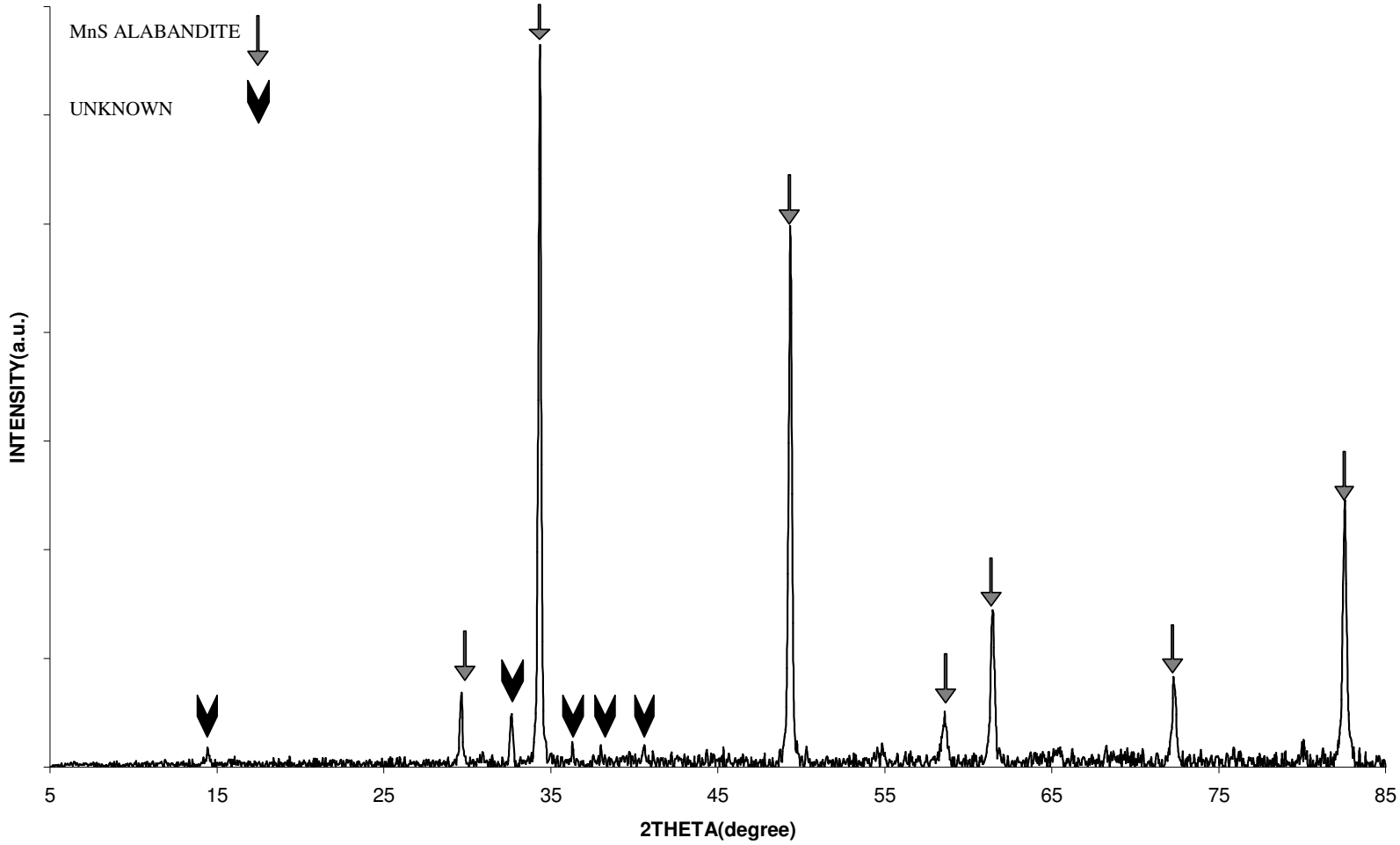

Figure Appendix C.6: X-Ray Powder Diffraction Pattern of Product obtained from the Sulfidizing Reaction of MnO_2 at 1150 ^{o}C

APPENDIX D

Table Appendix D.1: X-ray powder diffraction data of Reactant Hematite, Fe_2O_3 (JCPDS Card no: 33-664) that used in Sulfidizing Reactions of Fe_2O_3.

OBSERVED DATA		CARD DATA				
		Fe_2O_3 (Hematite, JCPDS Card no: 33-664)				
d-values	I/I_0	d-values	I/I_0	h	k	l
3.6746	23	3.68	37	0	1	2
2.6961	100	2.698	100	1	0	4
2.5129	75	2.516	74	1	1	0
2.2046	26	2.205	19	1	1	3
1.8398	50	1.840	35	0	2	4
1.6937	62	1.694	40	1	1	6
1.5989	14	1.598	8	0	1	8
1.4858	43	1.485	25	2	1	4
1.4535	43	1.453	24	3	0	0
1.3488	7	1.349	2	2	0	8
1.3112	17	1.310	9	1	0	10
1.2588	11	1.258	5	2	2	0
1.1897	11	1.189	3	1	2	8
1.1630	11	1.162	4	0	2	10
1.1407	15	1.140	6	1	3	4
1.1034	15	1.103	5	2	2	6
1.0558	16	1.056	7	2	1	10

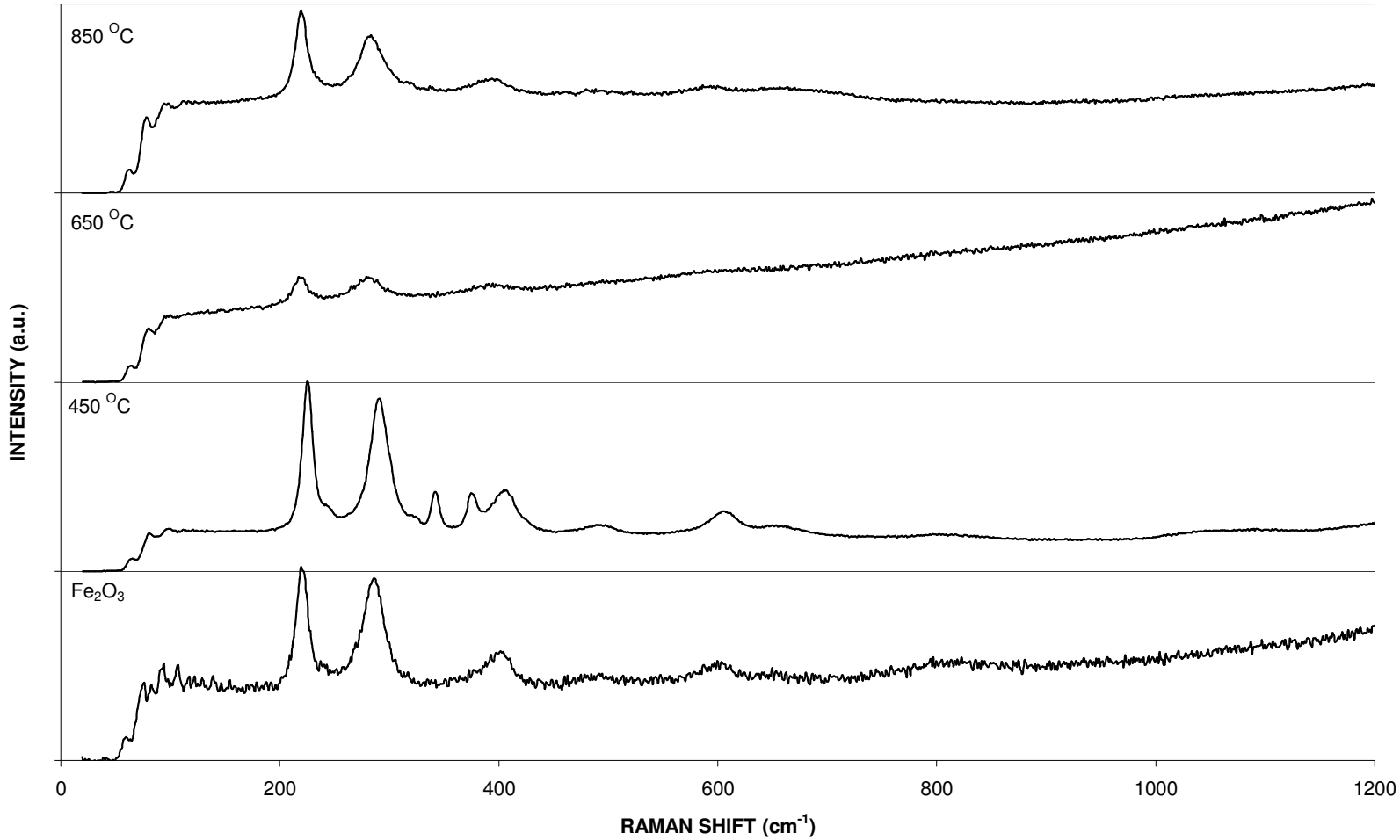

Figure Appendix D.1: Raman Scattering Spectra of Reactant and Products of Sulfidizing Reaction of Fe_2O_3

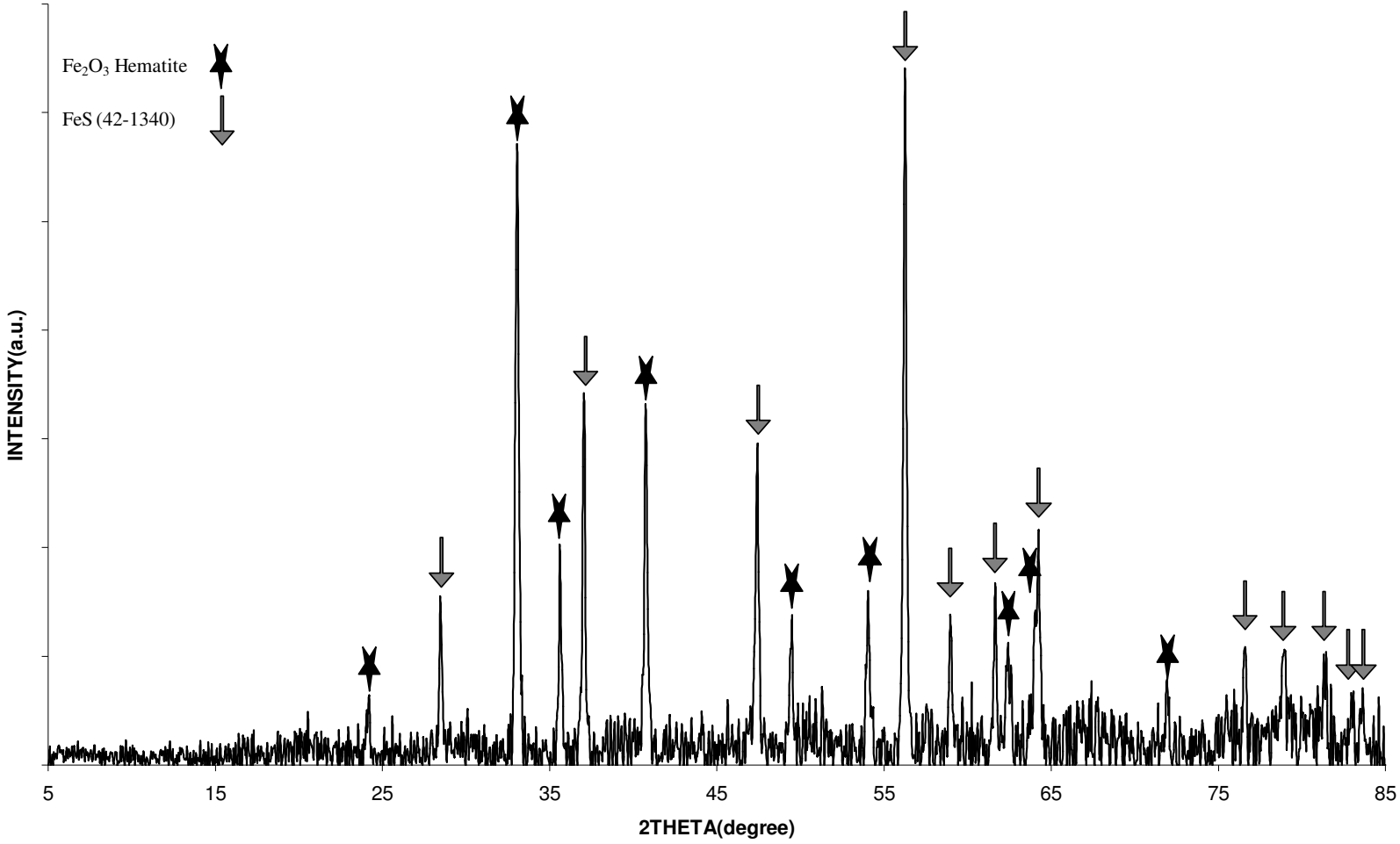

Figure Appendix D.2: X-Ray Powder Diffraction Pattern of Product obtained from the Sulfidizing Reaction of Fe_2O_3 at 450 ^oC

Table Appendix D.2: X-Ray Powder Diffraction Data of the Product obtained From the Sulfidizing Reaction of Fe_2O_3 at 450 ^{O}C

OBSERVED DATA		CARD DATA									
		FeS (JCPDS Card no: 42-1340)					Hematite, Fe_2O_3 (JCPDS Card no: 33-664)				
d-values	I/I_0	d-values	I/I_0	h	k	l	d-values	I/I_0	h	k	l
3.675	10						3.684	30	1	0	2
3.135	24	3.128	31	1	1	1					
2.708	90	2.705	100	2	0	0	2.700	100	1	0	4
2.520	32						2.519	70	1	1	0
2.424	54	2.421	53	2	1	0					
2.212	52	2.211	40	2	1	1	2.207	20	1	1	3
1.914	46	1.916	36	2	2	0					
1.840	22						1.841	40	2	0	4
1.695	26						1.694	45	1	1	6
1.634	100	1.633	69	3	1	1					
1.565	22	1.564	11	2	2	2					
1.503	27	1.502	13	3	2	0					
1.486	18						1.486	30	2	1	4
1.453	23						1.454	30	3	0	0
1.449	34	1.448	16	3	2	1					
1.311	13	1.314	1	4	1	0	1.311	10	1	0	10
1.243	17	1.243	6	3	3	1					
1.212	17	1.212	7	4	2	0	1.214	2	2	2	3
1.182	16	1.182	7	4	2	1					
1.163	10						1.163	5	2	0	1
1.155	10	1.155	3	3	3	2					

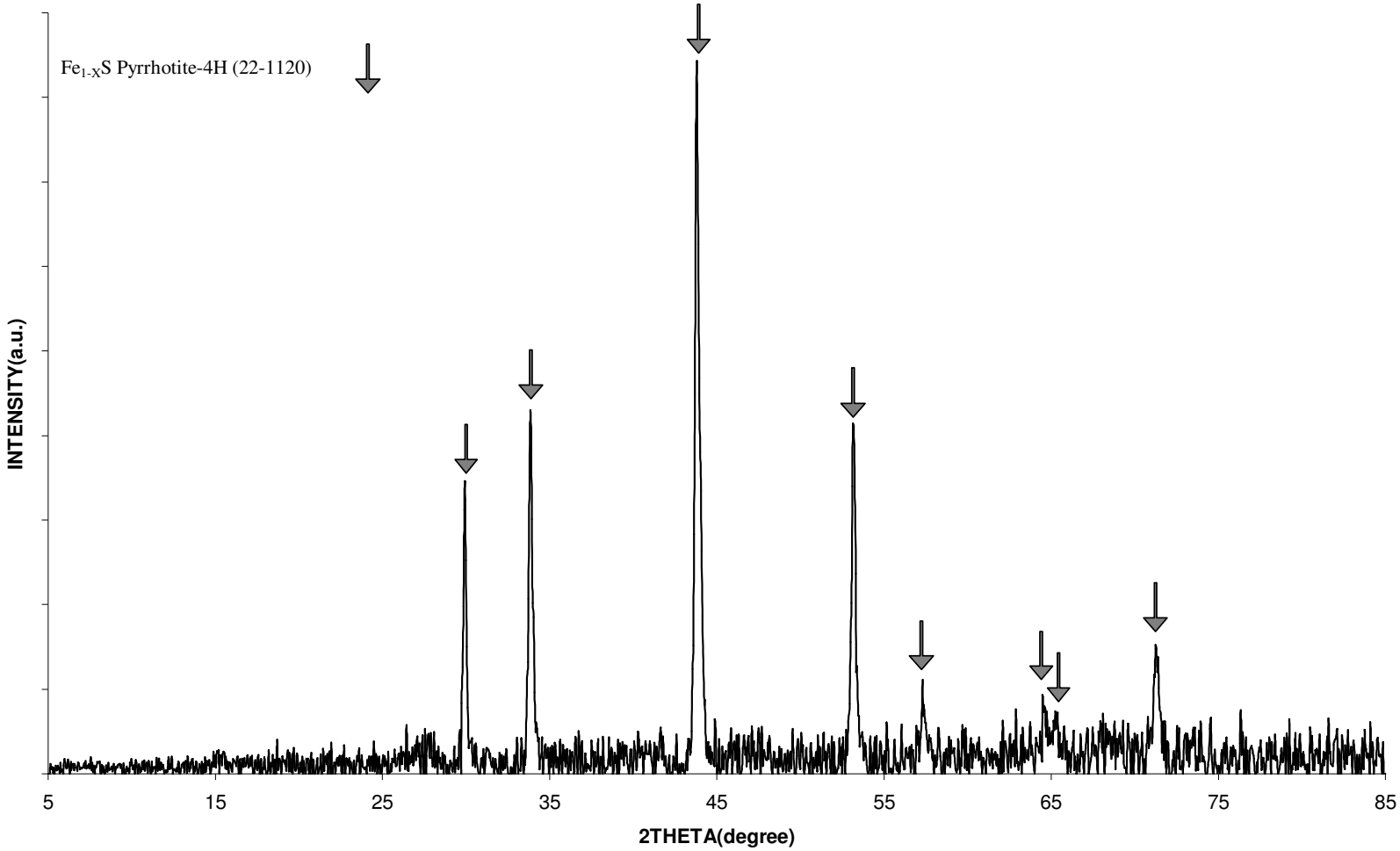

Figure Appendix D.3: X-Ray Powder Diffraction Pattern of Product obtained from the Sulfidizing Reaction of Fe_2O_3 at 650 ^oC

Table Appendix D.3: X-Ray Powder Diffraction Data of the Product obtained From the Sulfidizing Reaction of Fe_2O_3 at 650 ^{O}C

OBSERVED DATA		CARD DATA				
		Pyrrohotite-4H, $Fe_{1-X}S$ (JCPDS Card no: 22-1120)				
d-values	I/I_0	d-values	I/I_0	h	k	l
2.981	41	2.980	40	2	0	0
2.642	51	2.640	50	2	0	4
2.063	100	2.064	100	2	0	8
1.720	50	1.720	40	2	2	0
1.607	14	1.606	7	2	1	10
1.444	11	1.442	10	4	0	4
1.429	9	1.433	20	2	0	14
1.322	18	1.321	20	4	0	8

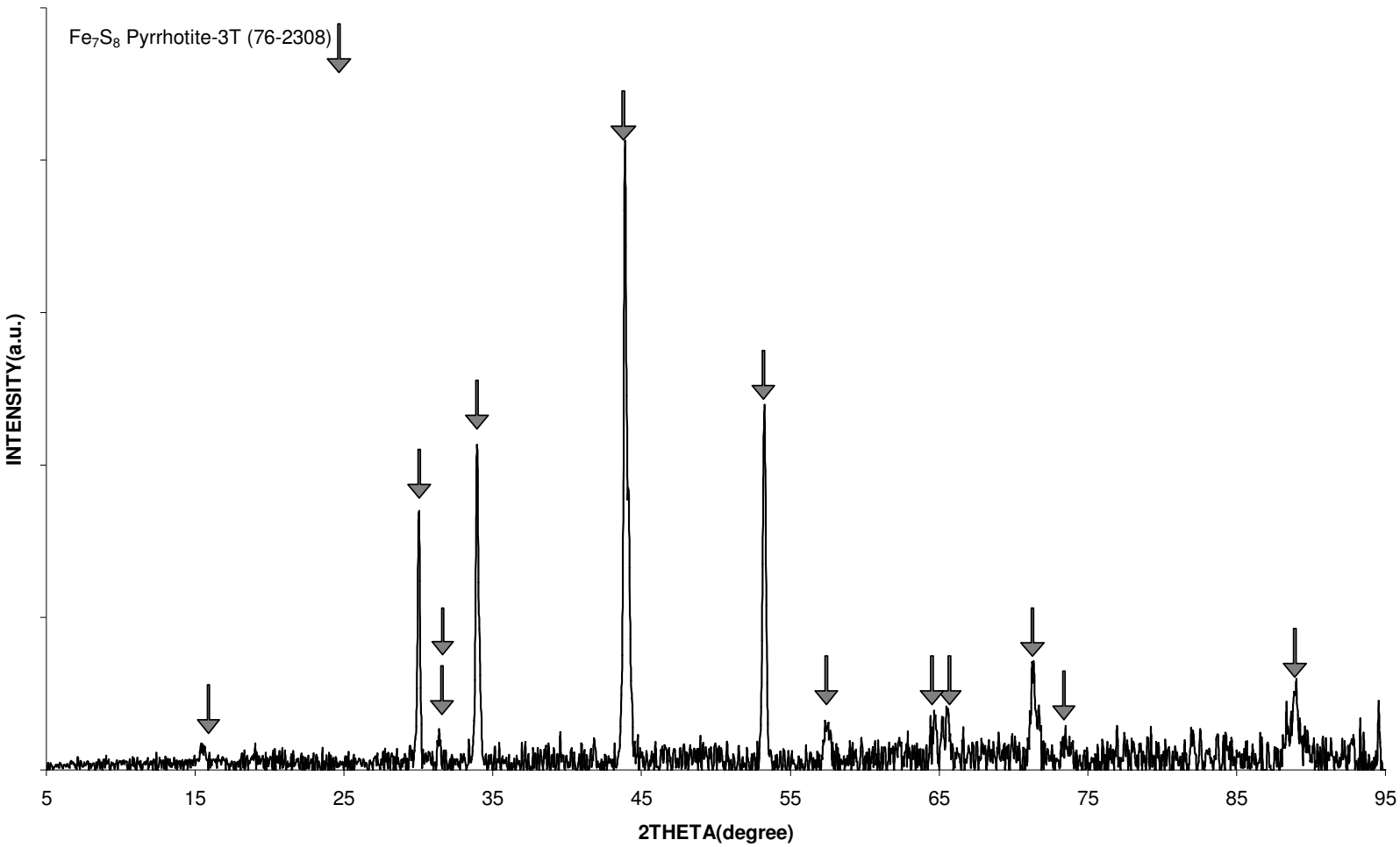

Figure Appendix D.4: X-Ray Powder Diffraction Pattern of Product b obtained from the Sulfidizing Reaction of Fe_2O_3 at 850 ^oC

Table Appendix D.4: X-Ray Powder Diffraction Data of the Product obtained From the Sulfidizing Reaction of Fe_2O_3 at 850 ^{O}C.

OBSERVED DATA		CARD DATA				
		Fe_7S_8 (Pyrrhotite-3T, JCPDS Card no:76-2308)				
d-values	I/I_0	d-values	I/I_0	h	k	l
5.712	5	5.696	5	0	0	3
5.658	5	5.616	8	1	0	1
2.971	46	2.973 2.963	40 27	2 0	0 1	0 5
2.847	7	2.848	4	0	0	6
2.638	55	2.636	56	2	0	3
2.061	100	2.657	100	2	0	6
1.719	56	1.717	34	2 0	2 3	0 5
1.600	9	1.6	8	0	0	9
1.438	10	1.438	5	0	4	3
1.424	11	1.424	6	0	0	12
1.318	15	1.318	11	0	4	6
1.315	12	1.315	6	1	1	12
1.282	7	1.284	3	0	2	12
1.097	15	1.096	8	3 2	0 2	13 12

APPENDIX E

Table Appendix E.1: X-ray powder diffraction data of Reactant Co_3O_4 (JCPDS Card No: 76-1802) that used in Sulfidizing Reactions of Co_3O_4

OBSERVED DATA		CARD DATA				
		Co_3O_4 (JCPDS Card No: 76-1802)				
d-values	I/I_0	d-values	I/I_0	h	k	l
4.643	10	4.660	18	1	1	1
2.851	29	2.854	33	2	2	0
2.431	100	2.434	100	3	1	1
2.328	13	2.330	10	2	2	2
2.017	26	2.018	21	4	0	0
1.647	16	1.148	9	4	2	2
1.553	47	1.553	32	5	1	1
1.427	58	1.427	37	4	4	0
1.277	9	1.276	3	6	2	0
1.232	17	1.231	8	5	3	3
1.052	20	1,052	12	7	3	1

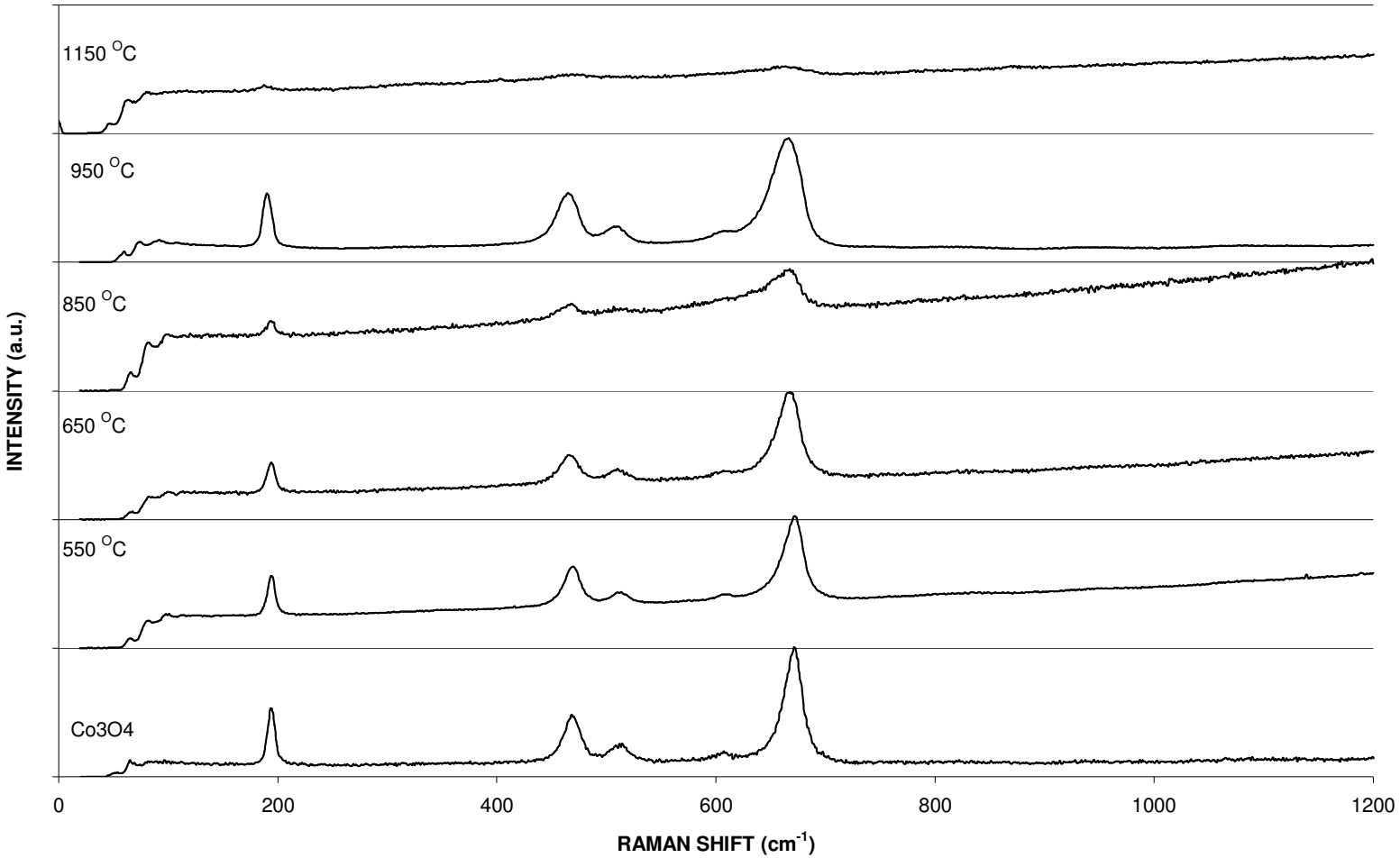

Figure Appendix E.1: Raman Scattering Spectra of Reactant and Product of Sulfidizing Reaction of Co_3O_4

Table Appendix E.2: X-Ray Powder Diffraction Data of the Product obtained From the Sulfidizing Reaction of Co_3O_4 at 550 ^{O}C

OBSERVED DATA		CARD DATA				
		Jaipurite, CoS (JCPDS Card no: 75-605)				
d-values	I/I_0	d-values	I/I_0	h	k	l
2.914	40	2.925	61	1	0	0
2.540	55	2.543	45	1	0	1
1.936	100	1.933	100	1	0	2
1.685	53	1.689	43	1	1	0
1.487	17	1.480	6	1	0	3
1.270	23	1.272	16	2	0	2

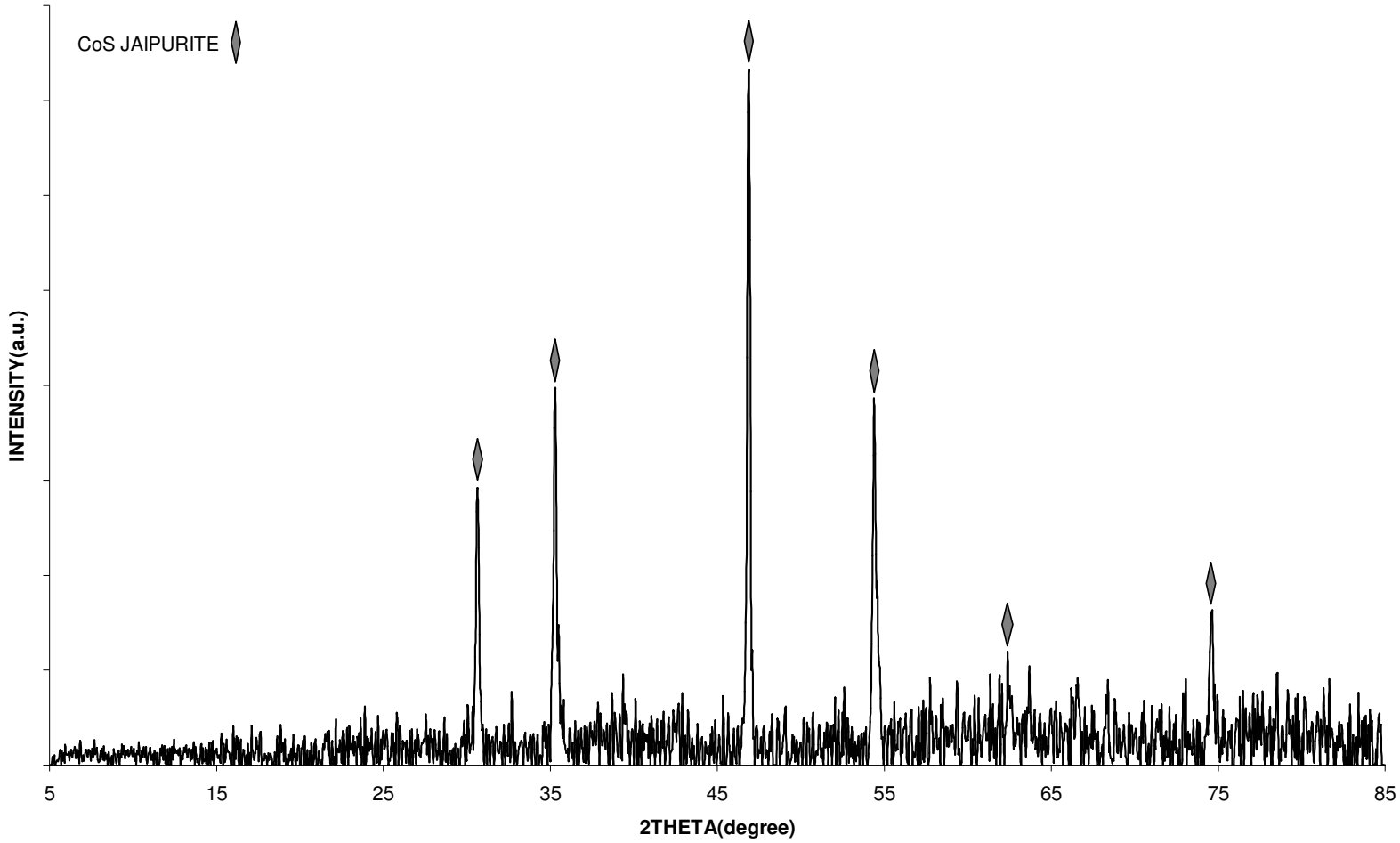

Figure Appendix E.2: X-Ray Powder Diffraction Pattern of Product obtained from the Sulfidizing Reaction of Co_3O_4 at 550 ^oC

Table Appendix E.3: X-Ray Powder Diffraction Data of the Product obtained From the Sulfidizing Reaction of Co_3O_4 at 650 ^{O}C.

OBSERVED DATA		CARD DATA				
		Jaipurite, CoS (JCPDS Card no: 75-605)				
d-values	I/I_0	d-values	I/I_0	h	k	l
2.919	36	2.925	61	1	0	0
2.544	55	2.543	45	1	0	1
1.936	100	1.933	100	1	0	2
1.685	67	1.689	43	1	1	0
1.485	16	1.480	6	1	0	3
1.272	32	1.272	16	2	0	2

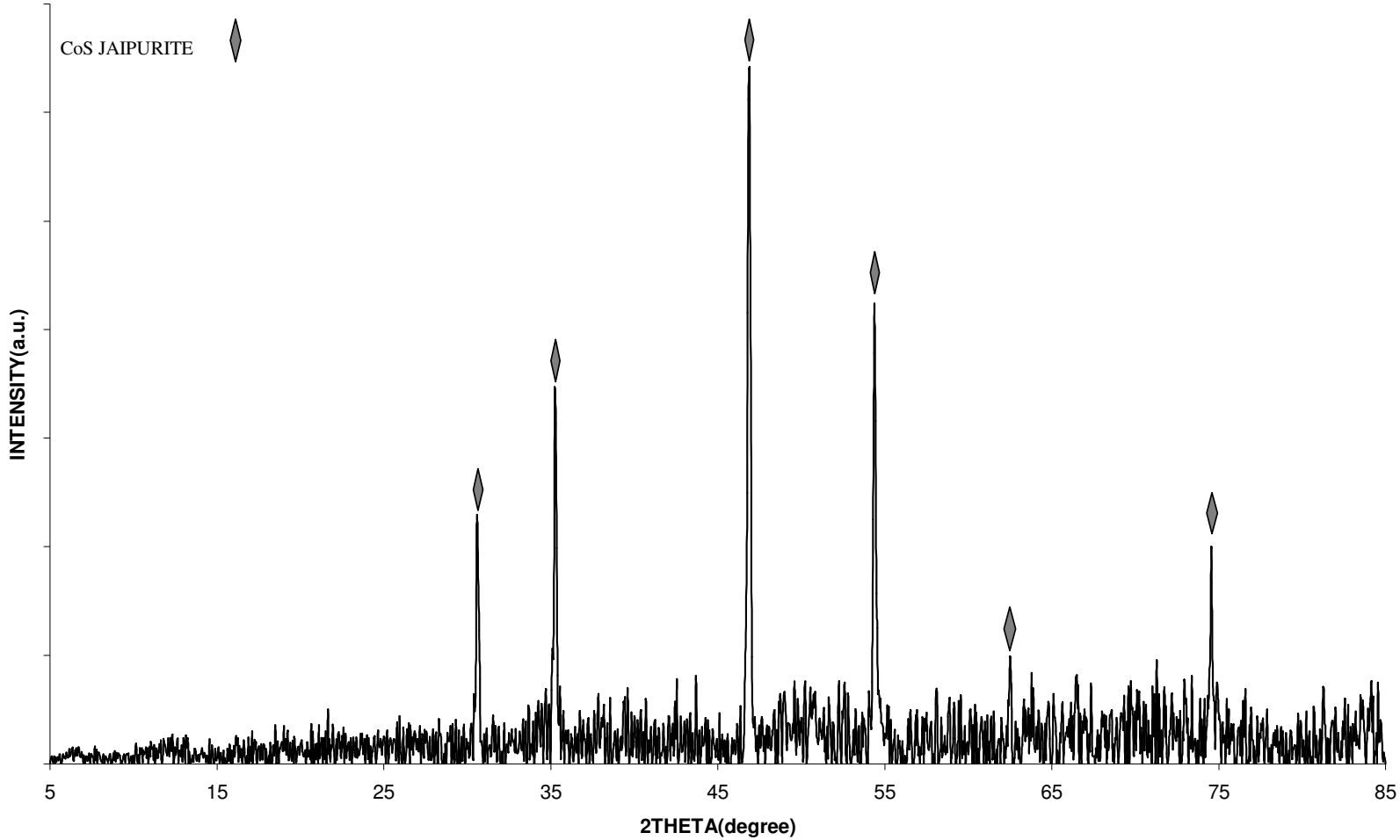

Figure Appendix E.3: X-Ray Powder Diffraction Pattern of Product obtained from the Sulfidizing Reaction of Co_3O_4 at 650 ^oC

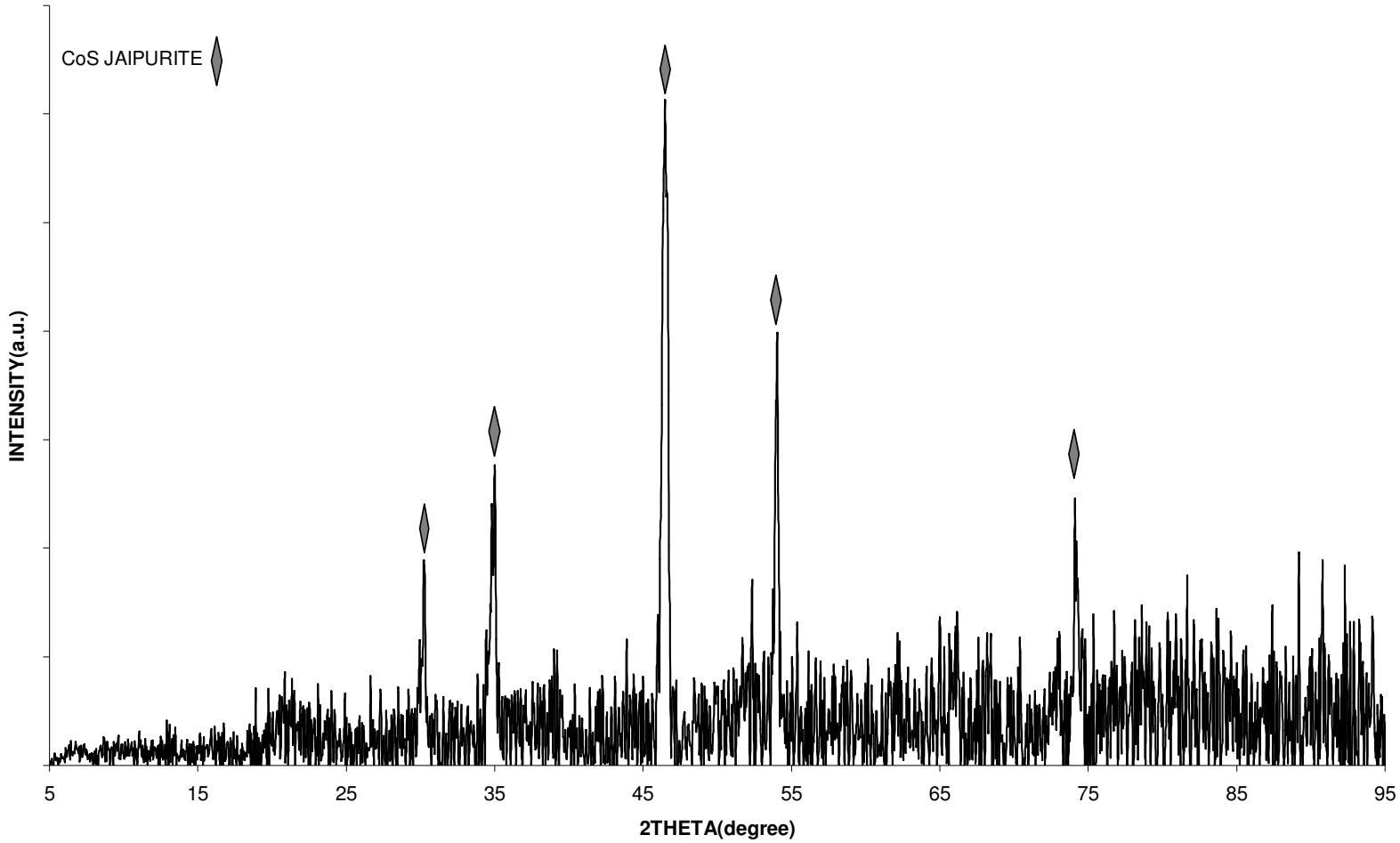

Figure Appendix E.4: X-Ray Powder Diffraction Pattern of Product obtained from the Sulfidizing Reaction of Co_3O_4 at 850 ^oC

Table Appendix E.4: X-Ray Powder Diffraction Data of the Product obtained From the Sulfidizing Reaction of Co_3O_4 at 850 ^{O}C

OBSERVED DATA		CARD DATA				
		Jaipurite, CoS (JCPDS Card no: 75-605)				
d-values	I/I_0	d-values	I/I_0	h	k	l
2.919	47	2.925	61	1	0	0
2.544	65	2.543	45	1	0	1
1.936	100	1.933	100	1	0	2
1.687	42	1.689	43	1	1	0
1.272	35	1.272	16	2	0	2

Table Appendix E.5: X-Ray Powder Diffraction Data of the Product obtained From the Sulfidizing Reaction of Co_3O_4 at 950 ^{O}C

OBSERVED DATA		CARD DATA									
		Cobaltpentlandite, Co_9S_8 (JCPDS Card no: 86-2273)					Jaipurite, CoS (JCPDS Card no: 75-605)				
d-values	I/I_0	d-values	I/I_0	h	k	l	d-values	I/I_0	h	k	l
5.730	13	5.729	31	1	1	1					
2.996	54	2.992	98	3	1	1					
2.919	29						2.925	61	1	0	0
2.864	34	2.865	32	2	2	2					
2.544	36						2.543	45	1	0	1
2.277	18	2.276	17	3	3	1					
1.940	80						1.933	100	1	0	2
1.913	35	1.910	34	5	1	1					
1.756	100	1.754	100	4	4	0					
1.688	88						1.689	43	1	1	0
1.408	20						1.407	5	2	0	1
1.293	40	1.292	12	7	3	1					

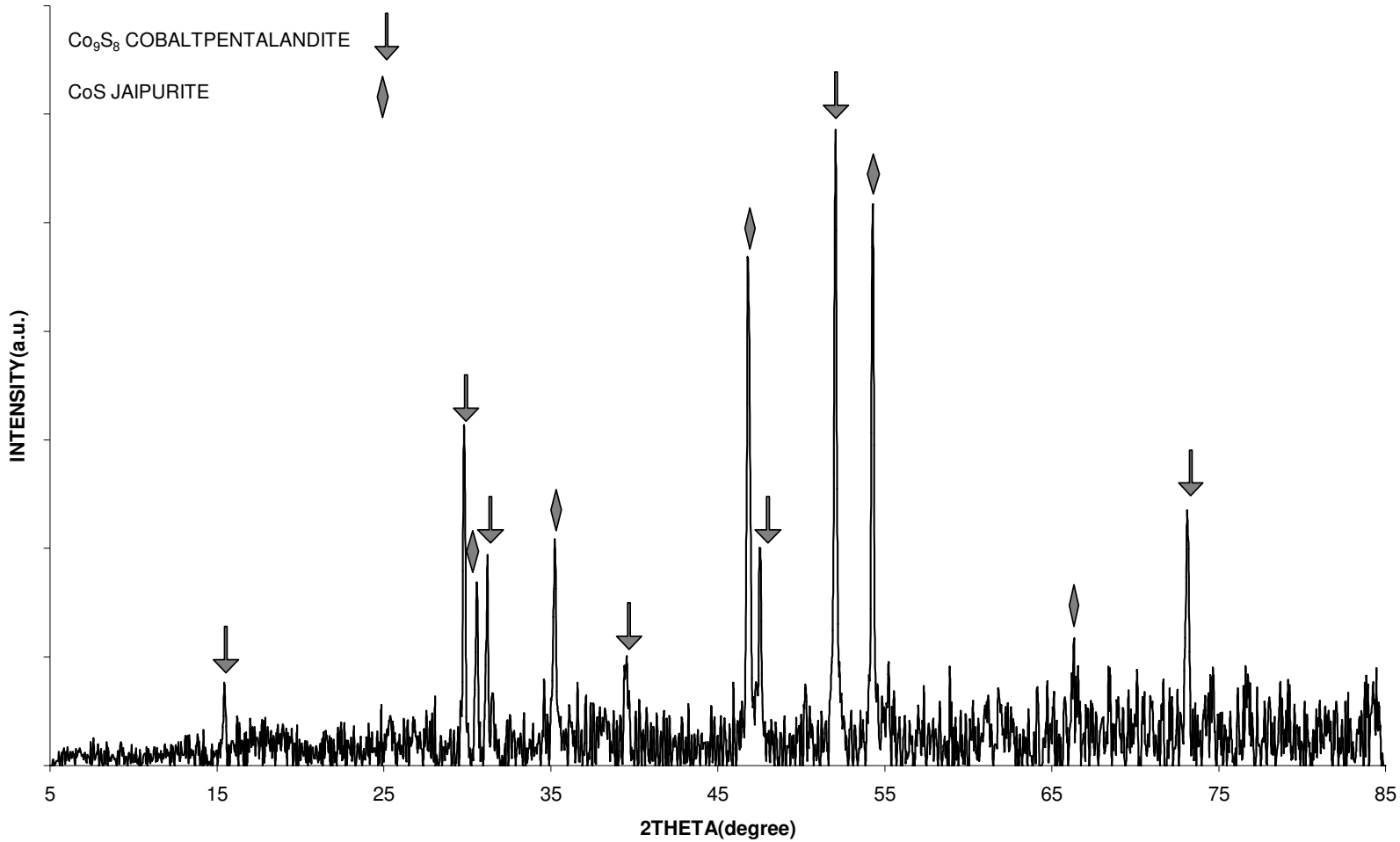

Figure Appendix E.5: X-Ray Powder Diffraction Pattern of Product obtained from the Sulfidizing Reaction of Co_3O_4 at 950 ^oC

Table Appendix E.6: X-Ray Powder Diffraction Data of the Product obtained From the Sulfidizing Reaction of Co_3O_4 at 1150 ^{O}C

OBSERVED DATA		CARD DATA				
		Cobaltpentlandite, Co_9S_8 (JCPDS Card no: 86-2273)				
d-values	I/I_0	d-values	I/I_0	h	k	l
9.157	11					
6.104	7					
5.712	8	5.729	31	1	1	1
4.607	5					
2.991	40	2.992	98	3	1	1
2.860	20	2.865	32	2	2	2
2.277	15	2.276	17	3	3	1
1.909	28	1.910	34	5	1	1
1.754	100	1.754	100	4	4	0
1.513	11	1.513	9	5	3	3
1.496	9	1.496	8	6	2	2
1.293	18	1.292	12	7	3	1
1.240	11	1.240	12	8	0	0
1.146	10	1.146	6	7	5	1

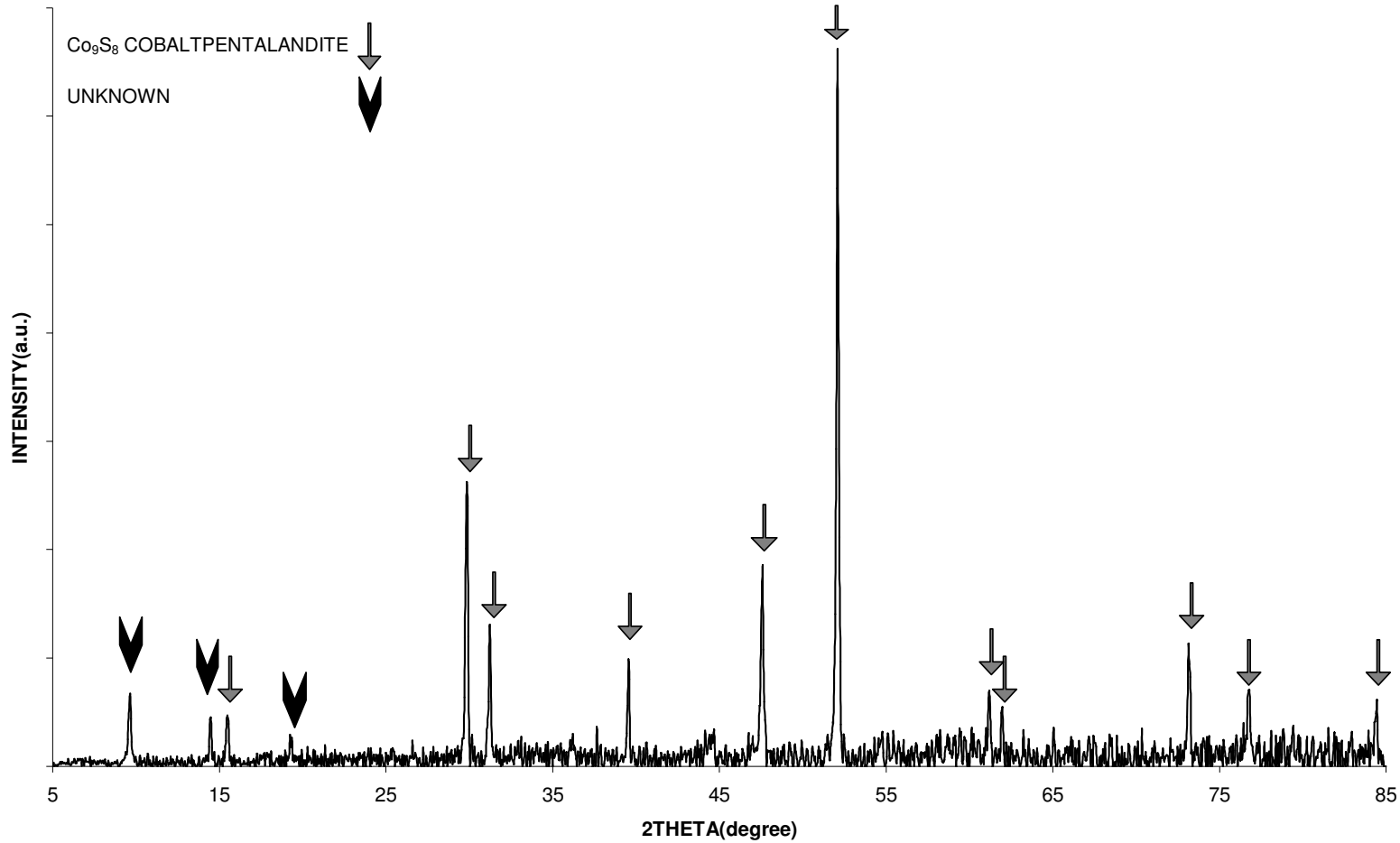

Figure Appendix E.6: X-Ray Powder Diffraction Pattern of Product obtained from the Sulfidizing Reaction of Co_3O_4 at 1150 ^oC

APPENDIX F

Table Appendix F.1: X-ray powder diffraction data of Reactant NiO (JCPDS Card No:73-1523) that used in Sulfidizing Reactions of NiO.

OBSERVED DATA		CARD DATA				
		NiO (JCPDS Card No: 73-1523)				
d-values	I/I_0	d-values	I/I_0	h	k	l
2.415	59	2.413	69	1	1	1
2.090	100	2.090	100	2	0	0
1.478	67	1.478	45	2	2	0
1.260	29	1.260	15	3	1	1
1.207	22	1.207	11	2	2	2

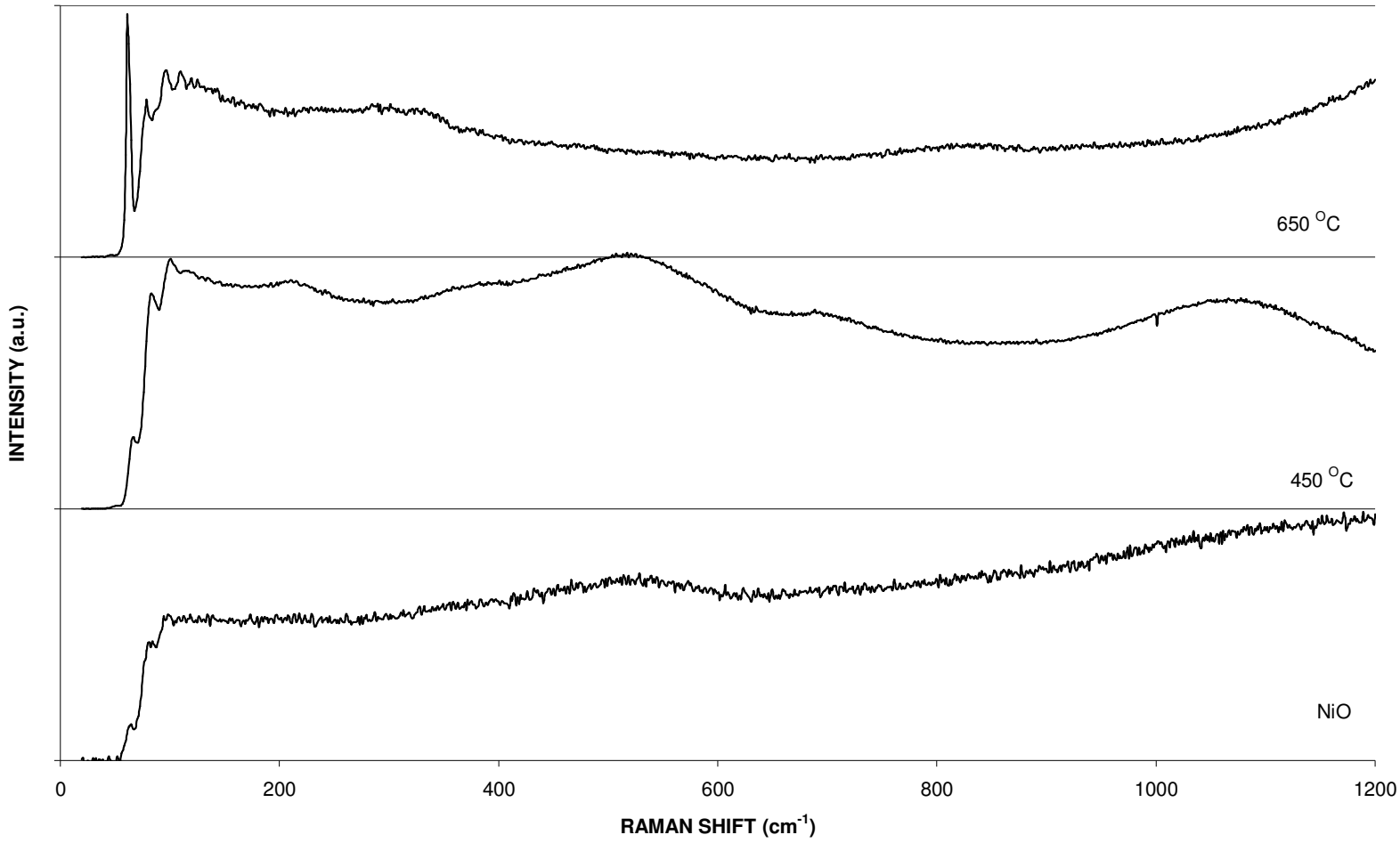

Figure Appendix F.1: Raman Scattering Spectra of Reactant and Product of Sulfidizing Reaction of NiO

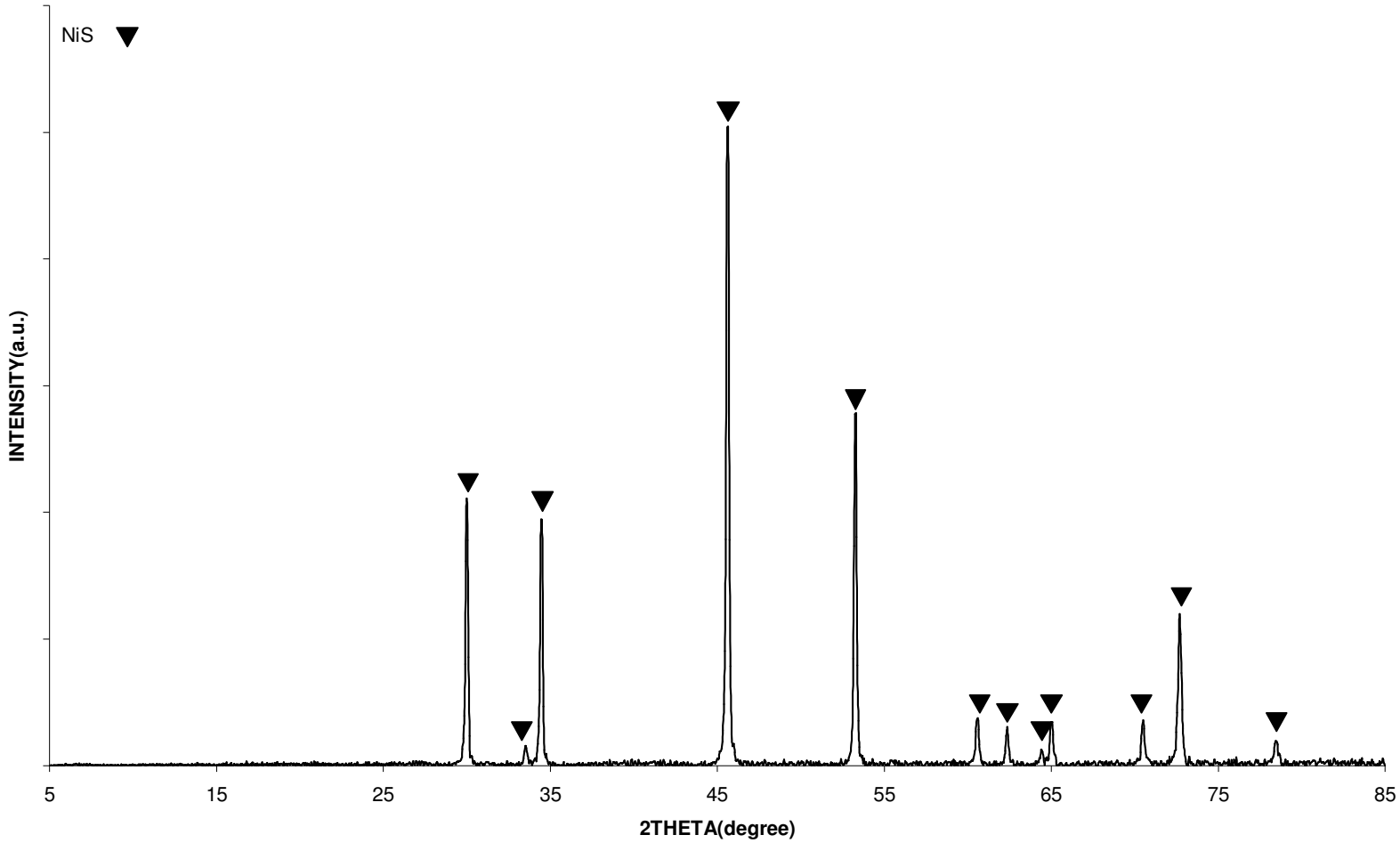

Figure Appendix F .2: X-Ray Powder Diffraction Pattern of Product obtained from the Sulfidizing Reaction of NiO at 450 ^{o}C

Table Appendix F.2: X-Ray Powder Diffraction Data of the Product obtained From the Sulfidizing Reaction of NiO at 450 ^{O}C

OBSERVED DATA		CARD DATA				
		NiS (JCPDS Card No: 77-1624)				
d-values	I/I_0	d-values	I/I_0	h	k	l
2.971	42	2.978	60	1	0	0
2.669	4	2.662	5	0	0	2
2.598	39	2.599	44	1	0	1
1.986	100	1.985	100	1	0	2
1.717	56	1.719	43	1	1	0
1.527	8	1.525	6	1	0	3
1.488	7	1.489	5	2	0	0
1.446	3	1.444	3	1	1	2
1.433	7	1.434	5	2	0	1
1.335	8	1.331	5	0	0	4
1.300	24	1.300	16	2	0	2
1.217	4	1.215	3	1	0	4

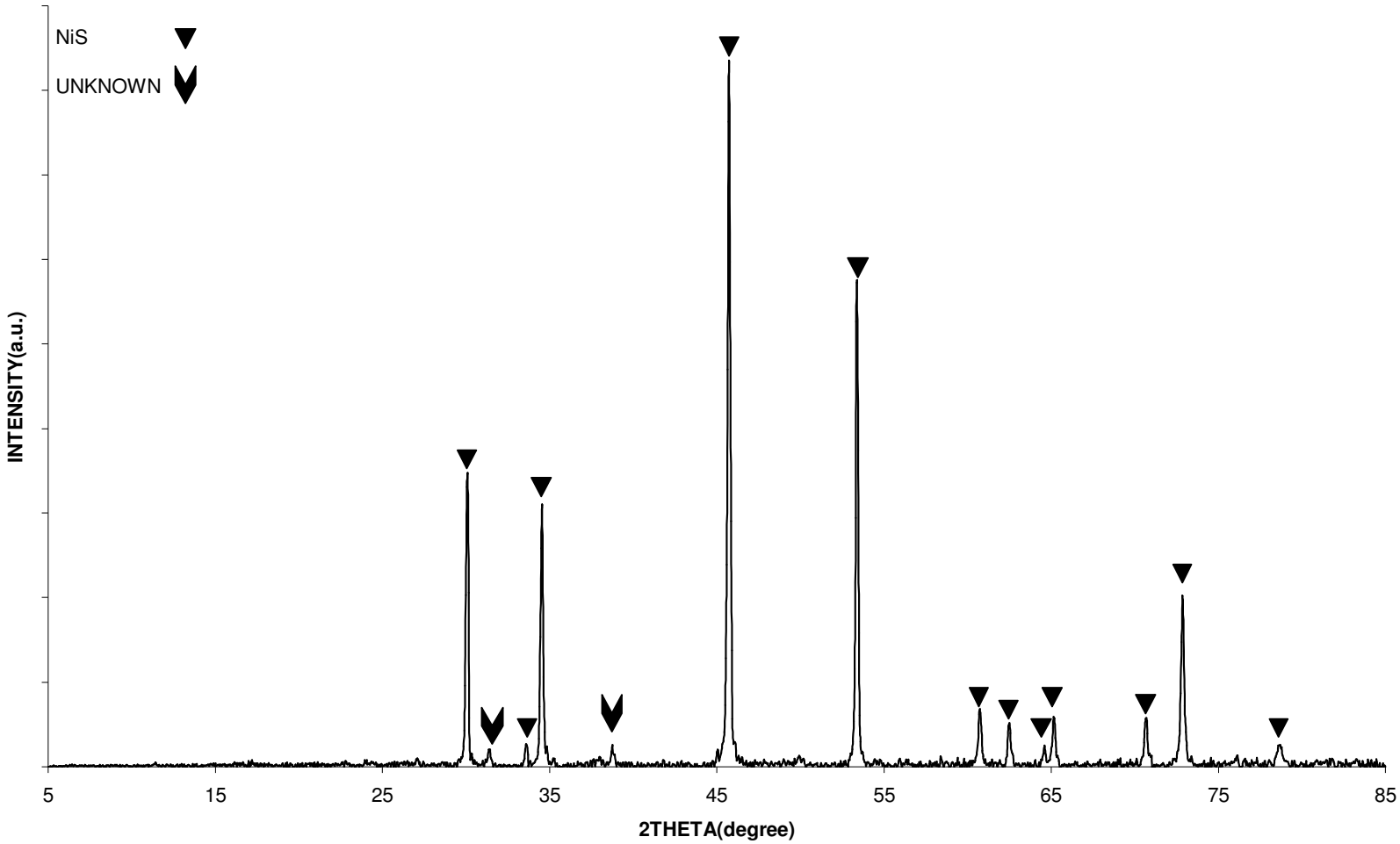

Figure Appendix F.3: X-Ray Powder Diffraction Pattern of Product obtained from the Sulfidizing Reaction of NiO at 650 ^{o}C

Table Appendix F.3: X-Ray Powder Diffraction Data of the Product obtained From the Sulfidizing Reaction of NiO at 650 ^{O}C

OBSERVED DATA		CARD DATA				
		NiS (JCPDS Card No: 77-1624)				
d-values	I/I_0	d-values	I/I_0	h	k	l
2.966	42	2.978	60	1	0	0
2.842	3					
2.661	4	2.662	5	0	0	2
2.594	38	2.599	44	1	0	1
2.322	4					
1.982	100	1.985	100	1	0	2
1.714	69	1.719	43	1	1	0
1.523	9	1.525	6	1	0	3
1.485	7	1.489	5	2	0	0
1.442	4	1.444	3	1	1	2
1.431	8	1.434	5	2	0	1
1.331	7	1.331	5	0	0	4
1.297	25	1.300	16	2	0	2
1.215	4	1.215	3	1	0	4

APPENDIX G

Table Appendix G.1: X-ray powder diffraction data of Reactant Tenorite, CuO (JCPDS Card No: 72-629) that used in Sulfidizing Reactions of CuO

OBSERVED DATA		CARD DATA				
		Tenorite, CuO (JCPDS Card No: 72-629)				
d-values	I/I_0	d-values	I/I_0	h	k	l
2.744	10	2.750	7	1	1	0
2.520	84	2.523	97	-1	1	1
2.319	100	2.322	100	1	1	1
1.865	27	1.866	28	-2	0	2
1.708	13	1.711	10	0	2	0
1.584	16	1.580	14	2	0	2
1.504	22	1.505	19	-1	1	3
1.410	35	1.409	14	-3	1	1
1.375	29	1.375	16	2	2	0
1.304	12	1.303	7	3	1	1
1.261	15	1.261	8	-2	2	2
1.168	9	1.169	4	-3	1	3
1.161	10	1.161	4	2	2	2
1.156	10	1.155	4	4	0	0
1.090	7	1.091	5	-1	3	1

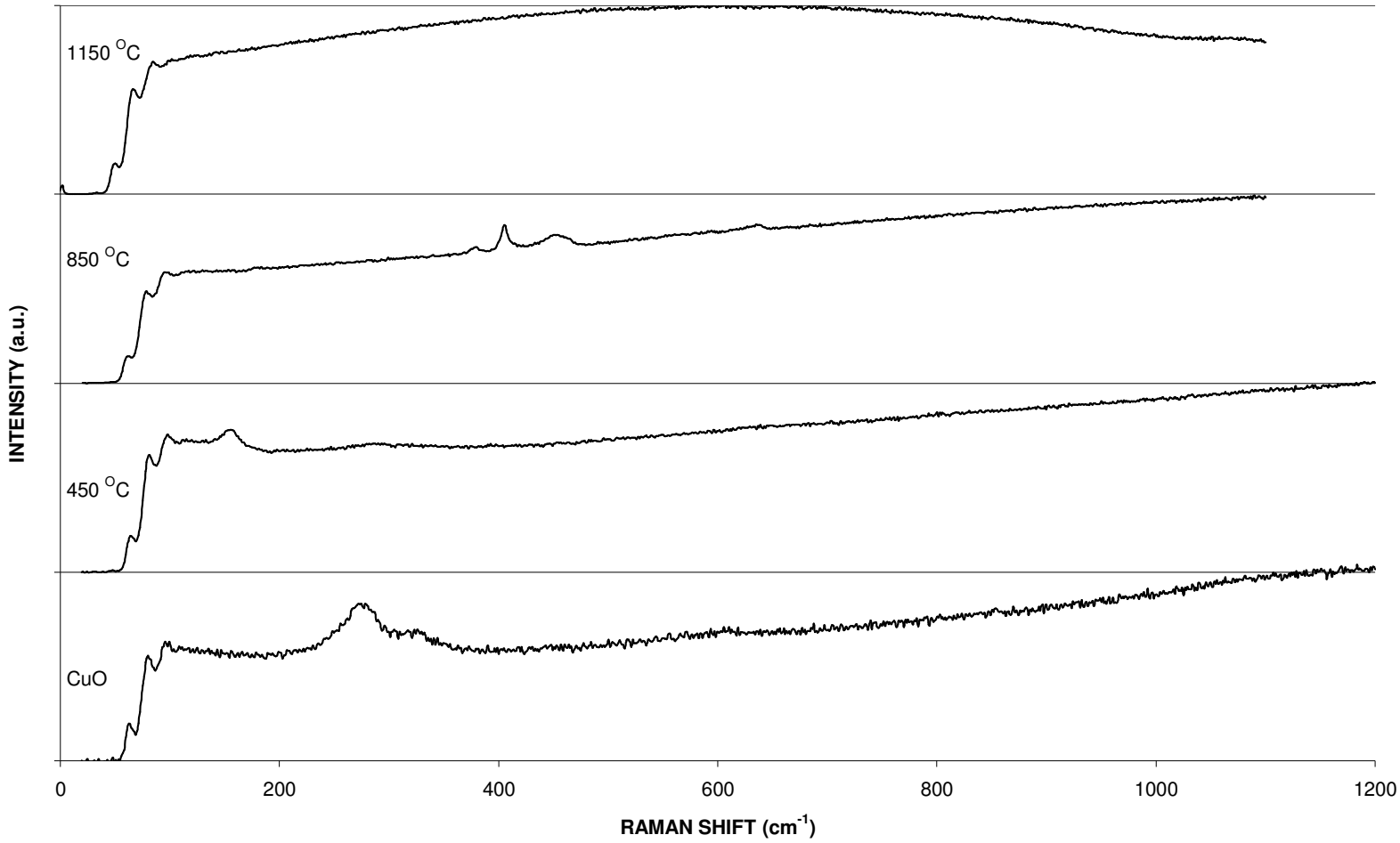

Figure Appendix G.1: Raman Scattering Spectra of Reactant and Product of Sulfidizing Reaction of CuO

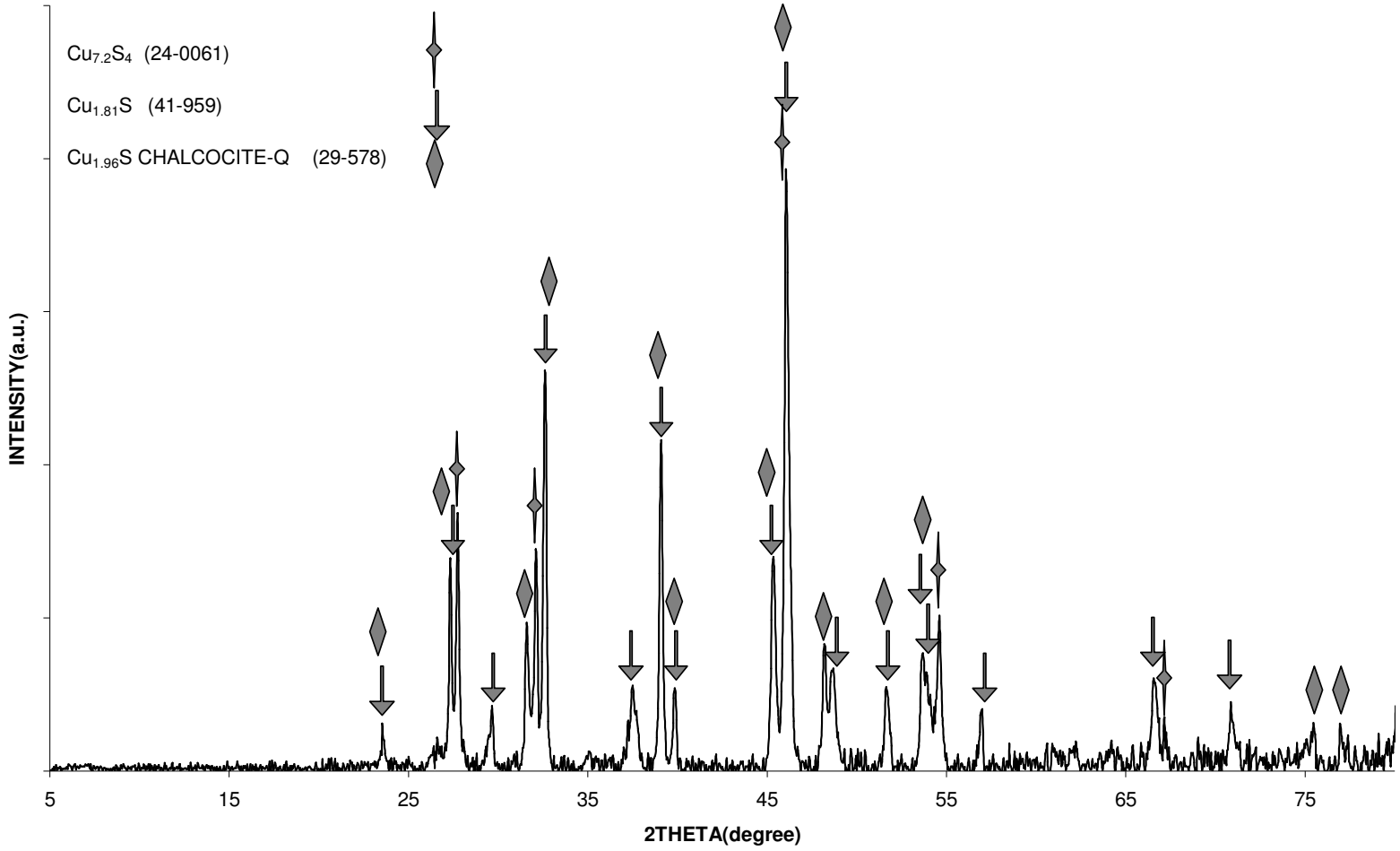

Figure Appendix G.2: X-Ray Powder Diffraction Pattern of Product obtained from the Sulfidizing Reaction of CuO at 650 ^{o}C

Table Appendix G.2: X-Ray Powder Diffraction Data of the Product obtained From the Sulfidizing Reaction of CuO at 650 ^{O}C

OBSERVED DATA		CARD DATA														
		$Cu_{7.2}S_4$ (JCPDS Card No: 24-61)					Chalcocite-Q,$Cu_{1.6}S$(JCPDS Card No:29-578)					$Cu_{1.81}S$ (JCPDS Card no: 41-959)				
d-values	I/I_0	d-values	I/I_0	h	k	l	d-values	I/I_0	h	k	l	d-values	I/I_0	h	k	l
3.774	8						3.783	9	2	0	0	3.770	10	1	0	1
3.258	36						3.270	29	1	0	5	3.270	16	1	0	2
3.212	43	3.216	40	1	1	1	3.225	19	2	0	3					
3.010	11						3.027	7	1	1	5					
3.829	25											2.827	20	1	1	0
2.786	37	2.785	68	2	0	0										
2.744	67						2.751	73	1	2	4	2.740	100	1	0	3
2.396	15						2.396	32	1	3	0					
2.302	56						2.306	58	1 2	3 2	2 4	2.302	80	1	0	4
2.260	14						2.265	18	1	2	6	2.259	30	1	1	3
1.998	36						1.998	61	1	3	5	1.998	30	2	0	0
1.969	100	1.969	100	2	2	0	1.968	100	0	1	9	1.967	30	2	0	1
1.886	22											1.883	35	2	0	2
1.872	17						1.874	49	2	2	7					
1.768	15						1.766	8	1	3	7	1.764	12	1	1	5
1.707	20						1.704	30	1	4	4	1.704	30	2	1	2
1.700	17						1.699	29	0	3	8					
1.679	26	1.679	14	3	1	1										
1.614	11						1.618	7	2	2	9	1.614	12	2	1	3
1.404	16						1.403	11	2	5	0					
1.393	9	1.393	3	4	0	0										
1.326	8						1.327	6	2	2	12	1.326	6	3	0	1
1.259	9											1.260	18	1	1	8
1.238	8											1.234	12	3	1	2
1.198	11						1.970	6	1 2	5 5	9 8	1.196	16	1	0	9

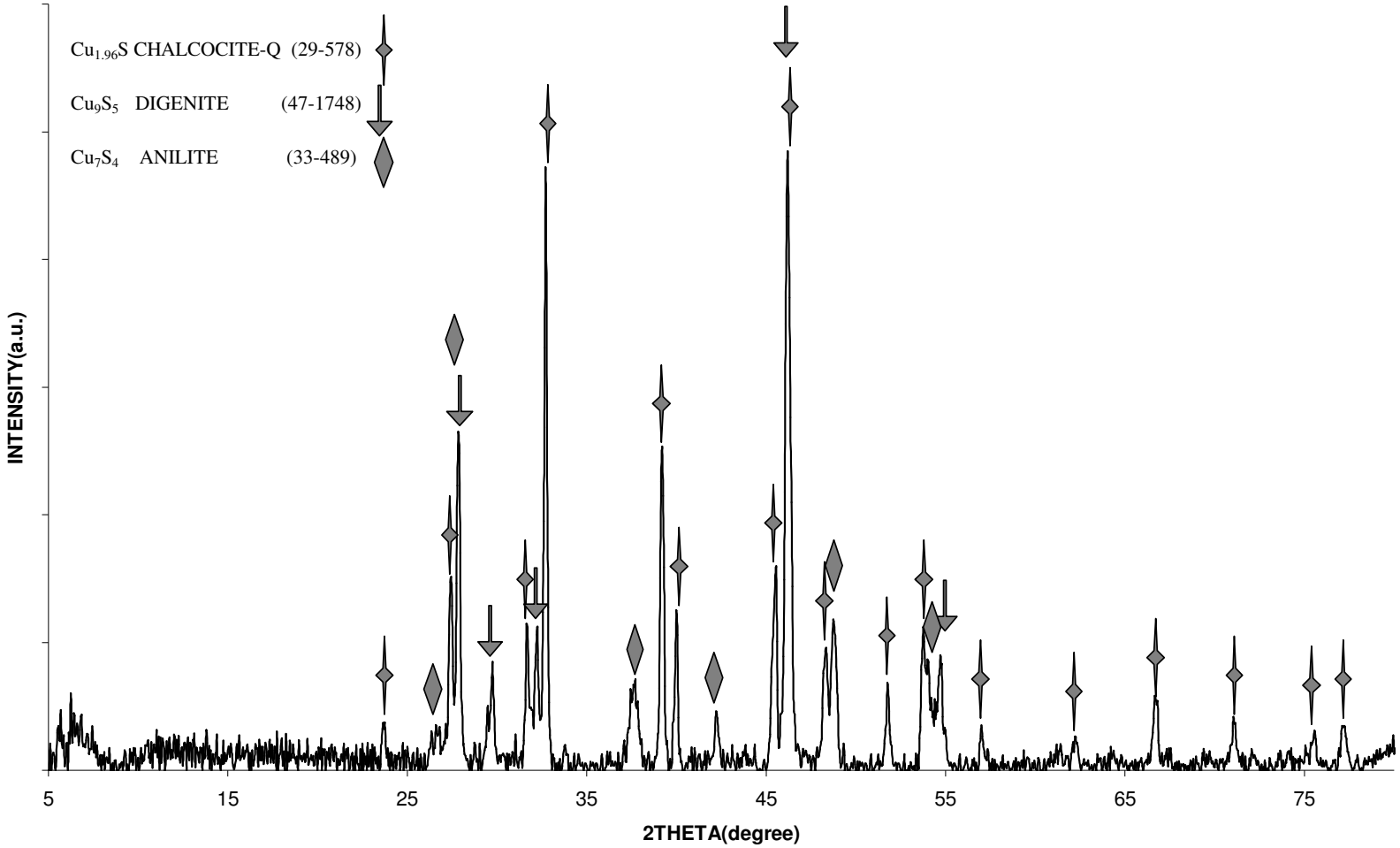

Figure Appendix G.3: X-Ray Powder Diffraction Pattern of Product obtained from the Sulfidizing Reaction of CuO at 850 ^{o}C

Table Appendix G.3: X-Ray Powder Diffraction Data of the Product obtained From the Sulfidizing Reaction of CuO at 850 ^{O}C

OBSERVED DATA		CARD DATA														
		Chalcocite-Q, $Cu_{1.6}S$ (JCPDS Card No: 29-578)					Digenite, Cu_9S_5 (JCPDS Card no: 47-1748)					Anilite, Cu_7S_4 (JCPDS Card no: 33-489)				
d-values	I/I_0	d-values	I/I_0	h	k	l	d-values	I/I_0	h	k	l	d-values	I/I_0	h	k	l
3.759	4	3.770	10	1	0	1										
3.348	5											3.343	25	1	0	3
3.246	19	3.270	16	1	0	2										
3.201	34						3.210	46	0	0	15					
3.025	7						3.051	11	1	0	7					
2.825	17	2.827	20	1	1	0										
2.773	17						2.781	46	1	0	10	2.780	55	2	2	0
2.736	70	2.740	100	1	0	3										
2.384	12											2.380	30	3	0	2
2.296	45	2.302	80	1	0	4										
2.252	23	2.259	30	1	1	3										
2.140	9											2.132	15	0	1	5
1.990	33	1.998 1.994	30 40	2 1	0 1	0 4										
1.963	100	1.967 1.959	30 20	2 1	0 0	1 5	1.964	100	1 0	1 1	0 20					
1.881	21	1.883	35	2	0	2										
1.866	26											1.861	30	3	2	3
1.765	16	1.764	12	1	1	5										
1.751	7											1.753	15	2	4	0
1.704	27	1.704 1.702	30 18	2 1	1 0	2 6										
1.697	21											1.696	20	3	0	5
1.677	22						1.676	17	1	1	15					
1.614	9	1.614	12	2	1	3										
1.493	7	1.495	6	1	0	7										
1.402	17	1.401	30	2	1	5										
1.326	13	1.326	6	3	0	1										
1.260	7	1.260	18	1	1	8										
1.234	12	1.234	12	3	1	2										

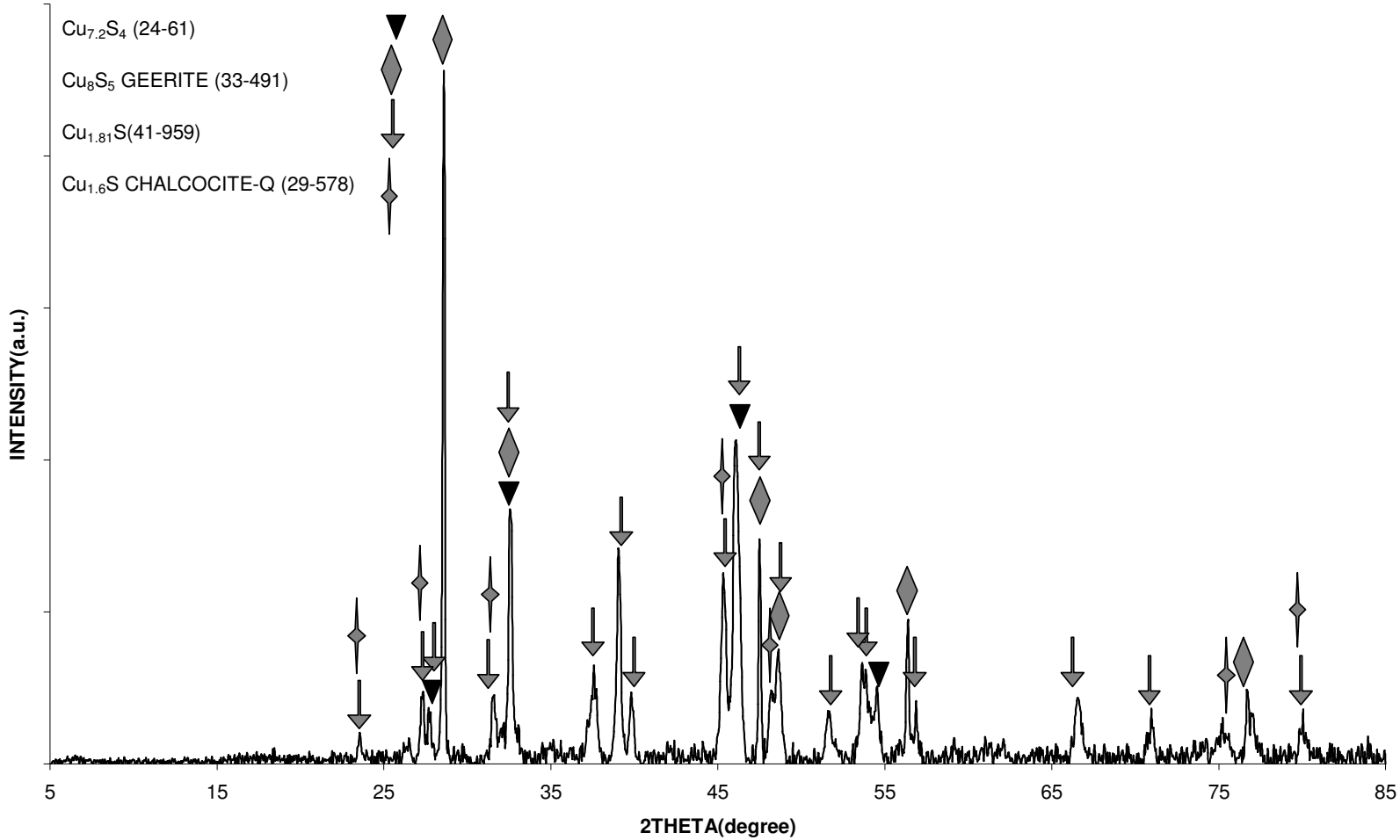

Figure Appendix G.4: X-Ray Powder Diffraction Pattern of Product obtained from the Sulfidizing Reaction of CuO at 1150 ^{o}C

Table Appendix G.4: X-Ray Powder Diffraction Data of the Product obtained From the Sulfidizing Reaction of CuO at 1150 ^{O}C

OBSERVED DATA		CARD DATA									
		$Cu_{7.2}S_4$ (JCPDS Card No: 24-61)					Geerite, Cu_8S_5 (JCPDS Card no: 33-491)				
d-values	I/I_0	d-values	I/I_0	h	k	l	d-values	I/I_0	h	k	l
3.775	5										
3.258	11										
3.218	9	3.216	40	1	1	1					
3.119	100						3.128	100	0	1	5
2.829	10										
2.749	37	2.785	68	2	0	0	2.712	10	1	0	10
2.390	15										
2.305	31										
2.263	11										
2.000	28										
1.969	47	1.969	100	2	2	0					
1.913	33						1.918	50	1	1	3
1.886	11						1.870	10	1	1	6
1.870	17										
1.768	7										
1.707	15										
1.701	14										
1.681	12	1.679	14	3	1	1	1.683	10	0	2	1
1.630	21						1.637	30	1	1	15
1.617	9										
1.404	10										
1.327	8										
1.262	7										
1.241	11						1.247	10	2	1	7
1.198	8										

Table Appendix G.4 (continued)

OBSERVED DATA		CARD DATA									
		$Cu_{1.81}S$ (JCPDS Card no: 41-959)					Chalcocite-Q, $Cu_{1.6}S$ (JCPDS Card No: 29-578)				
d-values	I/I_0	d-values	I/I_0	h	k	l	d-values	I/I_0	h	k	l
3.775	5	3.783	9	2	0	0	3.770	10	1	0	1
3.258	11	3.270	29	1	0	5	3.270	16	1	0	2
3.218	9	3.225 3.203	19 16	2 1	0 2	3 2					
3.119	100										
2.829	10	2.833	34	0	1	6	2.827	20	1	1	0
2.746	37	2.751	73	1	2	4					
2.390	15	2.396	32	1	3	0					
2.305	31	2.306	58	1 2	3 2	2 4					
2.263	11	2.265	18	1	2	6					
2.000	28	1.998	61	1	3	5	1.998 1.994	30 40	2 1	0 1	0 4
1.969	47	1.968	100	0	1	9					
1.913	33	1.909	8	2	3	4					
1.886	11						1.883	35	2	0	2
1.870	17	1.874	49	2	2	7					
1.768	7	1.771 1.766	11 8	3 1	3 3	1 7					
1.707	15	1.704	30	1	4	4					
1.701	14	1.699	29	0	3	8					
1.681	12										
1.630	21										
1.617	9	1.618	7	2	2	9					
1.404	10	1.403	11	2	5	0					
1.327	8	1.327	6	2	2	12					
1.262	7						1.26	18	1	1	8
1.241	11										
1.198	8	1.197	6	1 2	5 5	9 8					

APPENDIX H

Table Appendix H.1: X-ray powder diffraction data of Reactant ZnO (JCPDS Card No: 75-576) that used in Sulfidizing Reactions of ZnO

OBSERVED DATA		CARD DATA				
		ZnO (JCPDS Card No: 75-576)				
d-values	I/I_0	d-values	I/I_0	h	k	l
2.807	58	2.808	57	1	0	0
2.598	43	2.597	42	0	0	2
2.469	100	2.470	100	1	0	1
1.909	30	1.907	22	1	0	2
1.623	50	1.621	31	1	1	0
1.476	45	1.474	28	1	0	3
1.408	9	1.404	5	2	0	0
1.378	46	1.375	23	1	1	2
1.359	23	1.356	12	2	0	1
1.302	4	1.299	2	0	0	4
1.238	9	1.235	4	2	0	2
1.182	5	1.179	2	1	0	4

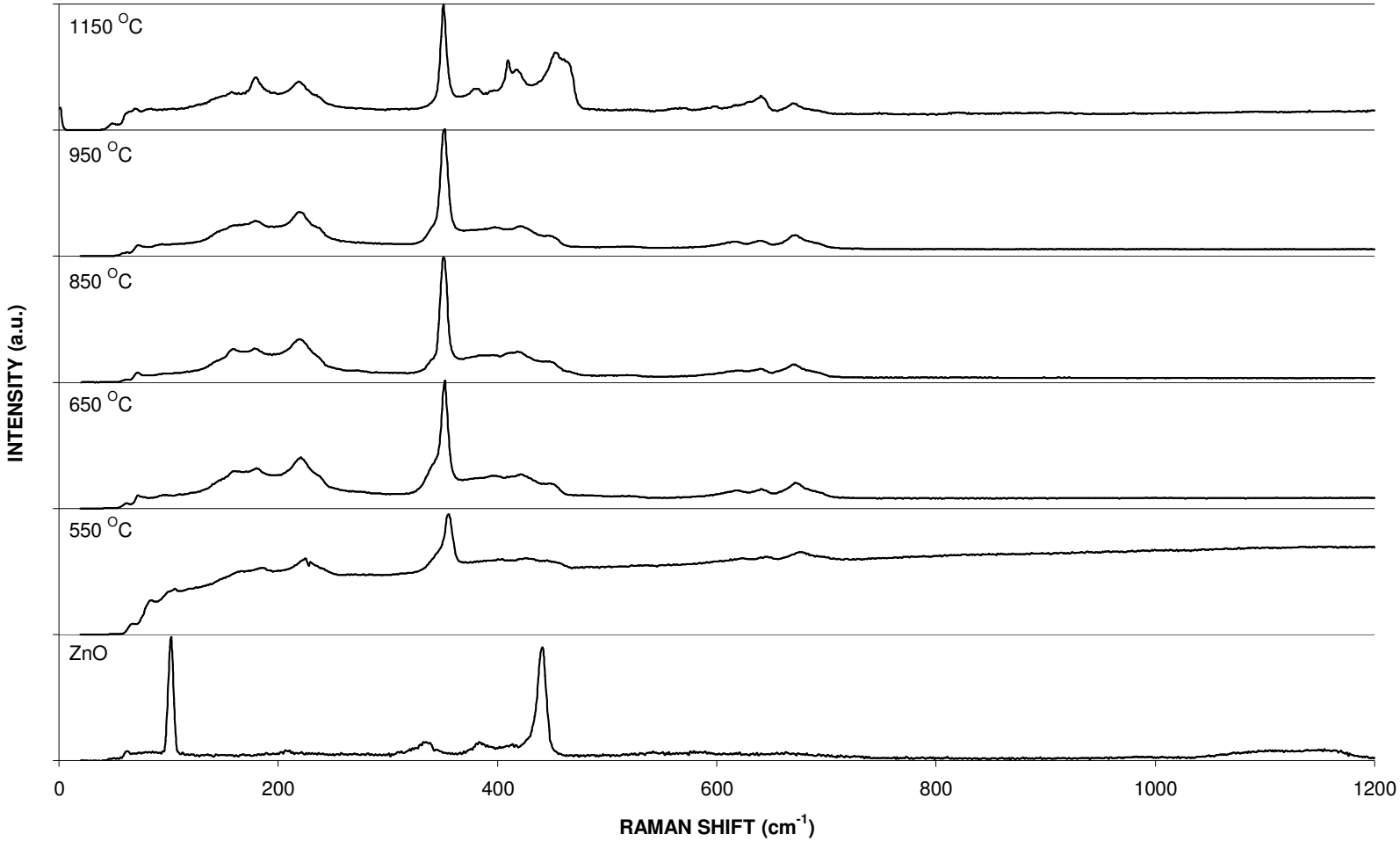

Figure Appendix H.1: Raman Scattering Spectra of Reactant and Product of Sulfidizing Reaction of ZnO

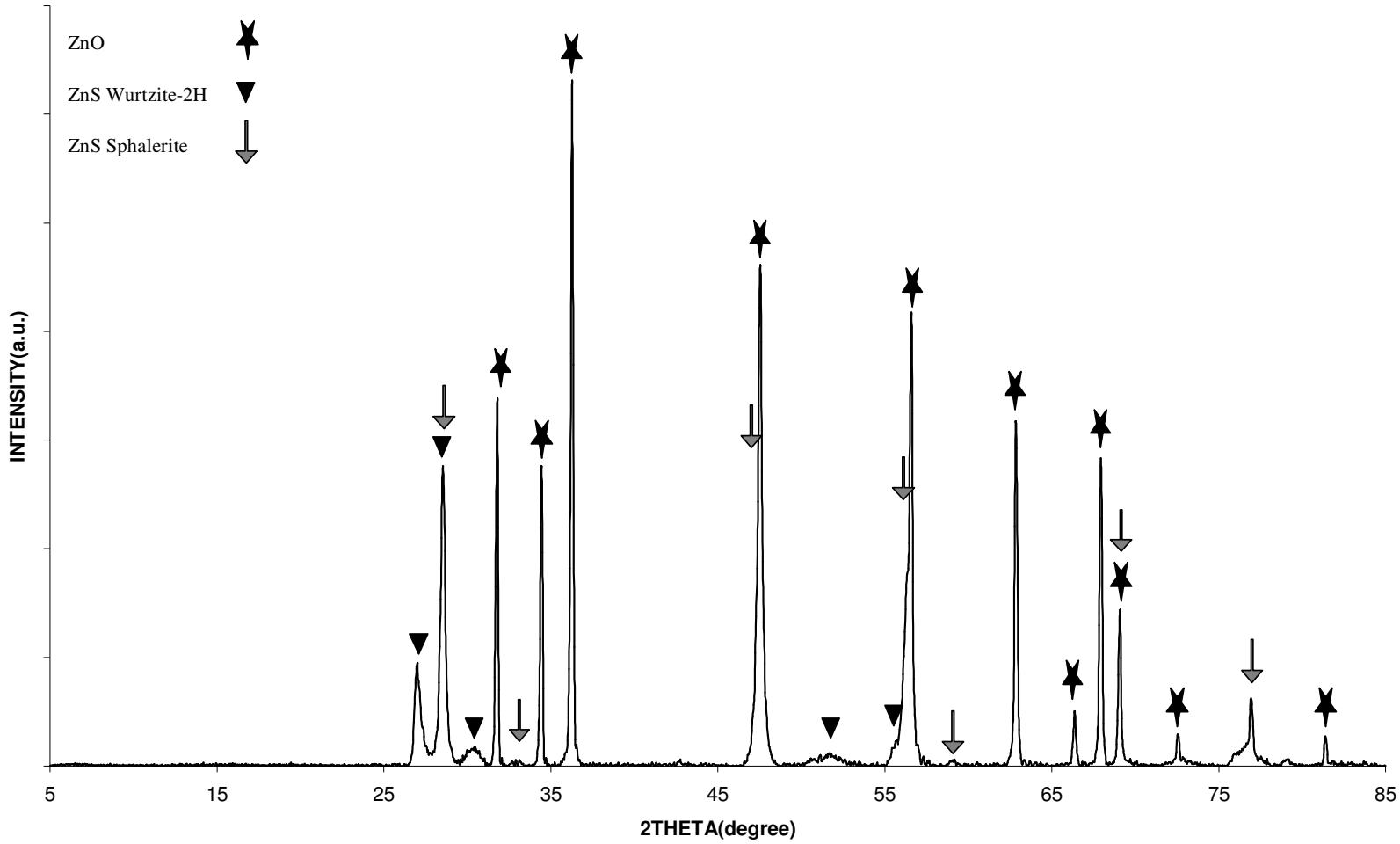

Figure Appendix H.2: X-Ray Powder Diffraction Pattern of Product obtained from the Sulfidizing Reaction of ZnO at 450 ^{o}C

Table Appendix H.2: X-Ray Powder Diffraction Data of the Product obtained From the Sulfidizing Reaction of ZnO at 450 ^{O}C

OBSERVED DATA		CARD DATA														
		Wurtzite-2H, ZnS (JCPDS Card No: 36-1450)					Sphalerite, ZnS (JCPDS Card no: 05-566)					ZnO (JCPDS Card No: 75-576)				
d-values	I/I_0	d-values	I/I_0	h	k	l	d-values	I/I_0	h	k	l	d-values	I/I_0	h	k	l
3.300	21	3.310	100	1	0	0										
3.124	54	3.129	84	0	0	2	3.123	100	1	1	1					
2.933	11	2.926	87	1	0	1										
2.812	57											2.808	57	1	0	0
2.720	4						2.705	10	1	1	1					
2.601	44											2.597	42	0	0	2
2.473	100											2.47	100	1	0	1
1.911	76	1.910	81	1	1	0	1.912	51	2	2	0	1.907	22	1	0	2
1.765	8	1.764	54	1	0	3										
1.652	11	1.654	11	2	0	0										
1.631	35						1.633	30	3	1	1					
1.625	68											1.621	31	1	1	0
1.561	5						1.561	2	2	2	2					
1.477	42											1.474	28	1	0	3
1.407	10											1.404	5	2	0	0
1.378	39											1.375	23	1	1	2
1.358	22						1.351	6	4	0	0	1.355	12	2	0	1
1.302	8	1.296	15	2	0	3						1.299	2	0	0	4
1.238	14						1.240	8	3	1	1					
1.209	6						1.209	2	4	2	0					
1.181	8											1.179	2	1	0	4

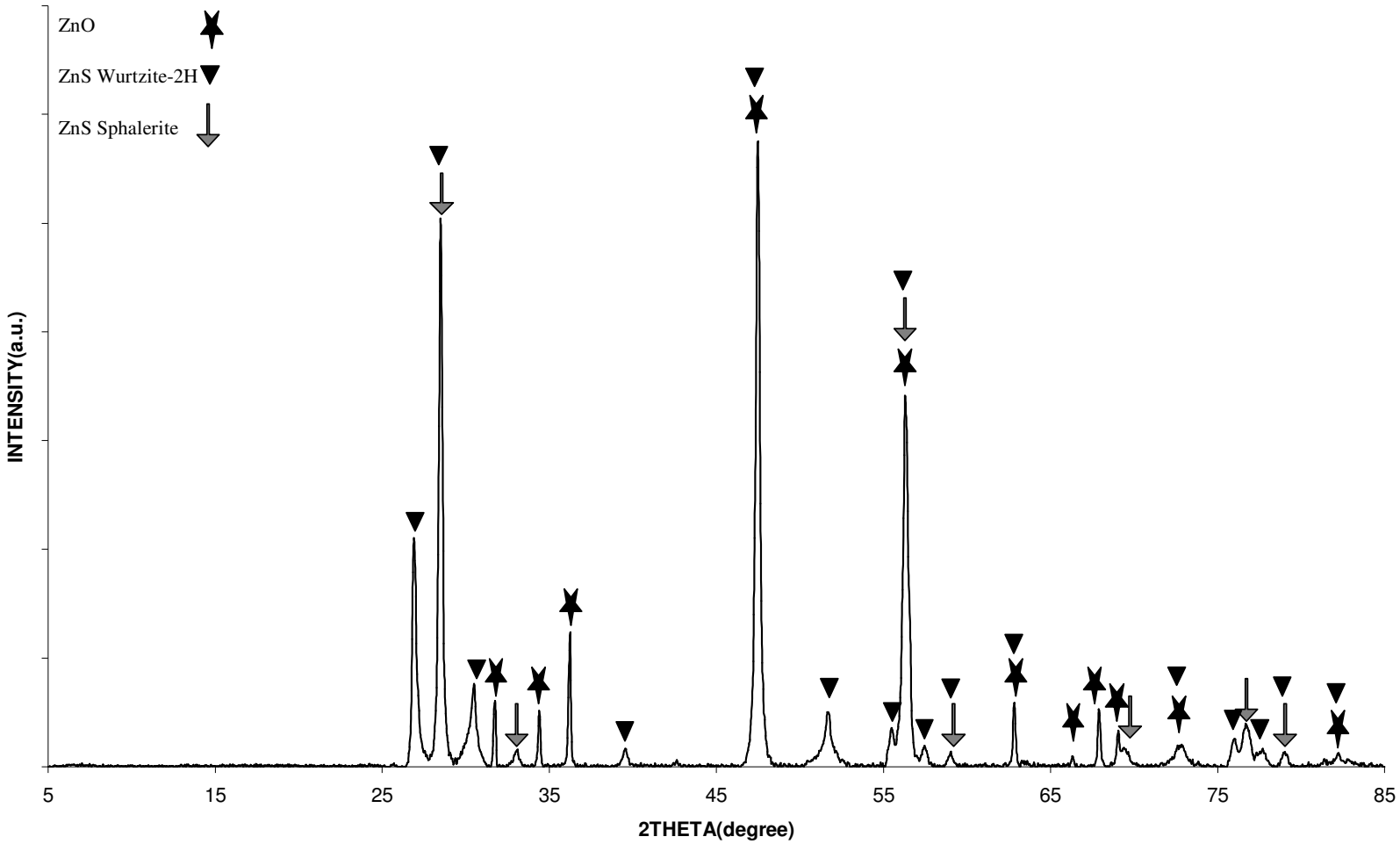

Figure Appendix H.3: X-Ray Powder Diffraction Pattern of Product obtained from the Sulfidizing Reaction of ZnO at 550 ^{o}C

Table Appendix H.3: X-Ray Powder Diffraction Data of the Product obtained From the Sulfidizing Reaction of ZnO at 550 ^{O}C

OBSERVED DATA		CARD DATA														
		Wurtzite-2H, ZnS (JCPDS Card No: 36-1450)					Sphalerite, ZnS (JCPDS Card no: 05-566)					ZnO (JCPDS Card No: 75-576)				
d-values	I/I_0	d-values	I/I_0	h	k	l	d-values	I/I_0	h	k	l	d-values	I/I_0	h	k	l
3.312	37	3.310	100	1	0	0	3.123	100	1	1	1					
3.129	88	3.129	84	0	0	2										
2.928	14	3.926	87	1	0	1										
2.816	11											2.808	57	1	0	0
2.704	3						2.705	10	2	0	0					
2.605	9											2.597	42	0	0	2
2.476	22											2.470	100	1	0	1
2.274	3	3.273	28	1	0	2										
1.913	100	1.910	81	1	1	0	1.912	51	2	2	0					
1.767	9	1.764	54	1	0	3										
1.654	7	1.654	11	2	0	0										
1.633	60	1.630	47	1	1	2	1.633	30	3	1	1					
1.603	4	1.599	12	2	0	1										
1.563	3	1.564	2	0	0	4	1.561	2	2	2	2					
1.477	11											1.474	28	1	0	3
1.409	2											1.404	5	2	0	0
1.379	10											1.375	23	1	1	2
1.359	6											1.355	12	2	0	1
1.353	4						1.351	6	4	0	0					
1.299	4	1.296	15	2	0	3						1.299	2	0	0	4
1.251	5	1.251	6	2	1	0										
1.241	7						1.240	9	3	3	1					
1.210	3	1.210	2	1	1	4	1.209	2	4	2	0					
1.171	3	1.171	11	1	0	5										

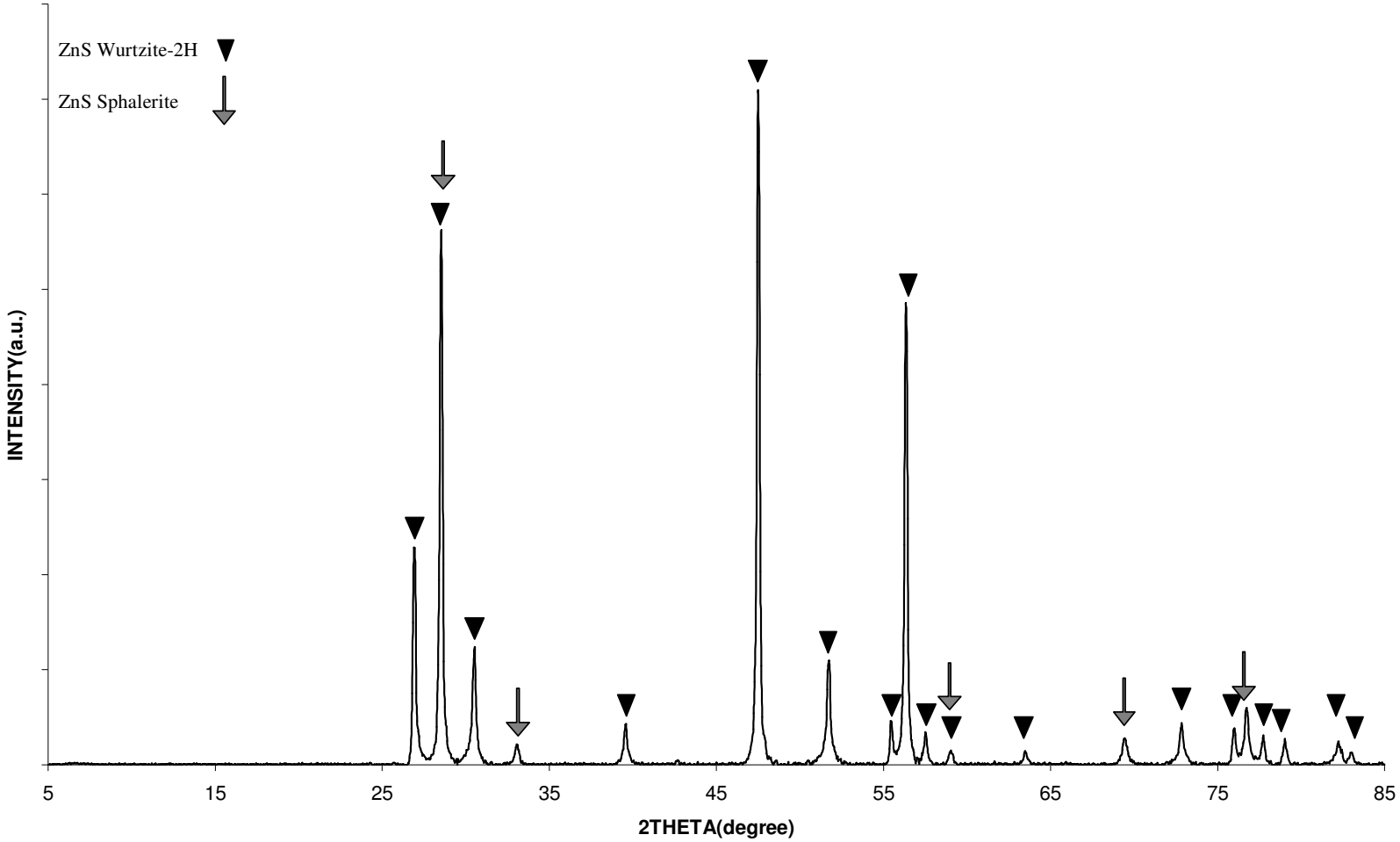

Figure Appendix H.4: X-Ray Powder Diffraction Pattern of Product obtained from the Sulfidizing Reaction of ZnO at 650 ^{o}C

Table Appendix H.4: X-Ray Powder Diffraction Data of the Product obtained From the Sulfidizing Reaction of ZnO at 650 ^{O}C

OBSERVED DATA		CARD DATA									
		Wurtzite-2H, ZnS (JCPDS Card No: 36-1450)					Sphalerite, ZnS (JCPDS Card no: 05-566)				
d-values	I/I_0	d-values	I/I_0	h	k	l	d-values	I/I_0	h	k	l
3.306	41	3.31	100	1	0	0					
3.124	94	3.129	84	0	0	2	3.123	100	1	1	1
2.924	25	2.926	87	1	0	1					
2.704	6						2.705	10	2	0	0
2.274	9	2.273	28	1	0	2					
1.911	100	1.910	81	1	1	0	1.912	51	2	2	0
1.765	20	1.764	54	1	0	3					
1.654	10	1.654	11	2	0	0					
1.631	66	1.630	47	1	1	2	1.633	30	3	1	1
1.600	8	1.599	12	2	0	1					
1.562	5	1.564	2	0	0	4	1.561	2	2	2	2
1.464	4	1.463	6	2	0	2					
1.351	6						1.351	6	4	0	0
1.297	9	1.296	15	2	0	3					
1.251	8	1.251	6	2	0	0					
1.241	12						1.240	9	3	3	1
1.227	8	1.226	9	2	1	1					
1.210	6	1.210	2	1	1	4	1.209	2	4	2	0
1.171	6	1.171	11	1	0	5					
1.162	5	1.161	6	2	1	2					

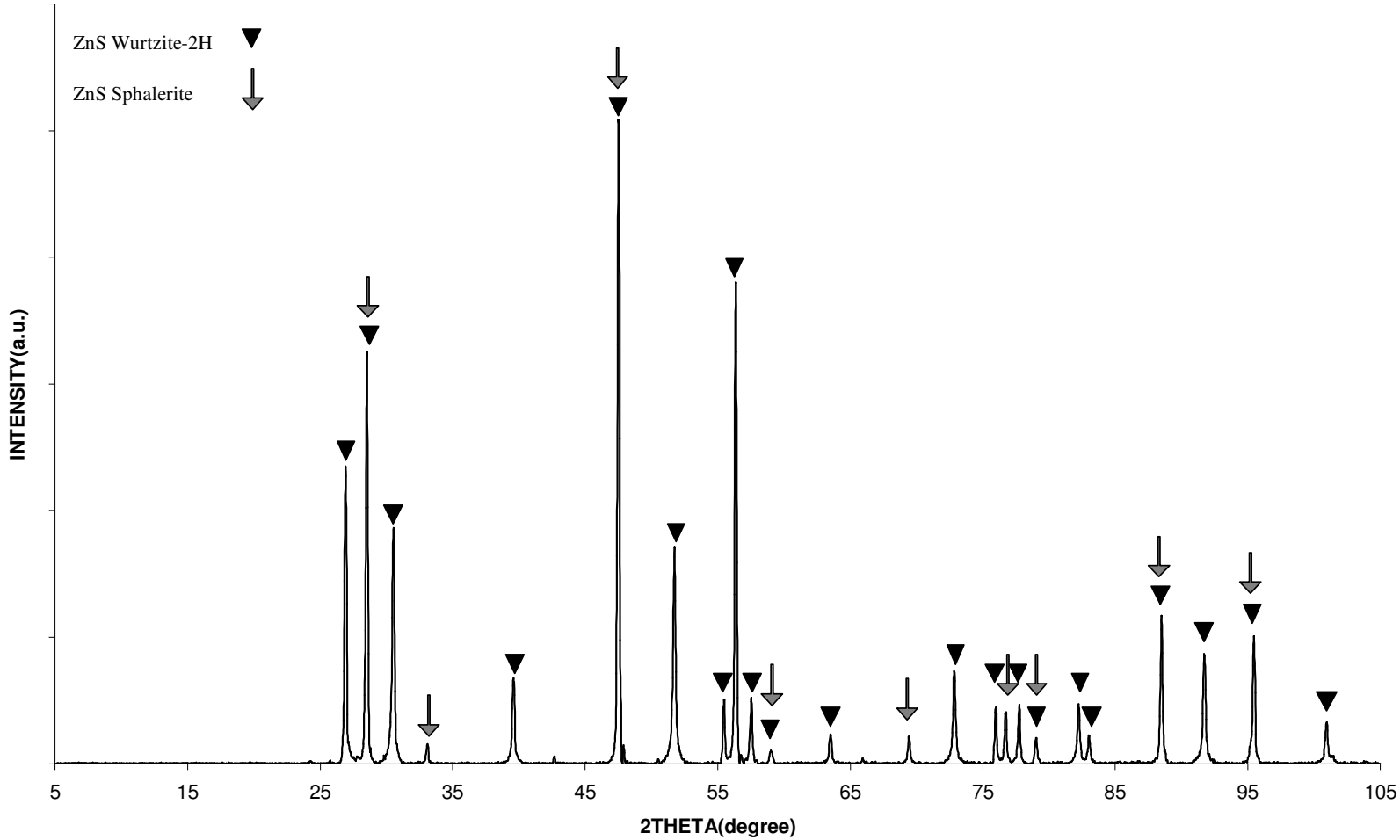

Figure Appendix H.5: X-Ray Powder Diffraction Pattern of Product obtained from the Sulfidizing Reaction of ZnO at 850 ^{o}C

Table Appendix H.5: X-Ray Powder Diffraction Data of the Product obtained From the Sulfidizing Reaction of ZnO at 850 ^{O}C

OBSERVED DATA		CARD DATA									
		Wurtzite-2H, ZnS (JCPDS Card No: 36-1450)					Sphalerite, ZnS (JCPDS Card no: 05-566)				
d-values	I/I_0	d-values	I/I_0	h	k	l	d-values	I/I_0	h	k	l
3.306	57	3.31	100	1	0	0					
3.124	78	3.129	84	0	0	2	3.123	100	1	1	1
2.924	45	2.926	87	1	0	1					
2.704	5						2.705	10	2	0	0
2.274	17	2.273	28	1	0	2					
1.911	100	1.91	81	1	1	0	1.912	51	2	2	0
1.765	83	1.764	54	1	0	3					
1.654	13	1.654	11	2	0	0					
1.631	71	1.63	47	1	1	2	1.633	30	3	1	1
1.600	13	1.599	12	2	0	1					
1.562	5	1.564	2	0	0	4	1.561	2	2	2	2
1.463	7	1.463	6	2	0	2					
1.352	6						1.351	6	4	0	0
1.297	16	1.296	15	2	0	3					
1.251	10	1.251	6	2	1	0					
1.241	10						1.24	9	3	3	1
1.227	11	1.226	9	2	1	1					
1.211	6	1.21	2	1	1	4	1.209	2	4	2	0
1.171	12	1.171	11	1	0	5					
1.162	7	1.161	6	2	1	2					
1.104	23	1.103	9	3	0	0	1.103	9	4	2	2
1.074	19	1.073	15	2	1	3					
1.041	20	1.04	10	3	0	2	1.04	5	5	1	1
0.999	9	0.998	7	2	0	5					

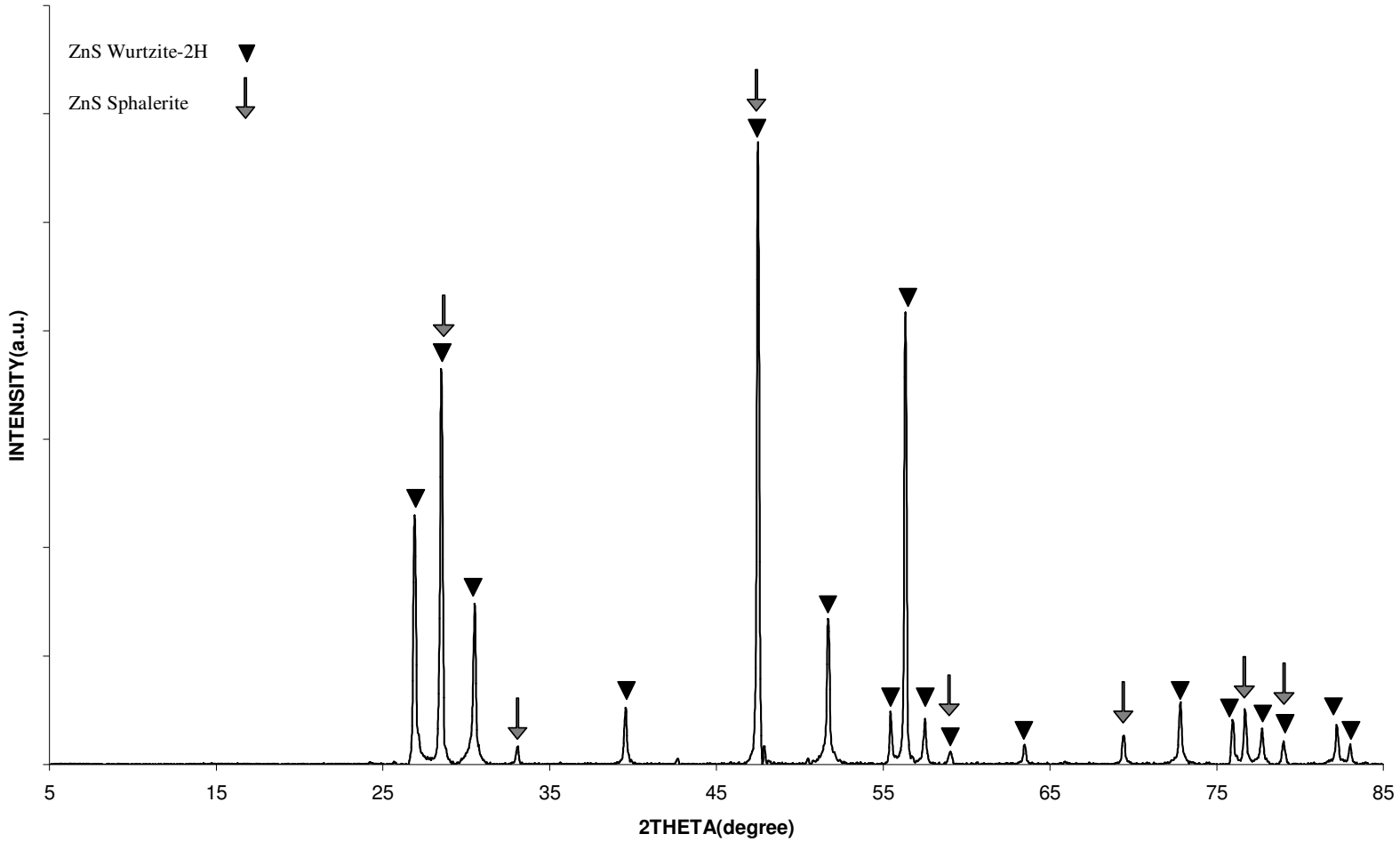

Figure Appendix H.6: X-Ray Powder Diffraction Pattern of Product obtained from the Sulfidizing Reaction of ZnO at 950 ^{o}C

Table Appendix H.6: X-Ray Powder Diffraction Data of the Product obtained From the Sulfidizing Reaction of ZnO at 950 ^{O}C

OBSERVED DATA		CARD DATA									
		Wurtzite-2H, ZnS (JCPDS Card No: 36-1450)					Sphalerite, ZnS (JCPDS Card no: 05-566)				
d-values	I/I_0	d-values	I/I_0	h	k	l	d-values	I/I_0	h	k	l
3.312	47	3.310	100	1	0	0					
3.124	79	3.129	84	0	0	2	3.123	100	1	1	1
2.924	33	2.926	87	1	0	1					
2.704	5						2.705	10	2	0	0
2.274	12	2.273	28	1	0	2					
1.913	100	1.910	81	1	1	0	1.912	51	2	2	0
1.767	27	1.764	54	1	0	3					
1.656	11	1.654	11	2	0	0					
1.631	71	1.630	47	1	1	2	1.633	30	3	1	1
1.601	10	1.599	12	2	0	1					
1.562	4	1.564	2	0	0	4	1.561	2	2	2	2
1.464	5	1.463	6	2	0	2					
1.352	7						1.351	6	4	0	0
1.297	12	1.296	15	2	0	3					
1.252	9	1.251	6	2	1	0					
1.241	11						1.240	9	3	3	1
1.227	9	1.226	9	2	1	1					
1.211	6	1.210	2	1	1	4	1.209	2	4	2	0
1.171	9	1.171	11	1	0	5					
1.162	6	1.161	6	2	1	2					

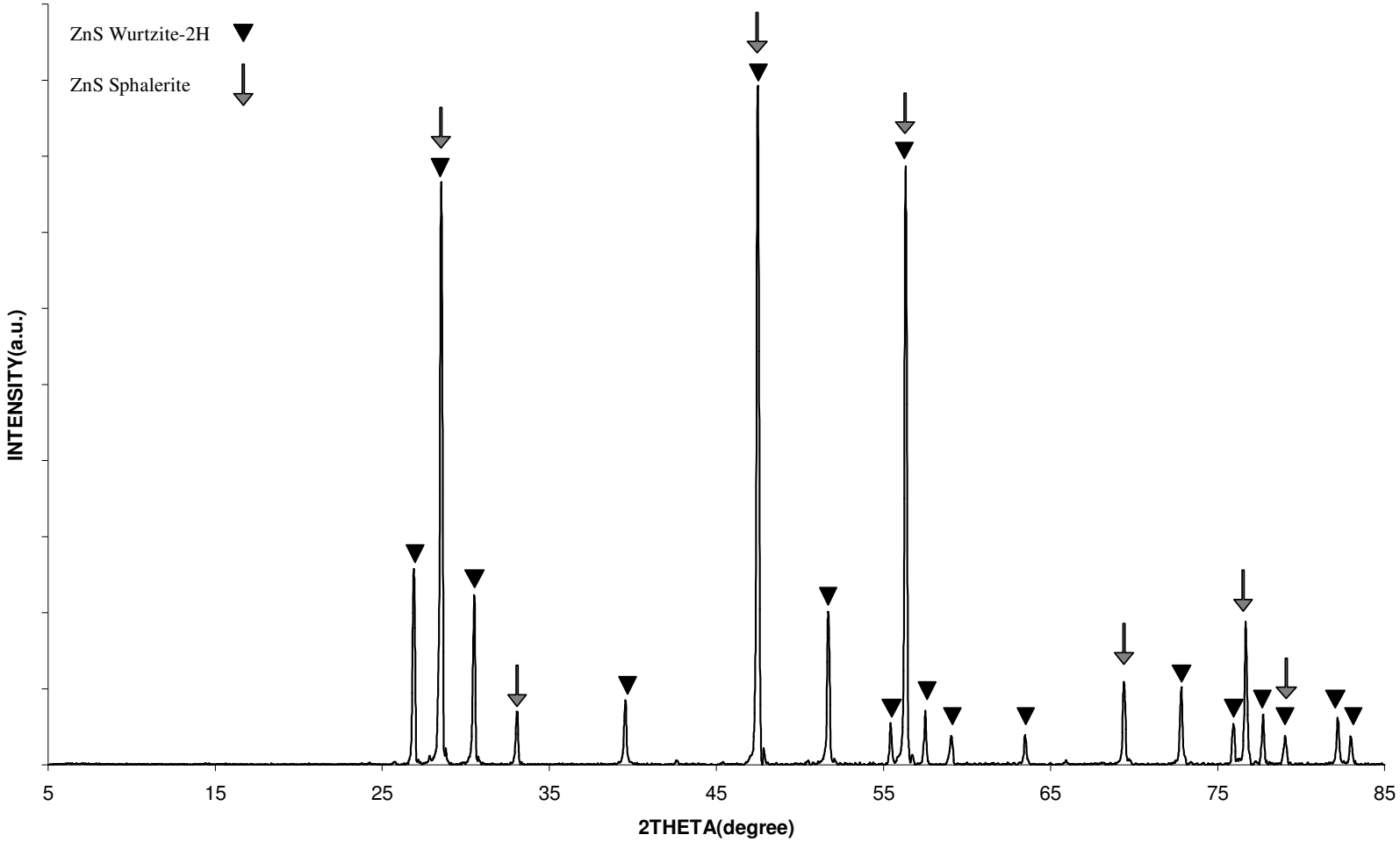

Figure Appendix H.7: X-Ray Powder Diffraction Pattern of Product obtained from the Sulfidizing Reaction of ZnO at 1150 ^{o}C

Table Appendix H.7: X-Ray Powder Diffraction Data of the Product obtained From the Sulfidizing Reaction of ZnO at 1150 ^{O}C

OBSERVED DATA		CARD DATA									
		Wurtzite-2H, ZnS (JCPDS Card No: 36-1450)					Sphalerite, ZnS (JCPDS Card no: 05-566)				
d-values	I/I_0	d-values	I/I_0	h	k	l	d-values	I/I_0	h	k	l
3.312	33	3.310	100	1	0	0					
3.124	98	3.129	84	0	0	2	3.123	100	1	1	1
2.924	29	2.926	87	1	0	1					
2.704	10						2.705	10	2	0	0
2.274	11	2.273	28	1	0	2					
1.913	100	1.910	81	1	1	0	1.912	51	2	2	0
1.767	22	1.764	54	1	0	3					
1.656	8	1.654	11	2	0	0					
1.631	81	1.630	47	1	1	2	1.633	30	3	1	1
1.601	9	1.599	12	2	0	1					
1.562	6	1.564	2	0	0	4	1.561	2	2	2	2
1.464	6	1.463	6	2	0	2					
1.353	12						1.351	6	4	0	0
1.297	12	1.296	15	2	0	3					
1.252	7	1.251	6	2	1	0					
1.241	20						1.240	9	3	3	1
1.227	8	1.226	9	2	1	1					
1.210	6	1.210	2	1	1	4	1.209	2	4	2	0
1.172	8	1.171	11	1	0	5					
1.163	6	1.161	6	2	1	2					